January 2012

Evaluation Of A Low Corrosion Method To Increase Mercury Oxidation And Scrubber Capture

Shuchita Sanjay Patwardhan

EVALUATION OF A LOW CORROSION METHOD TO INCREASE MERCURY OXIDATION AND SCRUBBER CAPTURE

by

Shuchita Sanjay Patwardhan
Bachelor of Science, Pune University, 2010

A Thesis
Submitted to the Graduate Faculty

of the

University of North Dakota

in partial fulfillment of the requirements

for the degree of

Master of Science

Grand Forks, North Dakota
December
2012

This thesis, submitted by Shuchita Sanjay Patwardhan in partial fulfillment of the requirements for the Degree of Master of Science from the University of North Dakota, has been read by the Faculty Advisory Committee under whom the work has been done and is hereby approved.

_____
Dr. Steve Benson, Chairperson

_____
Dr. Srivats Srinivaschar, Committee Member

_____
Dr. Michael Mann, Committee Member

This thesis meets the standards for appearance, conforms to the style and format requirements of the Graduate School of the University of North Dakota, and is hereby approved.

_____
Dr. Wayne Swisher, Dean of the Graduate School

_____
Date

PERMISSION

Title Evaluation of a Low Corrosion Method to Increase Mercury Oxidation and Scrubber Capture

Department Chemical Engineering

Degree Master of Science

In presenting this thesis in partial fulfillment of the requirements for a graduate degree from the University of North Dakota, I agree that the library of this University shall make it freely available for inspection. I further agree that permission for extensive copying for scholarly purposes may be granted by the professor who supervised my thesis work or, in his absence, by the chairperson of the department or the dean of the Graduate School. It is understood that any copying or publication or other use of this thesis or part thereof for financial gain shall not be allowed without my written permission. It is also understood that due recognition shall be given to me and to the University of North Dakota in any scholarly use which may be made of any material in my thesis.

Signature Shuchita Patwardhan

Date 12/06/2012

TABLE OF CONTENTS

LIST OF FIGURES

Figure Page

LIST OF TABLES

Table Page

AKNOWLEDGEMENT

I am greatly indebted to the Department of Chemical Engineering of University of North Dakota for giving me wonderful opportunities during my MS. I would like to express my immense gratitude to my advisor Dr. Steve Benson, who has supervised me with enormous support and encouragement. No words are sufficient to express how profoundly grateful I am for Dr. Srivats Srinivaschar's guidance in my research. I am also grateful to my research committee member, Dr. Michael Mann, for his guidance and insightful reviews. I would like to thank the US Environmental Protection Agency (EPA) and Minnesota's Department of Natural Resources (DNR) for their research funding. I am also thankful to all the taconite plants working in the Mesabi Iron Range for providing raw materials required for this research.

I wish to thank Mr. Harry Feilen for helping me with the experimental setup. My sincere thanks go to Dr. Nicholas Lentz for his guidance and support in analyzing the results of my experiments. I am grateful to Junior Nasah, Charles Thumbi and Jacob Bertram for their help in carrying out this research. I also wish to thank my family and friends for their support.Finally, I would like to thank all other people who have contributed directly or indirectly to my research that I am unable to thank individually.

ABSTRACT

The taconite industry located in the Mesabi iron range has been identified as one of the major contributors of the atmospheric mercury in the Lake Superior basin by the Lake Superior Lakewide Management Plan (LaMP). Mercury is a leading concern among air toxic metals due to its volatility, persistence and bioaccumulation as methylmercury in the environment, and its neurological health impacts.

Previous research work performed at taconite processing plants by Minnesota Department of Natural Resources (DNR) identified the taconite ore as the main source of mercury during the taconite processing. Magentite iron ore pellets are produced by balling moist concentrates to green balls, which are then dried, oxidized to hematite, sintered, cooled and transported to steelmaking plants. Mercury is released during the heat processing (induration) step of these green balls to a final product called as taconite pellets. In order to address the mercury emission problem, an approach was proposed by the University of North Dakota (UND) team which explores the possibility of oxidizing the mercury and thus, increasing the mercury capture from scrubbers.

The proposed technology employed a low corrosion method where brominated activated carbon (ESORB-HG-11) was added to green balls to promote mercury oxidation. In Phase I, mercury oxidation potential of ESORB-HG-11 was established. In Phase II, green balls produced from the ore concentrate and additives obtained from five different plants were mixed with trace amounts of ESORB-HG-11. The green balls were

then subjected to heating experiments to determine the mercury oxidation potential of the additive.

Heating tests of the green balls from four of the taconite facilities showed the mercury oxidation levels ranging between 43% and 78%, with averages of 52% (±8 %) and 58% (±11%) for 0.1 and 0.5 weigh percent loading respectively. Baseline oxidation levels averaged to 18% (±6%), while oxidation levels due to addition of ESORB-HG-11 averaged 42% (±9%) and 48% (±13%) for the 0.1 and 0.5 weight percent loading respectively. Results were in accordance with Phase I indicating that 0.1 wt% is optimum loading for mercury oxidation. The results from the fifth taconite facility have not been included in the averages since they showed significantly lower mercury oxidation levels when compared to other plants.

Phase analysis experiments and results from Phase I and Phase II suggest that there was little or no gas-phase mercury oxidation occurring during tests performed using the lab scale apparatus. This suggests that the mercury oxidation observed during these tests is a solid phase phenomenon occurring most likely on the carbon surface and within the green ball. Previous work indicated that the gas-phase mercury oxidation does occur in taconite facilities. Consequently, a full-scale demonstration of the technology might result in higher levels of mercury oxidation than observed during the bench scale tests in this project. The impact of the carbon additive on the fired taconite pellet needs to be investigated in future testing to further develop the process.

CHAPTER I

INTRODUCTION

The taconite industry located in Minnesota produces taconite pellets which are currently among one of the main source of iron for the iron and steel industries all over the world. Minnesota's taconite industry is located on the Mesabi Iron Range in the north east of the state of Minnesota.

Taconite pellet production process is divided into three major steps. The first step is mining of the ore from the open pits. In the second step, beneficiation is performed on the ore to increase the iron content and to improve the ore's physical structure. The third step involves agglomeration which includes pelletization (indurating) processes to oxidize the iron present in the ore. In this part the iron-rich concentrated ore is mixed with water and a binder and then the concentrate is rolled into green balls inside rotating cylinders. These green balls are then fed to the induration furnaces (Straight Grate or Grate Kiln) with the help of a moving shaft in which they are heated up to 2300 – 2500 °F. (2) Taconite ore has significant quantities of mercury deposited on it. Due to extensive research in this area, it was only recently recognized that mercury present in taconite concentrate is released during induration to process gases. Also, the majority of this mercury is not captured by the plant's wet scrubbers, but released to the atmosphere. (2)

Previous studies related to mercury release suggest that taconite processing in Minnesota releases approximately 350 to 400 kg (750 – 900 lbs) of mercury to the atmosphere each year. (3) Even though this amount is small compared to overall global emission rates, it is Minnesota's second largest industrial source of mercury to the atmosphere. Minnesota's existing taconite processing plants were built during the 1950's to 1970's well before mercury was recognized as a global pollutant. (1) Hence, The Environmental Protection Agency (EPA), the Minnesota Department of Natural Resources, and the taconite industry are examining methods to control the mercury emission from taconite plants. There are a number of methods to remove this mercury from a flue gas stream. Among the most common methods to control mercury emissions is to inject halogens into the taconite processing system to increase oxidation of mercury in the induration furnace to promote the capture of mercury in the scrubbers. Short term tests were conducted at different taconite facilities by the Minnesota Department of Natural Resources (DNR) to identify potential means to reduce mercury oxidation. These tests included addition of halogen additives such as chlorides and bromides to the green ball feed. (1)

NaCl was added to the straight grate furnace at the rate of 30 to 60 lbs per hour. NaCl addition decreased total mercury (Hg (T)) emission in stack-gases by 5 to 9%. Reductions of 6% to 13% were observed with addition of NaCl and salt solutions directly into the pre-heat zone of straight grate furnace. Reductions of 18% - 32% of Hg (T) emission was observed in grate-kiln facility when NaCl addition rates were kept similar to that of the straight grate facility. Compared to chloride salts, bromide salts proved to be more effective with a reduction of 62-64% across the scrubber when injected into

preheat zone of a straight grate furnace resulting in increase Hg oxidation. The maximum reduction (80% capture) was observed with proprietary U.S. Environmental Protection Agency (EPA) oxidant when it was added to scrubber solution. All the above mentioned methods showed an increase in average and dissolved mercury in scrubber waters. Each of these methods provides some level of mercury capture, but not at a high level (>95%).(1)

Even though halogen based additives showed promise in reducing mercury emissions, they also pose a problem to the taconite facilities. There is a possibility of increased corrosion in the system components due to the additives and an increase in particulate matter emissions due to additional fine particulate formation (4). However increased particulate emission would not be a problem with efficient scrubber system in taconite facilities. Hence, in this project, our strategy was to minimize the amount of bromine required for mercury oxidation and in turn, try to reduce the corrosion problem. An alternative oxidizing agent that is not corrosive is used in this project. Also, we have investigated the effectiveness of a special additive in achieving oxidation of the mercury using a two phased approach summarized as follows.

1. Preliminary Testing (Phase I)

In Phase I, research focuses on preliminary laboratory scale work performed to determine if the addition of a halogen containing carbon based material (ESORB HG-11) mixed with the green balls consisting of predominantly magnetite (Fe_3O_4) and other components (limestone flux, organic or bentonite binder and mineral contaminant) has a potential of oxidizing mercury significantly when included in the green ball formation process.

The work in phase I investigated:

- Examine methods to incorporate additive into the green balls
- Set up test equipment to vaporize mercury from green balls and measure mercury speciation
- Optimal additive to green ball ratio
- Additive and green ball combination method– through mixing or surface addition
- Effectiveness of halogen enhanced carbon against plain carbon
- Surface chemistry of green balls during testing

Green ball samples used during this testing were obtained in January, 2012 from the Utac plant, and October, 2011 and February, 2012 from the Minntac plant. The green balls were tested over a period of 4 to 5 months, during which the test equipment was optimized continuously.

2. Analysis of Mercury Oxidation Potential of ESORB-HG-11 (Phase II)

This phase of the work focused on laboratory scale testing performed to establish the extent of oxidation achievable when ESORB-HG-11 was included in the formulation of green balls obtained from all five taconite facilities. ESORB-HG-11 loadings of 0.1 weight percent (wt %) and 0.5 weight percent (wt %) were used for the duration of the test, based on the optimum loading established during the phase 1 testing.

The main goals of these tests were to:

- Determine the effects of the addition of ESORB –HG-11 on green ball physical properties.
- Establish potential oxidation levels achievable by including ESORB-HG-11 in green ball formulations.

- Perform chemical analyses on test products to better understand the mechanism of mercury oxidation.

Green balls used for the testing were prepared by the Coleraine Minerals Research Laboratory (CMRL). Preparation was done according to a batch balling procedure established by CMRL and based on the green ball formulations of each respective facility.

CHAPTER II

BACKGROUND

2.1 Taconite Industry Mining and Processing

Taconite is an iron ore concentrate that contains 25 to 30 percent iron minerals and is inter- layered with quartz, silica or carbonate. When taconite is heated in the presence of a reductant, it yields metallic iron (Fe). The forms of iron in taconite pellet includes iron oxides, mainly magnetite (Fe_3O_4 iron content 72 percent), hematite (Fe_2O_3 iron content 70 percent), and goethite (Fe_2O_3 H_2O iron content 63 percent).

I. Mining

In Minnesota's Mesabi Iron Range, iron containing rock is mined from open pits because most commercial ore bodies lie close to the surface of mines and their lateral dimensions are large. Mining activities at these sites involve overburden removal, drilling, blasting, and removal of waste rock and crude taconite from the open-pit (2). Mining in open pits is mostly done with large powerful shovels and trucks. Shovels at taconite mines are used to dig surface overburden as well as iron ore and waste rock. Rotary drills are used to create holes which are 16 inches in diameter and 45 to 55 feet in depth for explosives to be placed for blasting activities. Around 0.4 to 1.5 million tons of taconite ore is broken during individual blasts. Trucks then transport the crude iron ore to primary crushers. At some mining operations, trains are used to transport ore to the crushers (2, 5, 6).

II. Beneficiation

The beneficiation process increases the iron content by reducing the impurities in the ore and it also improves the physical structure of the ore. (7) The process includes milling (crushing and grinding), screening, washing, and processing that separate ore minerals from gangue (sand, rock, and other impurities surrounding the iron) by using differences in physical or chemical properties. Figure 1 illustrates the general beneficiation processes. (2, 6)

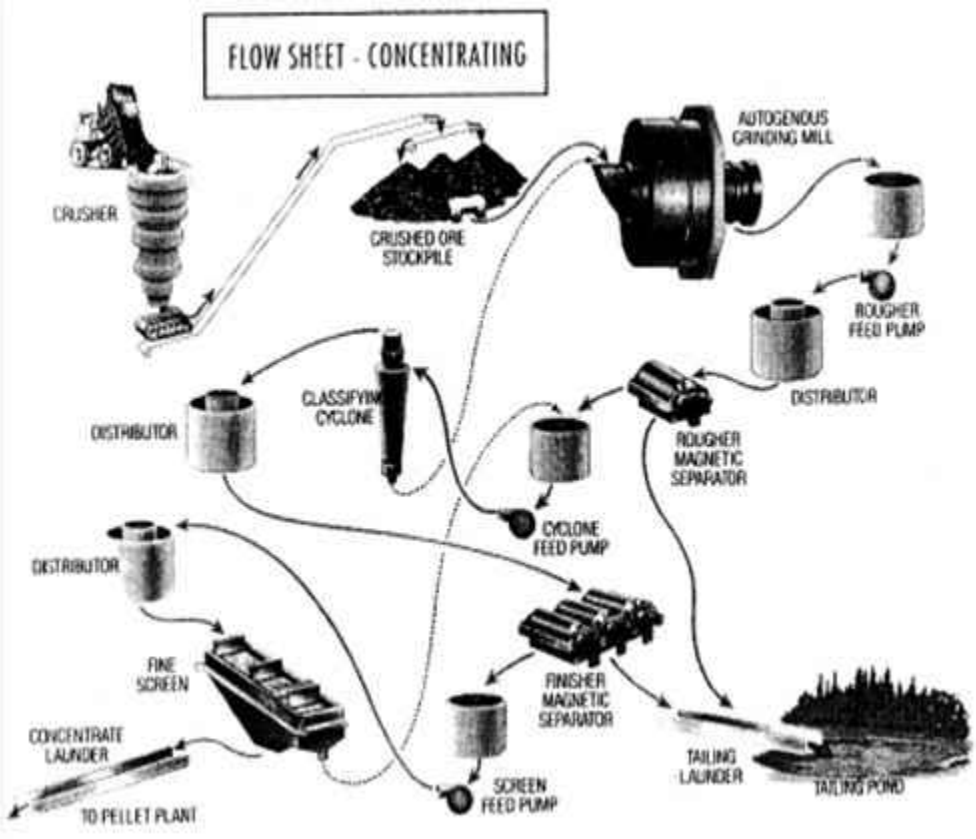

Figure 1 : Flow sheet of concentrating section for taconite plant. (2)

III. Crushing and Grinding

Crushing and grinding of the ore is an important step to produce concentrates from crude taconite ore. In the first step of crushing and grinding, taconite ore is fed to a

gyratory crusher. In the crusher, ore is crushed down to a size of approximately 6 inches. Secondary and tertiary fine-crushing stages are used to reduce the material to 3/4 inch. To remove the undersized material, there are a few intermediate vibratory screens between the crushing stages.

After crushing, the crushed ore is sent to rod mills for fine grinding. Product from rod mill will go to ball or pebble mills which are charged with heavy steel rods or balls and taconite ore with water slurry. The discharged taconite slurry from ball mill will be fed to the magnetic separator. (2)

IV. Magnetic Separation

Magnetic separation involves three stages of separation. The first stage is called cobbing, that is followed by cleaning of the ore and the final step is called as finishing. Each stage works on a finer particle size as compared to the previous ones by removing the oversized particles. Rejected oversized particles are sent to non magnetic tailings or gangue. Generally, 40 percent of the feed is rejected to non-magnetic tailings. Tailings from these two stages are sometimes re-ground or discharged to the tailing basin. (2, 8, 9)

V. Flotation

In the flotation process, excess water is removed from the iron-bearing slurry through gravity separation in a hydraulic concentrator. This is followed by a chemical flotation unit. In the flotation process, three types of additives are used to increase the iron contents namely frothers, collectors/amines, and anifoams. After this step, the iron-rich concentrates become the raw materials for producing taconite pellets in the agglomerating process.(2, 10)

VI. Agglomeration

Agglomeration is the third and the most important step in taconite pellet production since in this part the iron-rich concentrated ore is mixed with water and a binder (generally some mixture of bentonite, hydrated lime and/or organic material) and then the concentrate is rolled into green balls inside rotating cylinders. These green balls are then fed to the induration furnaces with the help of a moving shaft in which they are heated up to 2300 – 2500 °F. The induration or heating of the green balls can be done in a vertical shaft furnace on a travel grate (straight grate) or by a combination of a travel grate and a rotary kiln (grate-kiln). (2, 4) The finished product is taconite pellets. Figure 2 explains the pelletizing process in detail.

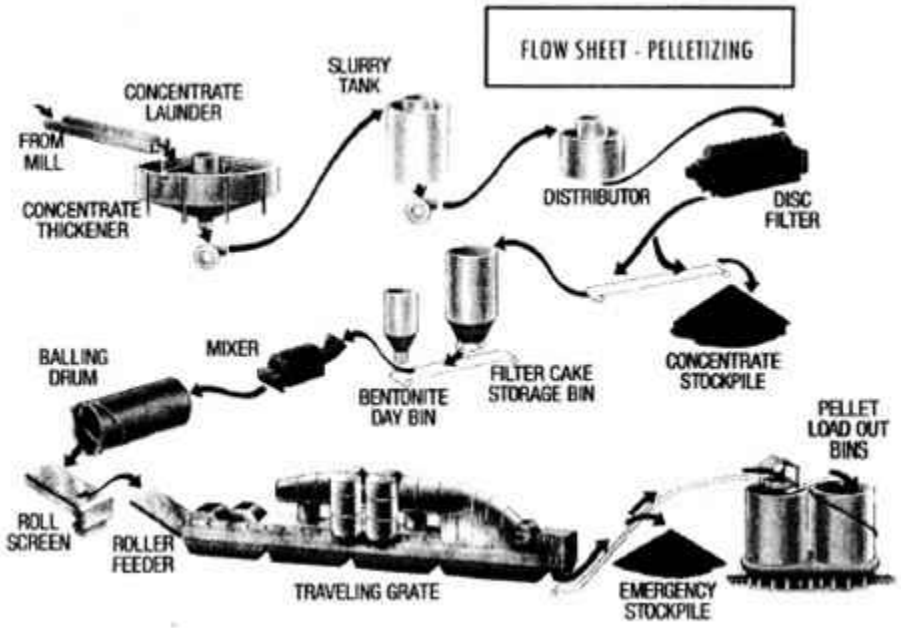

Figure 2 : Flow sheet of pelletizing section for taconite plant (2)

Travel Grate (Straight Grate). As shown in Figure 3, the green balls are fed to the updraft drying section of straight grate with the help of a moving shaft. In drying and preheat sections, the green balls are dried and preheated after which they are fed to the ignition section of the grate, where all the magnetite is oxidized to hematite. Finally, the pellets are cooled by intake air at cooling stages before they are discharged by conveyor belt to storage.

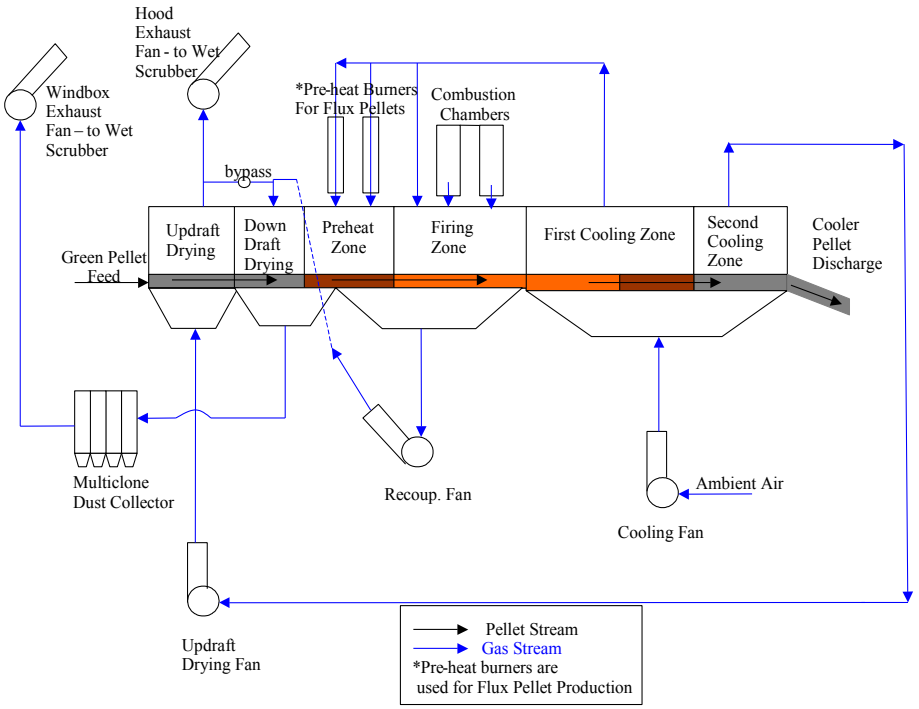

Figure 3: Straight Grate Furnace

Grate-Kiln. The grate-kiln system combines a travel grate, a rotary kiln, and an annular cooler (see Figure 3). Drying of the green pellets and partial induration occur at the grate while final induration is finished in the rotary kiln. The pellets are heated to a temperature of 2,000°F on the travel grate before being hardened in the rotary kiln furnace. Then the hardened pellets enter the cooling zone of the annular cooler.(2)

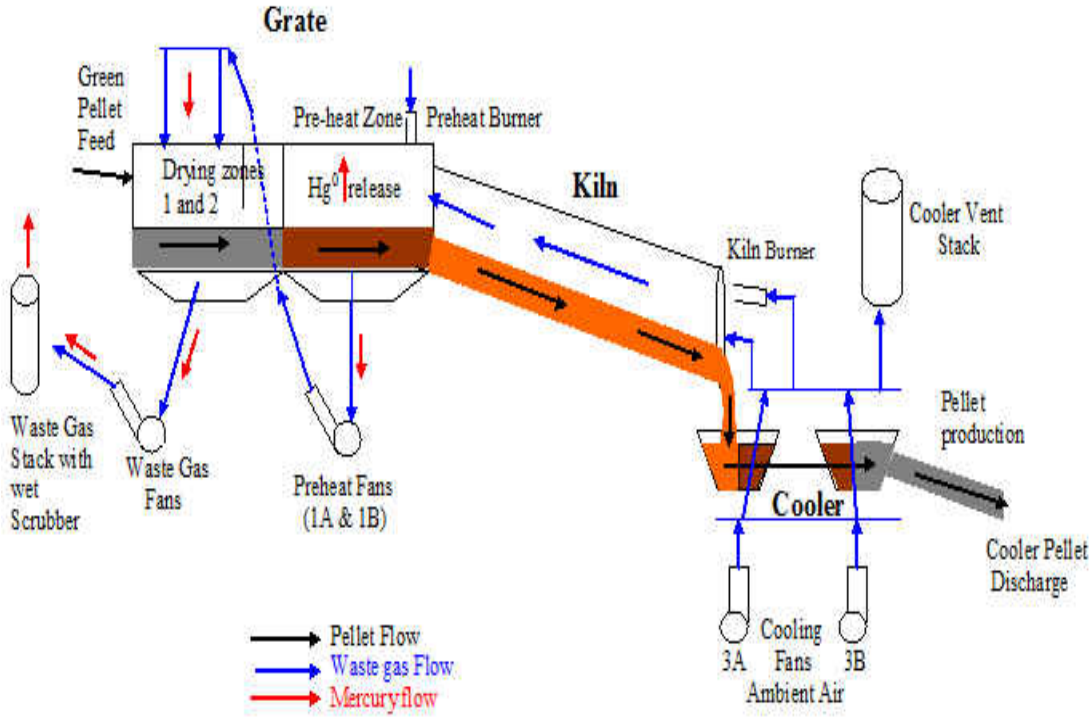

Figure 4: Grate Kiln

2.2 Mercury Release in Taconite Processing

To develop effective control measures for mercury emissions from taconite plants, it is important to understand processes involved in the release of mercury during taconite processing. Previous studies at taconite plants proved that the major source of mercury is taconite ore and not the fuel (coal) used in the induration furnaces. (1, 11, 12) Mercury release and transport during taconite processing involves a relatively complex series of reactions, whereby some of the mercury released at high temperatures in the furnace is recaptured by magnetite and/or magnetite solid-solutions with maghemite (magnetite/maghemite solid-solutions). In all plants, however, there is also mercury captured by scrubber systems that is dissolved in solution, indicating potential importance of a molecular reaction between mercury and gaseous species, most likely chlorine. To simplify the release process, we write four reactions:

$$2Fe_3O_{4(ss)} + \tfrac{1}{2}\, O_{2(g)} = 3Fe_2O_{3(ss)} \quad \text{(I)}$$

Magnetite Maghemite

$$2Fe_3O_4 + \tfrac{1}{2}\, O_{2(g)} = 3Fe_2O_3 \quad \text{(II)}$$

Magnetite Hematite

$$HgO_{(ss)} = Hg^0_{(g)} + 1/2O_{2(g)} \quad \text{(III)}$$

$$HgO_{(ss)} + 2HCl_{(g)} = HgCl_{2(g)} + H_2O_{(g)} \quad \text{(IV)}$$

Reactions (I) and (II) represent the formation of magnetite/maghemite solid-solutions and hematite, while Reactions (III) and (IV) represent release of mercury in reduced and oxidized form, respectively. In reaction (I), Magnetite is getting oxidized to give maghemite solid solution; in which maghemite interacts with mercury in flue gases,

while magnetite does not. The minerals have the same structure and form a solid solution but little is known about how mercury reacts with magnetite solid-solutions.

For reaction (II), when magnetite is converted to hematite in induration furnaces, Mercury is released. Hematite does not interact with mercury in flue gases. Reaction (III) is important because $Hg^0_{(g)}$ is insoluble in water and cannot be caught by wet scrubbers. $HgO_{(ss)}$ represents mercury associated with magnetite and magnetite/maghemite solid-solutions. Reaction (IV) determines the formation of $HgCl_{2\ (g)}$ from $HgO_{(ss)}$ in which $HgCl_{2(g)}$ is soluble in water and the Hg^{2+} base atom can adsorb to solids. Oxidized mercury is more easily captured by wet scrubbers than is $Hg^0_{(g)}$.(12)

The oxidation reaction of magnetite holds utmost important in mercury release since it determines the nature and composition of the dust in process gases. This dust will ultimately help to trap the oxidized mercury in process gases. Zygarlicke et al. (2003) and Galbreath et al. (2005) have demonstrated that magnetite and hematite does not participate in gaseous mercury reactions. During the formation of maghemite, oxygen is added to the spinel-type crystal lattice without any modification.(13, 14)

Data presented by Berndt et al. (2005) from the onsite testing demonstrate that magnetite/maghemite composition is close to the original composition of magnetite. Hence, there is a high probability that magnetite/maghemite solid solution interacts with mercury even for a low level of maghemitization. To understand this behavior, closer looks at the mineral reaction in preheat and firing zones is required. (Refer to figure 5.) When oxygen atom comes in contact with the magnetite surface, it reacts with the electrons from Fe^{+2} and forms Fe^{+3} and O^{-2} ions. This will result in extending the mineral lattice and a cation vacancy will develop.

This oxidation reaction takes place outside and progresses inwards. Hence, the full oxidation of the interior portion depends on the extent of diffusion of oxygen. The factors that impact diffusion include: oxygen availability, temperature, humidity, nucleation effects, and crystal orientation. (15). According to the literature, conversion of magnetite to magnetite/maghemite solid-solutions takes place starting from 400 to 500 ºC in a very short span of time. Hence, only the outer most surface gets converted to magnetite/maghemite solid-solutions. In the kiln, around 1200 to 1300 ºC complete conversion of magnetite to hematite takes place. Hematite is not a significant oxidant for Hg^0 in flue gases. Hence reaction (II) might limit the mercury oxidation and capture process.

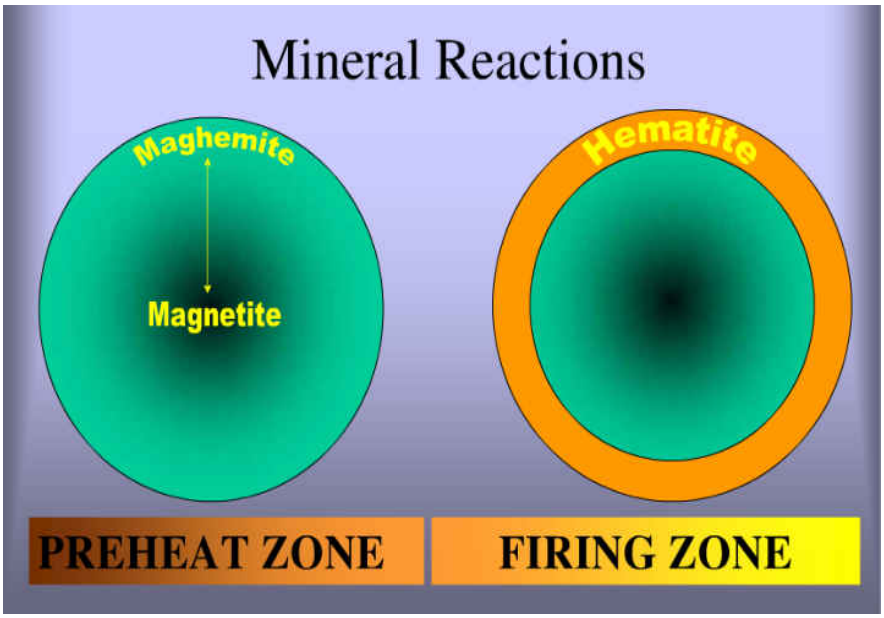

Figure 5 : Mineral Reactions in Preheat and Firing Zones

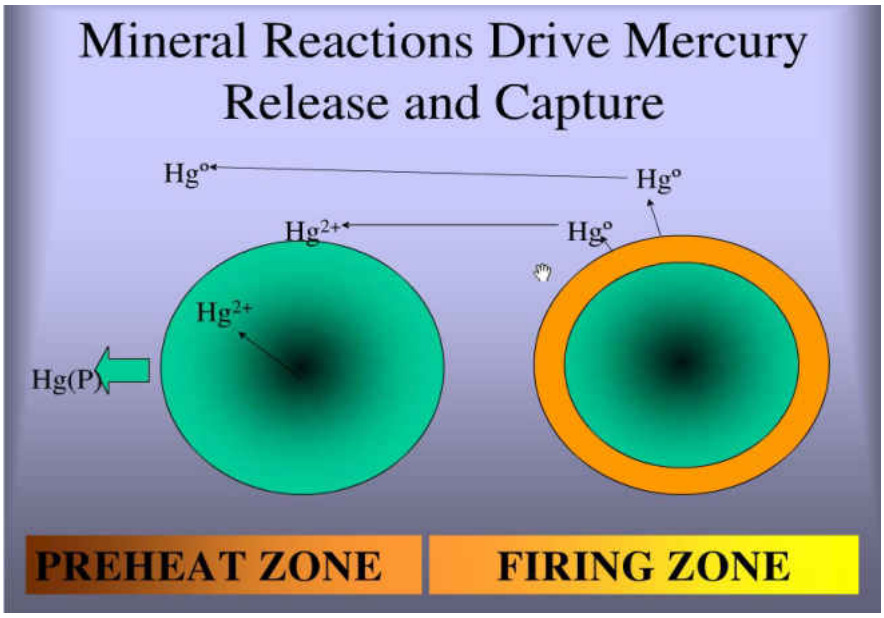

Figure 6 : Mercury Release in Preheat and Firing Zones

In reaction 3, oxidized mercury reduces to a volatile form of $Hg^0_{(g)}$. Previous studies have shown that mercury is dispersed throughout the green ball. Also, it is proved that the elemental mercury also exists on the surface of magnetite/maghemite solid-solutions in the cooler regions where the hematite formation reaction is not begun. Hence, the elemental mercury emerges from the surface of magnetite/maghemite solid-solutions to the process gases. Reaction (IV) is a hypothetical mechanism to generate $HgCl_2^0{}_{(g)}$. It is a molecule which is easily absorbed by scrubbers in taconite facilities. Relative rates of reaction (III) and reaction (IV) will determine the overall emission or capture of mercury in stack gases.(1, 11, 12) Mercury reaction pathways are influenced by the presence of HCl or HBr in process gases, which will favor reaction (IV) over (III) and thus will give good capture efficiencies. Hence, combining all the four reactions, we get:

$$Hg^{0}_{(g)} + 3Fe_2O_{3\,(ss)} + 2HCl_{(g)} = 2Fe_3O_{4(ss)} + HgCl_{2(g)} + H_2O_{(g)}\,.$$

Maghemite Magnetite

This reaction shows that if components on the left hand side of the reaction are elevated (maghemite and HCl), it will favor generation of $HgCl_{2\,(g)}$ relative to $Hg^{0}_{(g)}$ and, thus, greater capture efficiency.

Previous studies have shown that addition of halogens to taconite plants increase corrosion of the equipment and hence, this research will focus on finding a low corrosion method to achieve mercury oxidation. (1, 12, 13)

2.3 Mercury Cycle

Mercury (Hg) is a naturally occurring chemical element that is found in air, water, and soil. It exists in several forms: Mercury circulates through the environment in different chemical forms and different physical states. Mercury can exist in the environment in three forms: elemental mercury (Hg^0), oxidized mercury (mercurous [Hg_2^{2+}] or mercuric [Hg^{2+}]), and particulate-bound mercury (Hg^P). (16, 6, 17) Much of the mercury released into the atmosphere is in the form of elemental mercury. Elemental mercury can persist in the atmosphere for up to two years and travel thousands of miles, thus creating a global issue. Most of the oxidized and particulate-bound mercury will deposit in nearby water and soils, thus creating a local or regional issue. Bacteria can convert all forms of mercury to organic mercury, namely methyl mercury (CH_3Hg^+), most efficiently in the aquatic food chain. Once methyl mercury enters water, it bio-accumulates in fish and other aquatic animals. Humans are primarily exposed to mercury through the consumption of fish and other aquatic animals that come from contaminated lakes and streams.(16)

2.4 Health Effects

Mercury is a neurotoxin and long term exposure can lead to permanent damage of the brain, kidneys, and developing fetuses. (6, 18) In 2000, National Research Council declared that the EPA reference dose of 0.1 ug/kg of mercury intake is scientifically justifiable and this limit protect against the neurological effects of mercury exposure. (19) In the past, children born from women exposed to higher amounts of mercury during pregnancy have shown a variety of neurological abnormalities. Effect of methyl mercury exposure was noticed in Minamata, Japan, where 1000 deaths occurred and an additional 17,000 people were affected by methyl mercury exposure. Adverse effects on children born to these women included cerebellar symptoms, dysarthria, mental retardation, retention of primitive reflexes, hyperkinesia, hypersalivation, strabismus, and pyramidal symptoms. Another incident in Iraq where women mistakenly consumed bread made from methyl mercury treated wheat resulted in 500 deaths. Children born to these women showed delays in speech and motor development, mental retardation, reflex abnormalities, and seizures.(18, 20)

Dietary intake of methyl mercury was also associated to increased risk of coronary heart diseases and cardiovascular diseases. In Amazonian women, a significant decrease in vision, manual dexterity, and muscular strength was found with an increase in hair mercury levels. (21) A recent study found that exposure to methyl mercury near electric generating facilities is correlated with mental retardation in thousands of American babies each year. Environmentally released mercury has also been shown to increase rates of special education services and autism. (17)

2.5 Existing and Future Federal Regulations

Mercury pollution poses a problem to human health and environmental risks. Although, mercury is naturally present in the environment after industrial revolution, human activities have increased the amount of mercury cycling among land, ocean and atmosphere. Mercury is generally emitted in elemental form and gets converted to methylmercury in aquatic system and enters the food chain. Mercury accumulated in fish tissue in now the leading cause of advisories issued for fish consumption in Minnesota lakes. In 1997, US legislation has mandated emission regulations for coal-fired power plants, previously identified as the largest anthropogenic emitter of mercury to the atmosphere. Decreased emission from power plants and other sources in Minnesota led to reductions goals for mercury emission from 1990 levels by 60% in 2000 and 70% in 2005. However, the decreases in percentage of mercury emissions from coal fired power plants have resulted in an increase in the proportion for industries where control measures are either not available or difficult to implement. Taconite is one such industry whose share increased from 16% in 1995 to 20% in 2000. Important timeline for reduction of mercury emission from these taconite plants include 2007 and 2010 when mercury limits were set for Great Lakes Basin and Minnesota, respectively. (3)

In 1999, due to Lakewide Management Plans (LaMPs) reduction schedule and the requirements of Clean Water Act, Minnesota's legislature developed a plan for attaining the reduction requirements. The proceedings required the taconite industry to reduce emissions to 210 lbs by 2025 which accounts for 75 percent reduction in total. In an attempt to achieve these reduction targets, Minnesota Department of Natural Resources

(DNR) and others have funded the research for identifying the control technologies capable of achieving 75% reduction.

Referring to Title 40, Part 63, 63.8980 for taconite industry from EPA website (45):

(a) For existing ore pretreatment processes, you must emit no more than 127 pounds of mercury per million tons of ore processed.

(b) For existing carbon processes with mercury retorts, you must emit no more than 2.2 pounds of mercury per ton of concentrate processed.

(c) For existing carbon processes without mercury retorts, you must emit no more than 0.17 pounds of mercury per ton of concentrate processed.

(d) For existing non-carbon concentrate processes, you must emit no more than 0.2 pounds of mercury per ton of concentrate processed.

(e) For new ore pretreatment processes, you must emit no more than 84 pounds of mercury per million tons of ore processed.

(f) For new carbon processes with mercury retorts, you must emit no more than 0.8 pounds of mercury per ton of concentrate processed.

(g) For new carbon processes without mercury retorts, you must emit no more than 0.14 pounds of mercury per ton of concentrate processed.

(h) For new non-carbon concentrate processes, you must emit no more than 0.1 pounds of mercury per ton of concentrate processed.

(i) The standards set forth in this section apply at all times.

2.6 Control Technologies

Existing air pollution control technologies employed at taconite facilities capture only a small percentage of mercury. Most of the taconite plants have wet scrubbers which are effective in capturing oxidized mercury (Hg^{2+}) but not elemental mercury (Hg^{0}). Wet scrubbers capture 10 to 40 percent of mercury in the taconite facilities. (13, 22) A study conducted by Minnesota Department of Natural Resources (DNR) evaluated potential approaches for mercury reduction as follows:

- Injection of mercury sorbents into the gas stream.
- Use of fixed bed sorbent reactors to oxidize a higher percentage of the mercury
- Use of chemical oxidants to the gas stream, such as chloride and bromide salts or hydrogen peroxide.
- Use of halogenated oxidants in conjunction with activated carbon injection. (23)

In previous studies, they have found a significant number of possible approaches to control mercury emissions but there is no single best technology that can be broadly applied to taconite industries. Hence, a standard technology would be very difficult to implement worldwide. On the basis of current developments, the costs for mercury control ranges from $2500 to $1.1 million per kg of mercury isolated from the environment, generally making mercury control a better option. (24) Hence, policy makers and industry show growing interest in multi-pollutant removal to achieve environmental quality and reduction cost.

In the literature, a variety of potential mercury oxidation catalysts have been investigated which includes gold, palladium and iron oxides. Gold was found to be extremely useful since it absorbs mercury and chlorine and does not adsorb other species

like nitric oxide and water.(25) (26) Palladium was found to be a good oxidizer since it has oxidized >95 percent of elemental mercury in pilot scale tests. Iron oxides ($Fe_2O_3$and $Fe_3O_{4)}$ have been shown to promote mercury oxidation (27)(28). Al_2O_3 and TiO_2 have been shown to oxidize 50-60 percent of mercury in pilot scale tests. Other metal catalysts shown to promote mercury oxidation include iridium (29), MnO_2 (30), and CuO (30).

Olson et al (1998) studied the detailed chemistry mechanism of mercury oxidation and it's binding on activated carbon in the stream of flue gas. Olson has also studied the effect of carbon sorbents and their performance with different sorbent properties, process conditions, and other flue gas constituents.(31) In coal fired power plants, carbon has proved to be a good additive to control mercury emissions.(32) Although, the conditions in a coal fired power plant and a taconite plant are entirely different, mercury behavior and oxidation properties are similar.As compared to other catalysts used in oxidation reaction carbon is inexpensive and will not interfere with the taconite industry process. Hence, we conclude that carbon will be a good additive for mercury oxidation and capture.

2.7 Previous work in the Taconite Industry

The Department of Natural Resources (DNR) conducted a study to understand the mercury release in taconite processing and also summarized the result of the research. DNR's study on scrubber waters in taconite plants showed that mercury is present in two forms viz. dissolved and particulate bound. By applying the technology which captures mercury in process gases, we could reduce the dissolved mercury percent but particulate bound mercury values vary over time.(3) Berndt et al. found that there is a correlation between capture rate of mercury in wet scrubbers to the rate at which HCl and scrubber dust were generated during induration.(1, 11, 12) Thermal mercury release experiments conducted by Benner and Galbreath, spectroscopic measurements for heated taconite pellets suggest that mercury release during taconite induration is rather a complex process. (33, 13)

Also, the structural conversion of magnetite to hematite generates maghemite solid solution was found to be closely tied to the release of mercury. Mercury is released in either as Hg^0 or $HgCl_2$, depending on availability of HCl in the process gas environment. This in turn affects its capture since oxidized form gets captured easily. Literature shows that 10 – 15 percent of mercury was captured in a straight grate kiln while approximately 30 percent was captured in grate kiln. (22) Berndt et al. also found that mercury gets adsorbs onto non-magnetic surfaces easily. (1, 11, 12) Hence, we need to promote the oxidation of mercury which in turn will get captured in scrubber waters and can be discarded with mercury adsorption and magnetic separation processes. In the literature, there are two ways in promote mercury oxidation viz addition of halogens (Cl, Cl_2, Br_2, HCl) and addition of oxidizing compounds to scrubber waters. (24, 33, 34)

Other methods like ozone or activated carbon injection to process gases may also have application to the taconite industry. (16) Although, mercury oxidation and capture studies have been conducted at similar types of facilities such as waste incinerators, gold mining facilities, coal-fired power plant, the taconite industry is unique in a sense that induration includes formation of iron oxides which takes part in mercury release reactions and also plays a vital role in mercury speciation in the process gas stream.(16, 47)

2.8 Phase Analysis

During taconite processing, wet green balls consisting of predominantly magnetite and other components such as limestone flux, binder and none-ore components are conveyed into the furnace and converted to hematite by heating them up to 1200-1300°C in the presence of air. To gain better understanding of the conversion of magnetite to hematite and the oxidation reaction, it is important to perform some surface characterization analysis particularly from mineralogical point of view. Oxidation of magnetite to hematite is highly exothermic reaction. The oxidation reaction is as mentioned below. (35)

$$4\ FeO{\cdot}Fe_2O_3 + O_2 = 6\ Fe_2O_3 \qquad \Delta H = -119\ kJ/mol\ magnetite$$

Schmidt and vermaas, with the help of Differential Thermal Analysis and X-Ray Diffraction Techniques, found that magnetite particle undergo a surface oxidation forming a protective hematite layer on the surface. (36) Oxidation of magnetite particles to hematite starts by the formation of hematite needles (lamellae) at particle surface. Gruner found that when magnetite is oxidized to hematite, product develops inside the crystal structure in such a way that the basal planes of the hematite lattice lie parallel to the octahedral plane of magnetite lattice.(37) The distance between closed packed planes is greater in hematite than in magnetite (0.687 and 0.485 nm), which implies that perpendicular growth is halted due to the shortage of space in magnetite. This can also imply that needles grow faster in length as compared to their width.

According to Bentell and Mathisson, the hematite needles are formed when Fe^{2+}/Fe^{3+} ions diffuse into the magnetite phase. The rate of diffusion of these particles

can be affected due to dislocations, vacancies and impurities, i.e. the properties of the magnetite mineral and its surroundings.(38) At the surface of the magnetite particle, Fe^{2+} ions lose one electron to oxygen which is adsorbed on the surface forming Fe^{3+} and O_2^- ions. At higher temperatures, hematite tends to recrystallize and becomes porous. This allows oxygen to diffuse through hematite structure and accomplish the final oxidation.

In the literature review, it was found that many of the authors postulated the formation of γ hematite which could be the intermediate product. Like magnetite, γ hematite is also magnetic in nature. γ hematite changes into α - hematite around 400 to 500°C which is a more stable phase.(39) Zetterstorm found that the rate of oxidation is high in the initial phase which drastically decreases as the reaction proceeds.(39) Edstorm proved that the oxidation reaction takes place at the concentric front between oxidized and non-reacted material which is controlled by rate of mass transfer.(40, 41, 42, 43) Papanastassiou et al. proved that up to 420°C, a surface type of chemical reaction was the controlling step. Above 420°C, mass transfer through the gaseous boundary layer was the controlling and dominated the reaction rate. (43)

CHAPTER III

PRELIMINARY TESTING (PHASE I)

The proposed technology for oxidizing mercury employs the use of low-corrosive carbon based additive that is added to green balls to promote the oxidation of elemental mercury to oxidized forms. The additive is proprietary enhanced Powedered Activated Carbon (PAC) known as ESORB-HG-11. (47, 48) ESORB-HG-11 is a proven effective catalytic oxidation agent that acts as a fixed bed catalyst for mercury oxidation. ESORB-HG-11 contains only trace amounts of halogens thus reducing the possible occurrence of halogen driven corrosion. Phase I testing is divided into two major sections as follows.

I. Carbon addition in the flue gas

The preliminary testing was carried out in a laboratory scale reactor to optimize the equipment required for carbon addition to the flue gas.

II. Carbon addition to the green balls

In this section, research was focused on the preliminary laboratory scale work. This was done to determine if the technology has a potential of oxidizing mercury significantly when included in the green ball formation process.

The work in phase I investigated:

- Optimal additive to green ball ratio
- Additive and green ball combination method – through mixing or surface addition

- Effectiveness of halogen enhanced carbon against plain carbon
- Surface chemistry of green balls during testing.

Green ball samples used during this testing were obtained in January, 2012 for Utac, and October, 2011 and February, 2012 for Minntac. The green balls were tested over a period of 4 to 5 months, during which the test equipment was optimized continuously.

3.1 Carbon addition in the flue gas

Experimental Setup

Experimental setup for carbon addition in the process gas includes setting up a fixed bed laboratory-scale reactor with simulated flue gas introduction and continuous exhaust mercury measurement. The bed will include pellets and carbon catalyst. The fixed bed reactor is sized to be 2” diameter and the bed depth will be varied (8 to 16”) depending on the type of kiln. This setup will help us to evaluate the behavior of activated carbon in the pellet bed. A schematic of the fixed bed reactor system is shown in Figure 7. It consists of a fixed bed reactor which is 2” in diameter. Nitrogen gas was used instead of simulated flue gas. This helps us to understand activated carbon behavior under different conditions inside the reactor. We are using a PVC pipe of 2” diameter as our reactor for visibility purposes. Activated carbon is added into the carbon fluidized bed assembly through which it is carried out to the reactor with the help of gas flow through the assembly.

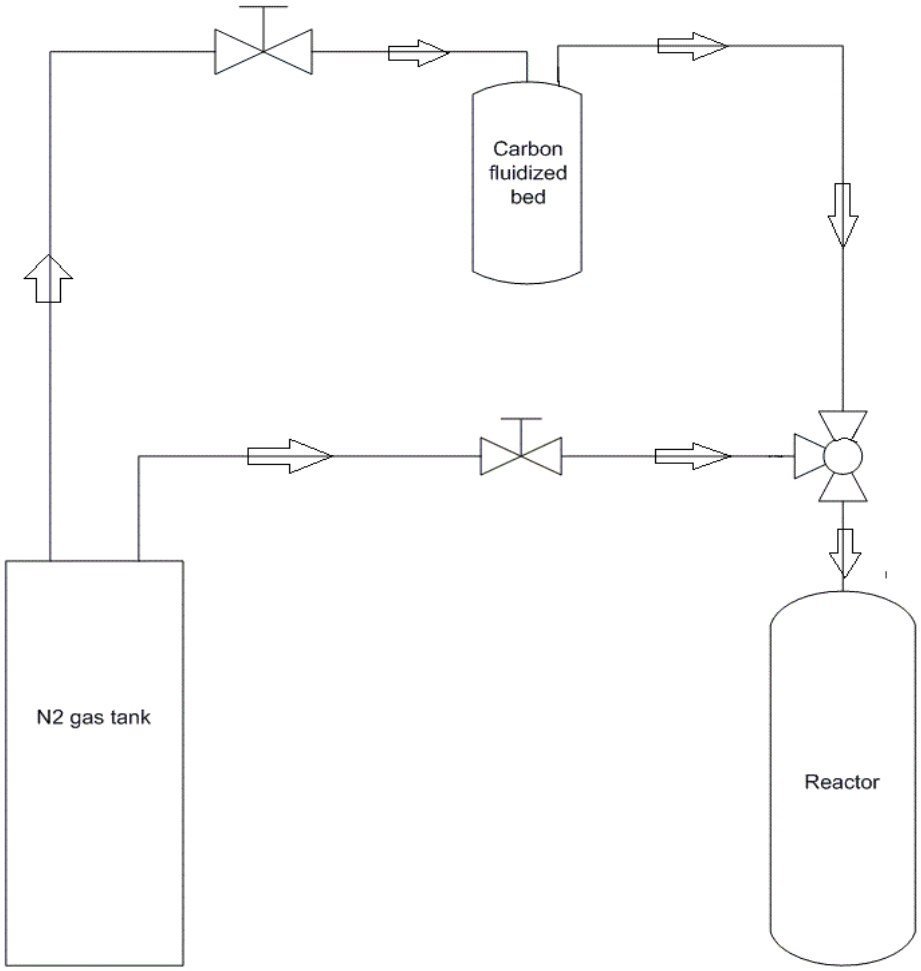

Figure 7: Experimental Setup for carbon addition into the flue gas

3.2 Experimental Observations

I. Dust Collection for dry pellets

Experimental Procedure

1. Weigh 1 kg of taconite fired pellets.
2. Weigh the filter. (Filter weight = "A")
3. Attach a filter at the reactor outlet for collecting the dust.
4. Place taconite pellets inside the reactor and attach the reactor to the assembly.
5. Check all the connections from N2 gas tank.
6. Switch on the gas flow. (Gas flow rate = 110 lpm)
7. Collect the dust particles at the outlet.
8. Let the gas flow for 15 minutes.
9. Remove the filter at the outlet and weigh the filter with dust. (B)
10. Attach a new filter at the outlet.
11. Calculate the weight of dust particles collected in first 15 minutes. (B-A)
12. Repeat the experiments for every 15 minutes till the dust accumulation on the filter becomes negligible.

Table 1 : Dust collection for dry pellets

Time	Dust weight at the outlet(g)	Cumulative Dust Collection(g)
15 minutes	0.0856	0.08562
30 minutes	0.0456	0.13122
45 minutes	0.0225	0.15372
60 minutes	0.0195	0.17322
75 minutes	0.0050	0.17822
90 minutes	0.0030	0.18122

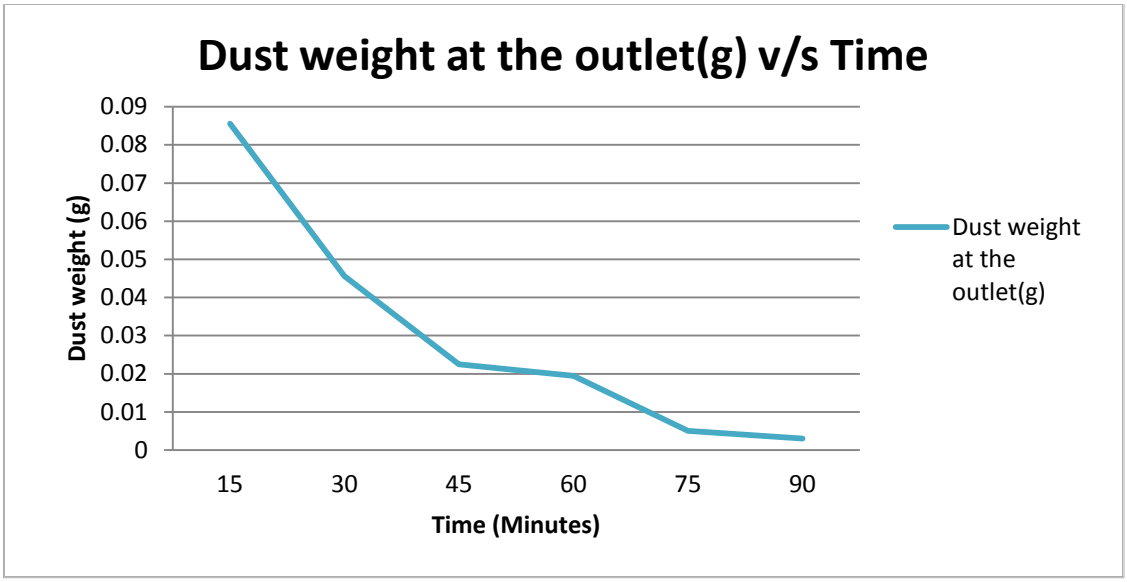

Figure 8 : Dust collection at the outlet v/s Time graph

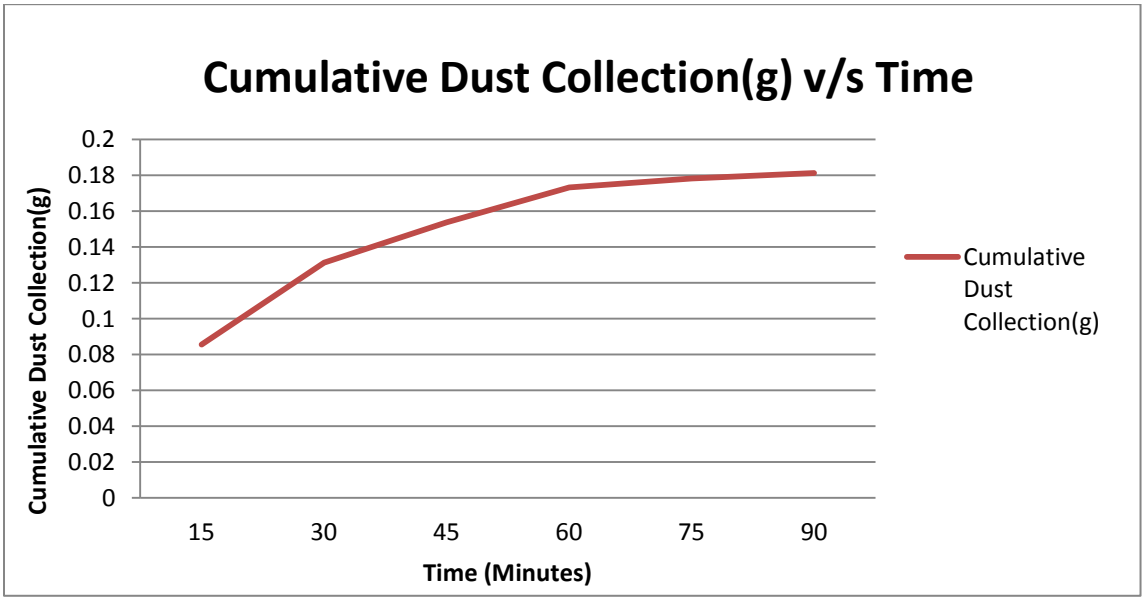

Figure 9 : Cumulative dust collection at the outlet v/s Time graph

II. Dust collection for wet pellets

Experimental Procedure

1.Weigh 1 kg of taconite fired pellets.

2.Weigh the filter.(A)

3.Add 100 ml of distilled water into a squeeze bottle.

4.Coat the pellets with water.

5.Remove the excess water from the pellets by drying them in the oven at 105 °C.

6.Place the wet pellets into the reactor.

7.Attach the filter at the outlet.

8.Switch on the gas flow. (Flow rate = 110 lpm)

9.Let the gas flow for 15 minutes.

10. Remove the filter at the outlet and weigh the filter with dust.(B)

11. Attach a new filter at the outlet.

12. Calculate the weight of dust particles collected in first 15 minutes. (B-A)

13. Repeat the experiments for every 15 minutes till the dust accumulation on the filter becomes negligible.

Table 2 : Dust collection for wet pellets

Time	Dust weight at the outlet(g)	Cumulative Dust Collection(g)
15 minutes	0.0654	0.0654
30 minutes	0.0324	0.0978
45 minutes	0.0224	0.1202
60 minutes	0.0089	0.1291
75 minutes	0.0050	0.1341
90 minutes	0.0020	0.1361

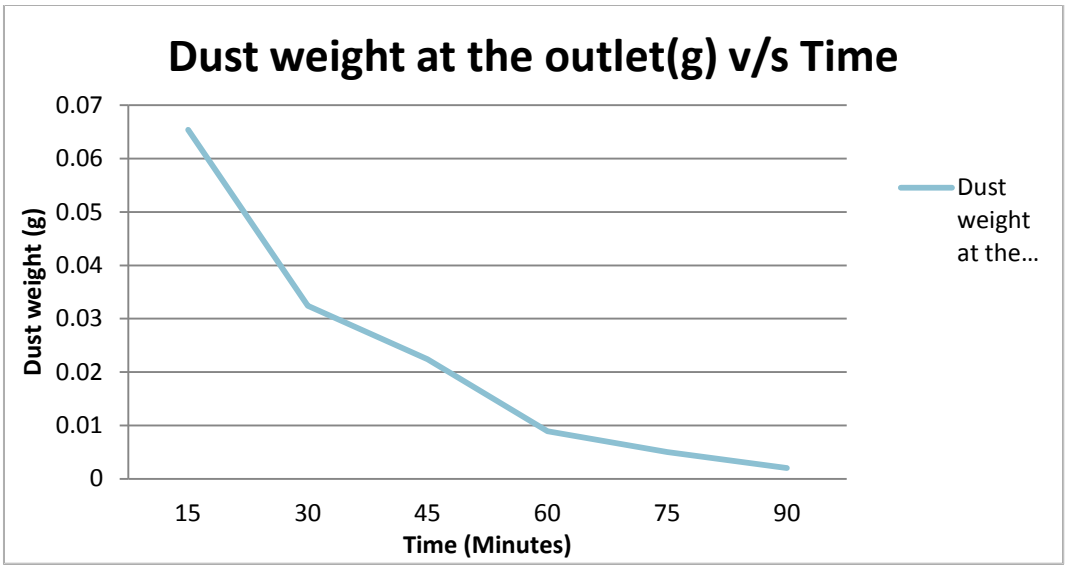

Figure 10 : Dust collection at the outlet v/s Time graph

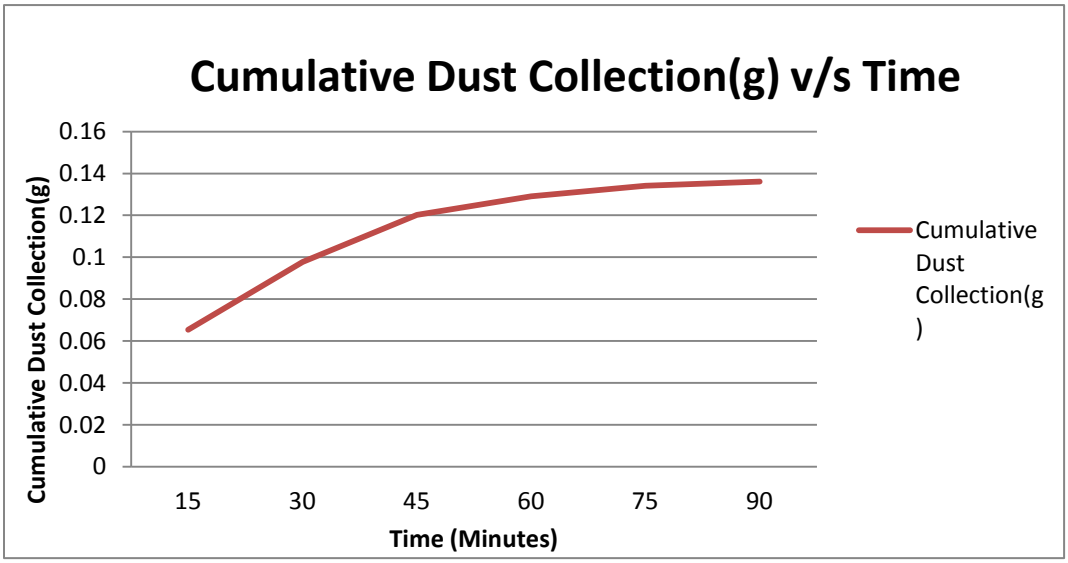

Figure 11 : Dust collection at the outlet v/s Time graph

III. Experiments with dry pellets

Experimental Procedure

1. Weigh 1 kg of taconite fired pellets.
2. Weigh 1 gram of activated carbon.
3. Weigh the filter. (Filter weight = "A")
4. Attach a filter at the reactor outlet for collecting the activated carbon.
5. Place taconite pellets inside the reactor and attach the reactor to the assembly.
6. Check all the connections from N2 gas tank.
7. Switch on the gas flow for 5 minutes. (Gas flow rate = 110 lpm)
8. Collect the dust particles at the outlet.
9. Add activated carbon.
10. Slowly increase the flow rate through activated carbon bed so as to obtain fluidized bed of carbon.
11. Let the gas flow for 20 minutes.
12. Weigh the outlet carbon on the filter.(Filter weight after = "B")
13. Obtain the percentage recovery of activated carbon. ((B-A)/1*100)

Table 3 : Percentage recovery of carbon with dry pellets

Experimental Run	% Recovery
Run 1	60
Run 2	61
Run 3	82
Run 4	85
Run 5	86
Average	75

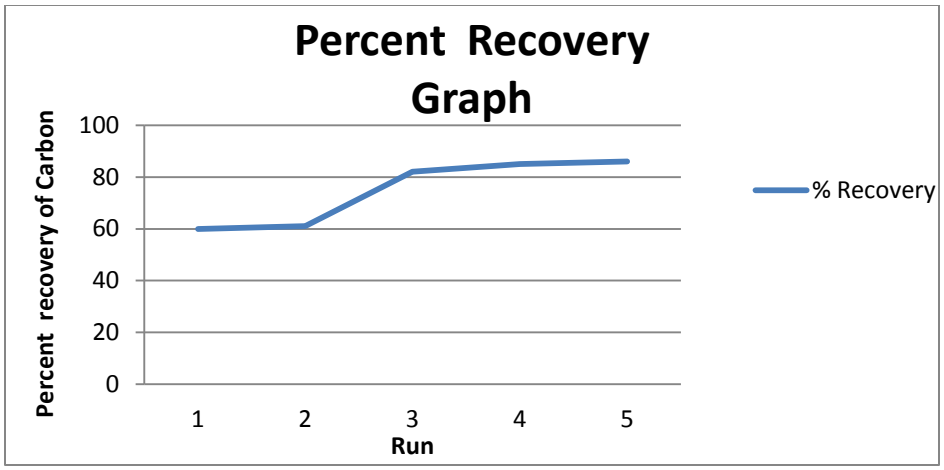

Figure 12 : Percent recovery of activated carbon for each run with dry pellets

IV. Experiments without pellets

Experimental Procedure

1. Weigh 1 gram of activated carbon.
2. Weigh the filter. (Filter weight = “A”)
3. Attach filter at the reactor outlet for collecting the activated carbon.
4. Attach the reactor to the holder.
5. Check all the connections.
6. Switch on the gas flow for 5 minutes. (Gas flow rate = 110 lpm)
7. Collect the dust particles at the outlet.
8. Add activated carbon.
9. Slowly increase the flow rate through activated carbon bed so as to obtain fluidized bed of carbon.
10. Let the gas flow for 20 minutes.
11. Weigh the outlet carbon on the filter.(Filter weight after = “B”)
12. Obtain the percentage recovery of activated carbon. ((B-A)/1*100)

Table 4 : Percentage recovery of carbon without pellets

Experimental Run	% Recovery
Run 1	82
Run 2	78
Run 3	70
Run 4	78
Run 5	94
Average	81

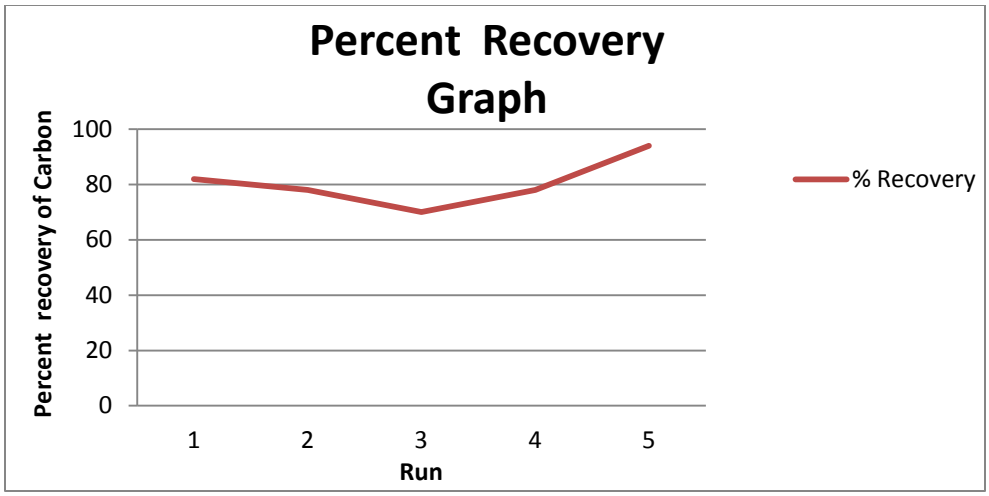

Figure 13 : Percent recovery of activated carbon for each run without pellets

V. Experiments with wet pellets

Experimental Procedure

1.Weigh 1 kg of taconite fired pellets.

2.Weigh the beaker. (Bw)

3.Add dry pellets to this beaker.

4.Measure 100 ml of distilled water

5.Add this distilled water to pellets.

6.Weigh the beaker containing pellets and distilled water.(Pw)

7.Keep the beaker into oven to evaporate excess water. Maintain oven temperature around 105 C.

8.After every 15 minutes, weigh the pellets.

9.Continue evaporating the water until weight of wet pellets comes to 1.1 kg.

10. Weigh 1 gram of activated carbon.

11. Weigh the filter. (Filter weight = “A”)

12. Attach a filter at the reactor outlet for collecting the activated carbon.

13. Place taconite pellets inside the reactor and attach the reactor to the assembly.

14. Check all the connections from N2 tank.

15. Switch on the gas flow. Let the gas flow for 5 minutes. (Gas flow rate = 110 lpm)

16. Collect the dust particles at the outlet.

17. Add activated carbon.

18. Slowly increase the flow rate through activated carbon bed so as to obtain fluidized bed of carbon.

19. Let the gas flow for 20 minutes.

20. Weigh the outlet carbon on the filter.(Filter weight after = “B”)

21. Calculate the percentage recovery of activated carbon. ((B-A)/1*100)

Table 5 : Percentage recovery of carbon for experiments with wet pellets

Experimental Run	% Recovery
Run 1	7
Run 2	11
Run 3	13
Average	10

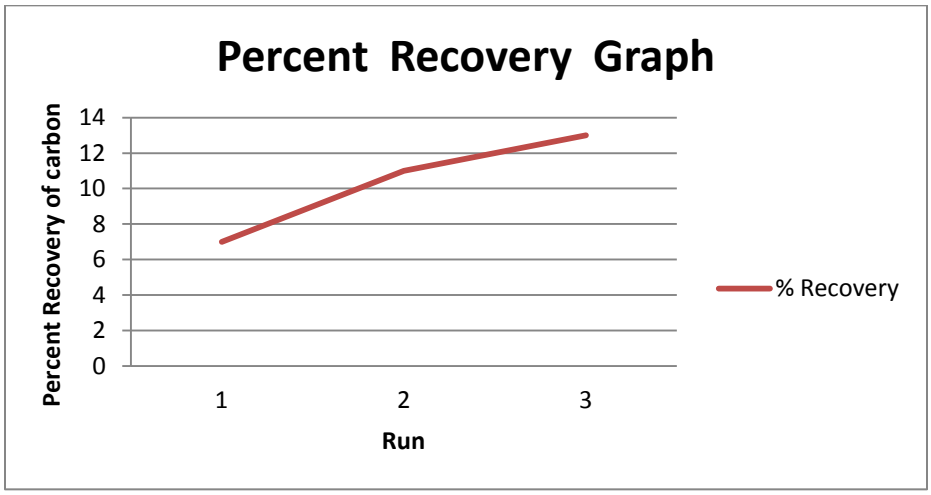

Figure 14 : Percent recovery of activated carbon for each run with wet pellets

VI. Experiments for different carbon sizes

Experimental Procedure

1.Weigh 1 kg of taconite fired pellets.

2.Weigh 1 gram of activated carbon.

3.Weigh the filter. (Filter weight = “A”)

4.Attach filter at the reactor outlet for collecting the activated carbon.

5.Place taconite pellets inside the reactor and attach the reactor to the assembly.

6.Check all the connections from N2 tank.

7.Switch on the gas flow. Let it flow for 5 minutes. (Gas flow rate = 110 lpm)

8.Collect the dust particles at the outlet.

9.Add activated carbon.

10. Slowly increase the flow rate through activated carbon bed so as to obtain fluidized bed of carbon.

11. Let the gas flow for 20 minutes.

12. Weigh the outlet carbon on the filter.(Filter weight = “B”)

13. Obtain the percentage recovery of activated carbon. ((B-A)/1*100)

14. Repeat the experiment for other sizes of carbon.

Table 6 : Percentage recovery of carbon for experiments with different carbon sizes

Carbon Type	Size	% Recovery
C1	carbon "C" > 1.2 mm	10
C2	1.2 mm >"C"> 0.853 mm	75
C3	0.853mm > "C" > 0.599 mm	69
C4	0.599mm> "C" > 0.251 mm	69
C5	0.251mm> "C" > 0.178 mm	81

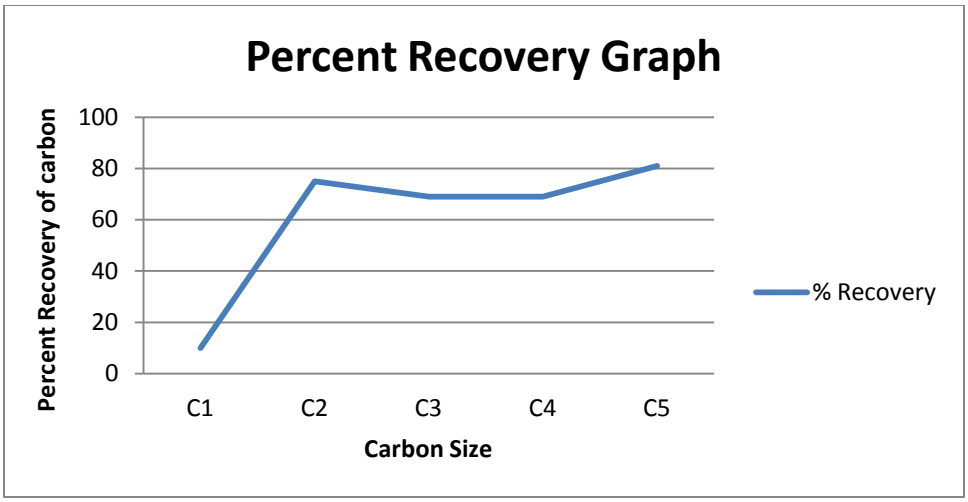

Figure 15 : Percent recovery of carbon for different sizes of carbon

VII. Experiments with low flow rate (20 lpm)

Experimental Procedure

1.Weigh 1 kg of taconite fired pellets.

2.Weigh 1 gram of activated carbon.

3.Weigh the filter. (Filter weight = “A”)

4.Attach a filter at the reactor outlet for collecting the activated carbon.

5.Place taconite pellets inside the reactor and attach the reactor to the assembly.

6.Check all the connections from N2 tank.

7.Switch on the gas flow for 5 minutes. (Gas flow rate = 20 Lpm)

8.Collect the dust particles at the outlet.

9.Add activated carbon.

10. Slowly increase the flow rate through activated carbon bed so as to obtain fluidized bed of carbon.

11. Let the gas flow for 20 minutes.

12. Weigh the outlet carbon on the filter.(Filter weight = “B”)

13. Obtain the percentage recovery of activated carbon. ((B-A)/1*100)

Table 7 : Percentage recovery of carbon for experiments with low flow rate

Experimental Run	% Recovery
Run 1	20
Run 2	14
Average	17

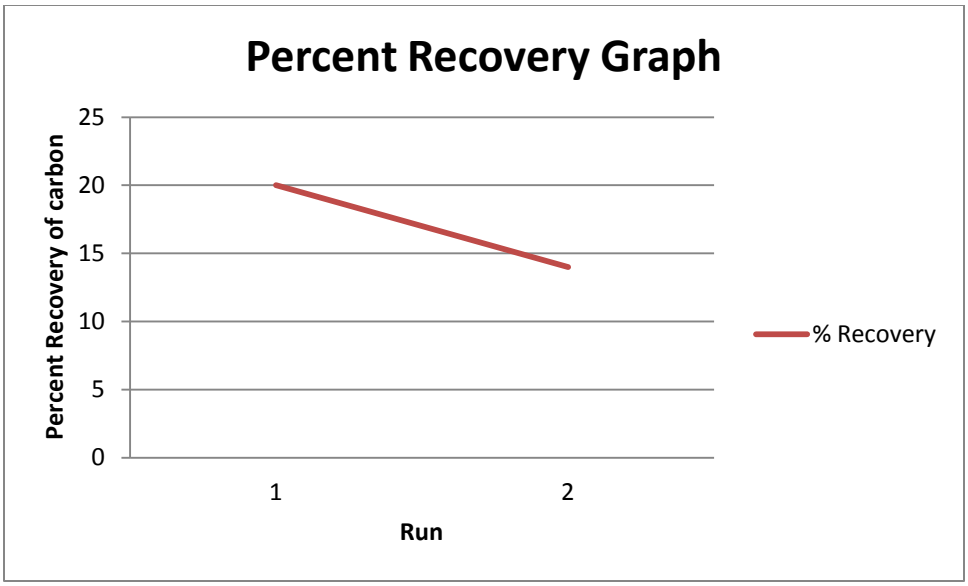

Figure 16 : Percent recovery of carbon for dry pellets with low flow rate

VIII. Experiments for Activated Carbon coated pellets

Experimental Procedure

1.Weigh 1 gram of activated carbon.

2.Add 100 ml of distilled water and activated carbon into a squeeze bottle.

3.Weigh 1 kg of taconite fired pellets.

4.Coat pellets with activated carbon slurry.

5.Keep the pellets into oven to evaporate excess water. Maintain the oven temperature at 105 C.

6.Weigh the filter. (Filter weight = “A”)

7.Attach a filter at the reactor outlet for collecting the activated carbon.

8.Place taconite pellets inside the reactor and attach the reactor to the assembly.

9.Check all the connections from N2 tank.

10. Switch on the gas flow. (Gas flow rate = 110 lpm)

11. Let the gas flow for 20 minutes.

12. Weigh the outlet carbon on the filter.(Filter weight = “B”)

13.Obtain the percentage recovery of activated carbon. ((B-A)/1*100)

Table 8 : Percentage recovery of carbon for experiments with activated carbon coated pellets

Experimental Run	% Recovery
Run 1	63
Run 2	56
Run 3	58
Average	59

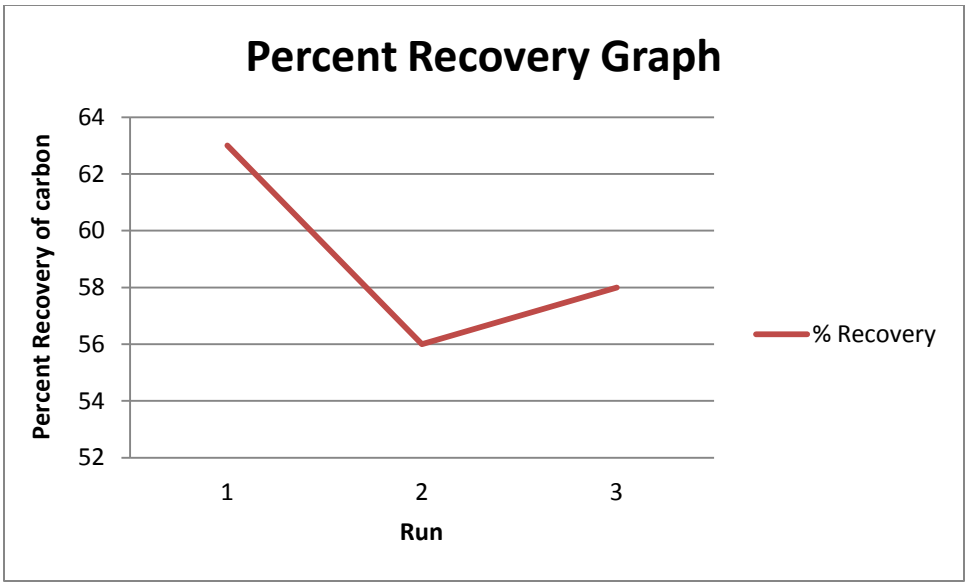

Figure 17 : Percent recovery of carbon for activated carbon coated pellets

3.3 Analysis of Data - Carbon addition to flue gas

Observed values for percent recovery of carbon leads us to following conclusions:

1. Dust collection values for dry pellets are gradually decreasing with time.
2. Percentage recovery of carbon decreases as the size of the carbon particle increases.
3. Carbon sticks to wet pellets and hence percentage recovery for wet pellets is very low.
4. With lower flow rates (20 lpm), percentage recovery of carbon has a very low value.
5. We are losing 10-20% carbon during its passage from fluidized bed to outlet. This could be due several reasons. Since the pipe develops static charge, carbon sticks to the walls of the reactor. Similarly, it could get clogged in the valves or pipelines.

Hence, after careful review of the results obtained from the experiments for carbon addition to the flue gas, it was determined that in the given circumstances it is important to evaluate the possibility of addition of carbon to the green ball feed.

3.4 Carbon Addition to Green Ball feed

Previous studies conducted by Minnesota Department of Natural Resources (DNR) suggested that ore is the main source of mercury and mercury is released during taconite processing in the agglomeration step. Most of the mercury release takes place between 200 ^{o}C up to 600 ^{o}C. (35) This temperature is observed in the pre-heat section of the induration kilns. Hence, in order to oxidize the elemental mercury and in turn to capture it in the scrubbers, it is important to understand and evaluate the possibility of adding oxidizing agent in to the green ball feed. This approach explores the possibility of oxidizing the mercury in the preheat section as soon as or even before the release of mercury to the flue gases.

In order to evaluate this possibility, green balls were obtained from two plant sites namely United Taconite (Utac) and Minnesota Taconite (Minntac). Green ball samples used from Utac were obtained in January, 2012 and those from Minnesota Taconite were obtained in two batches October, 2011 and February, 2012. Green balls were tested over a period of 4 to 5 months in which the test equipment was continuously optimized. Results presented under this section are obtained before and after the equipment was optimized.

The proposed technology involves use of carbon based additive known as ESORB-HG-11 which will be added to the green ball feed prior to induration to increase mercury oxidation and to potentially reduce mercury emissions. This is a proprietary enhanced Powdered Activated Carbon (PAC) which contains trace amounts of halogens and hence it is a low corrosion method to enhance mercury oxidation. In this section,

research mainly focuses on the preliminary work done in the laboratory to determine if this technology has a potential to oxidize the mercury significantly when included in the green ball formulation.

The research work done under this section mainly investigated:

- Examine methods to incorporate additive into the green balls
- Set up test equipment to vaporize mercury from green balls and measure mercury speciation
- Optimal additive to green ball ratio
- Additive and green ball combination method– through mixing or surface addition
- Effectiveness of halogen enhanced carbon against plain carbon
- Surface chemistry of green balls during testing

3.4.1 Experimental Setup

The bench scale apparatus is illustrated in Figures 18 and 19. It consists of a tube furnace, reaction vessel, a gas metering system, gas conditioning unit, mercury pretreatment system, and mercury analyzer.

The procedure for testing involves placing approximately 100 grams of green balls into the reaction vessel and heating the green balls up to 700 °C. During the heating process, air passes through the vessel at 7.5 lpm (during initial testing, flowrate = 5 lpm), and flows through heated PFA tubing to a pretreatment system and then directly to the analyzer for an elemental mercury determination.

Before each run, the Horiba mercury analyzer undergoes a calibration or calibration verification. While this goes on, the PFA tubing is disconnected from the impinger train and preheated to 170^0C to prevent condensation or reduction of oxidized mercury in the lines with the help of heating tape. The furnace reactor is also heated to 700 ^{0}C and then allowed to cool to 250^0C to drive out residual mercury in the furnace and simulate average temperatures experienced by green balls during induction at a Taconite facility. During testing, once the green balls are added to the reactor the temperature of the reactor is increased to 700 ^{0}C with a ramp rate of 20 ^{0}C per minute based on calculations from field testing conditions. Note that due to heat losses in the bench scale assembly, the actual ramp rate decreases as the temperature of the reactor bed increases, resulting in a slower overall ramp rate when compared with the field conditions.

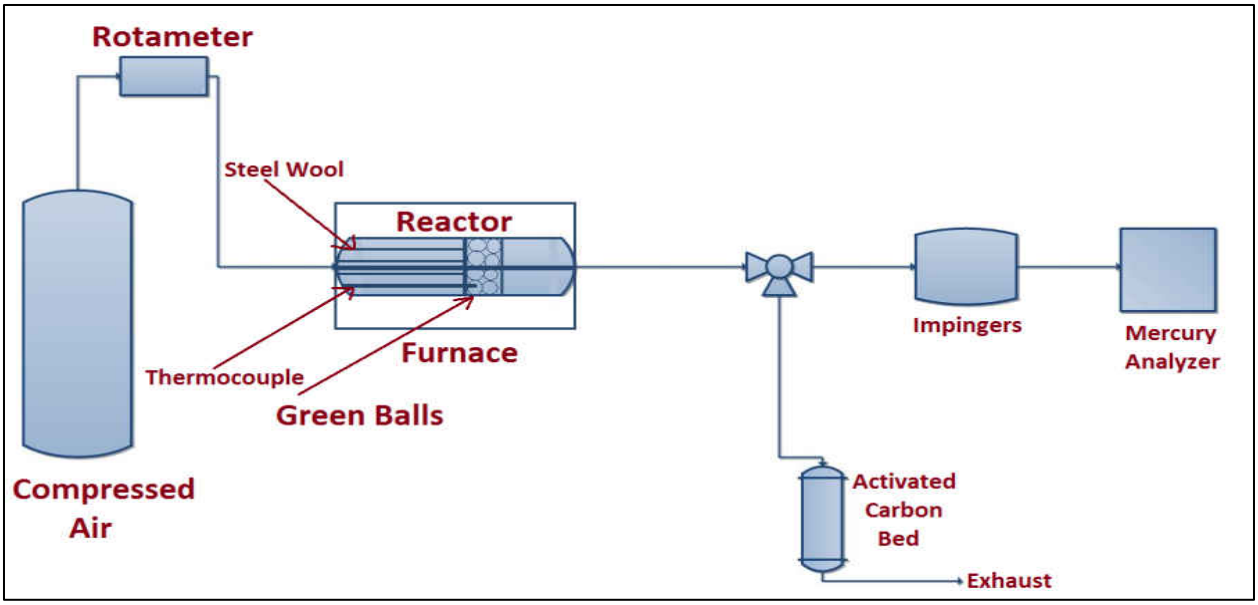

Figure 18 : Schematic of testing equipment – Phase I

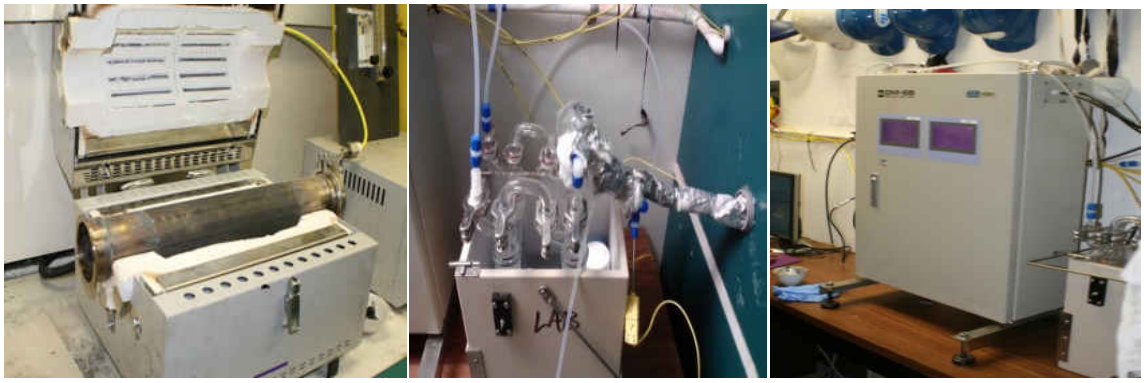

Figure 19 : Pictures showing reactor vessel, Wet-chemistry impinger train and Horiba DM-6B mercury analyzer.

As shown in Figure 19 and 20, a wet pre-treatment unit was used to condition the flue gas before it enters the Horiba mercury analyzer. It consisted of two parallel sets of impingers (4 impingers in total). One set is used to determine the elemental mercury concentration (Hg^0) while the other set is used to determine the total mercury concentration (Hg^T) in the sample flue gas. The set-up was designed based on a modified wet chemistry PS Analytical pre-treatment conversion system and ASTM D6784-02 (also known as the Ontario Hydro [OH] method).

The first impinger train is for conditioning the elemental mercury stream that consists of two impingers in series: The first impinger contains a 150 ml of 10 weight percent potassium chloride (KCl) and 0.8 weight percent of Sodium Thiosulfate ($Na_2S_2O_3$) solution that captures the oxidized mercury in order to obtain only elemental mercury concentration, while the second impinger sits in an ice bath and traps all moisture present in the gas sample before analysis by the mercury analyzer.

The second impinger train is for conditioning the total mercury stream. Here, the first impinger contains 150 ml of 0.8 weight percent stannous chloride ($SnCl_2$) solution and 20 weight percent of Sodium Hydroxide (NaOH). The $SnCl_2$ reduces the oxidized mercury in order to obtain a total mercury measurement of the flue gas. The second impinger also sits in an ice bath and traps all moisture present in the gas sample before analysis. The trains were modified from a continuous flow to a batch system. The Horiba mercury analyzer simultaneously and continuously measures both total and elemental mercury. The difference between the total and elemental is assumed to be oxidized mercury. Gas flow rates are measured with rotameters and were validated with mass flow controllers.

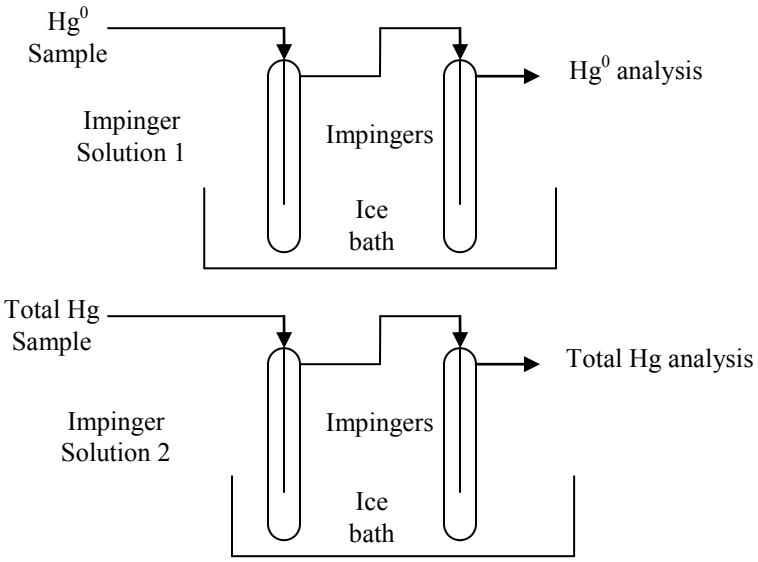

Figure 20 : Schematic diagram of impinger train – Phase I

3.4.2 Carbon Addition Method

Two methods for adding trace amounts of carbon to the green balls were used for the phase one testing:

- Mixed addition
- Surface addition

Mixed Addition Procedure

- Crush a random sample of green balls from the given sample.
- Weigh 100 grams of crushed sample.
- Weigh the mass of additive to be tested.
- Mix the additive with 100 grams of crushed green ball sample.
- Add 1 to 2 ml of water to the given mixture.
- Roll the mixture into balls with required size.

Surface Addition Method

- Crush a random sample of green balls from the given sample.
- Weigh 90 grams of crushed sample.
- Add 1 to 2 ml of DI water to the crushed sample.
- Roll the mixture into balls with a smaller size, (90 percent of average taconite size was used.)
- Weigh 10 grams of crushed sample.
- Weigh the mass of additive to be tested.
- Mix the additive with 10 grams of crushed green ball sample.

- Roll the smaller green balls in this mixture so as to get a coat of additive and green ball on the surface.

During baseline runs, the green balls were also prepared using the same procedure as for the mixed addition; however, no carbon was added to the new green balls. This ensured that any impact the production process had on the mercury release profile would be inherent to both baseline and mixed/surface tests. Figure 21 is a picture of the final green balls produced by hand. Once produced the green balls were then subjected to heating tests to determine the amount of oxidation occurring as a result of carbon addition.

Figure 21 : Picture of new green balls produced for phase one testing

3.5 Test Matrix

The test matrix was designed to achieve objectives explained in Section 3.4 of this thesis. In Phase I, green balls from two different plants (Minntac and Utac) were evaluated for mercury release and effect of additives on level of mercury oxidation was studied. We conducted tests based on the following preliminary test matrix. Slight variations in the testing may result based on intermediate findings. Continuous Mercury Monitors system was measuring elemental (Hg^0) and total mercury (Hg^T) continuously. Difference between elemental and total mercury is assumed to be oxidized mercury. From previous studies, it is proved that oxidized mercury gets captured into scrubber systems; hence the percent mercury oxidation was used as an estimate for percent mercury reduction in emissions.

Oxidation formula used to calculate the percent oxidation is as follows:

$$\% \text{ Hg Oxidation} = \frac{\{Hg^T - Hg^0\}}{Hg^T} * 100$$

Where,

Hg^T = Total mercury emission during the run

Hg^0 = Elemental Mercury emission during the run

(Hg^0 and Hg^T are measured with the help of Horiba DM-6B Cold Vapor Atomic Absorption Spectroscopy CMM.)

Table 9 : Minntac Green Ball Test Matrix

Plant	Flow Rate	Maximum Bed Temp.	Impinger Solution	Additive	Method	Additive Loading (wt%)
Minntac	7.5	700	KCl +$Na_2S_2O_3$	None	-	0
Minntac	7.5	700	KCl +$Na_2S_2O_3$	ESORB-HG-11	Mixed	0.1
Minntac	7.5	700	KCl	ESORB-HG-11	Mixed	0.1
Minntac	7.5	700	KCl +$Na_2S_2O_3$	ESORB-HG-11	Mixed	0.2
Minntac	7.5	700	KCl +$Na_2S_2O_3$	ESORB-HG-11	Mixed	0.3
Minntac	7.5	700	KCl +$Na_2S_2O_3$	ESORB-HG-11	Mixed	0.5
Minntac[1]	5	700	KCl	None	-	0
Minntac[1]	5	700	KCl	ESORB-HG-11	Mixed	0.1
Minntac[1]	5	700	KCl	ESORB-HG-11	Mixed	0.2
Minntac	5	700	KCl +$Na_2S_2O_3$	ESORB-HG-11	Mixed	0.05
Minntac	5	700	KCl +$Na_2S_2O_3$	ESORB-HG-11	Mixed	0.2
Minntac	5	700	KCl +$Na_2S_2O_3$	ESORB-HG-11	Mixed	0.3
Minntac	7.5	700	KCl	Halogenated salt	Mixed	0.01
Minntac	7.5	700	KCl +$Na_2S_2O_3$	PAC	Mixed	0.2
Minntac	5	700	KCl	ESORB-HG-11	Surface	0.2

Minntac[1] are the green balls obtained from Minntac site from October, 2011.

Table 10 : Utac Green Ball Test Matrix

Plant	Flow Rate	Maximum Bed Temperature	Impinger Solution	Additive	Method	Additive Loading (wt%)
Utac	5	700	KCl	None	-	0
Utac	5	700	KCl +$Na_2S_2O_3$	None	-	0
Utac	5	700	KCl	ESORB-HG-11	Mixed	0.1
Utac	5	700	KCl	Halogenated salt	Mixed	0.01
Utac	5	700	KCl	PAC	Mixed	0.1
Utac	5	700	KCl	ESORB-HG-11	Surface	0.1
Utac	5	700	KCl	ESORB-HG-11	Surface	0.2

3.6 Experimental Results and Discussion

Results presented in this section are broadly divided into two sections depending on the plant from which the green balls are obtained. Results presented in this section are mostly after the equipment was optimized and experiments are carried out at similar conditions for consistency.

I. Minntac Results

In Phase I, Minntac green balls testing had several objectives as follows:

- Evaluating effectiveness of different additives for mercury oxidation.
- Optimizing the additive loading amount.
- Comparing surface versus mixed addition results.
- Comparing carbon free halogen addition with ESORB-HG-11
- Comparing plain activated carbon with ESORB-HG-11

1. Effectiveness of different additives for mercury oxidation

Table 11 summarizes the results obtained from three different additives namely ESORB-HG-11, Powdered Activated Carbon (PAC) and halogenated salt with a baseline run. Baseline runs green balls are formed with the same procedure as mentioned in section 3.4.2 except that there is no additive in the mixture.

No significant oxidation was observed with PAC or Halogenated salts. In the literature, addition of halogenated salts into the grates during the field testing was proved to be effective in Hg oxidation. (1) However, during the lab scale testing of PAC addition into the green ball feed did not show any significant reduction. This can be due to several reasons such as lack of residence time of carbon in the lab scale setup as well as lack of halogens in the flue gas. This could also suggest that Hg oxidation in the full-scale facility is more significant than the levels observed in the lab scale setting. Figure 23, 24, 25 and 26 represents the mercury release profiles with different additives versus pellet bed temperature(°C).

Table 11 : Minntac Test Results with different additives

	Additive Loading	Loading Ratio	Oxidation
Additive	(wt.%)	(mg/kg)	(%)
None	0	0	7.00
PAC	0.2	2000	1.01
Halogenated Salt	0.2	2000	19.47
ESORB-HG-11	0.2	2000	67.00

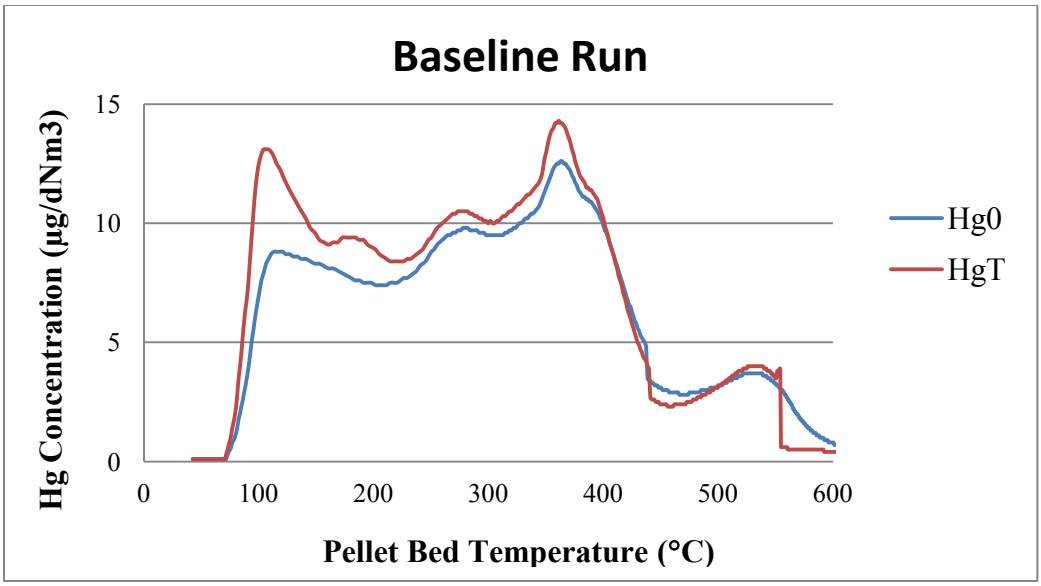

Figure 22 : Mercury release profile during heating of Minntac green balls with no additive (Baseline)

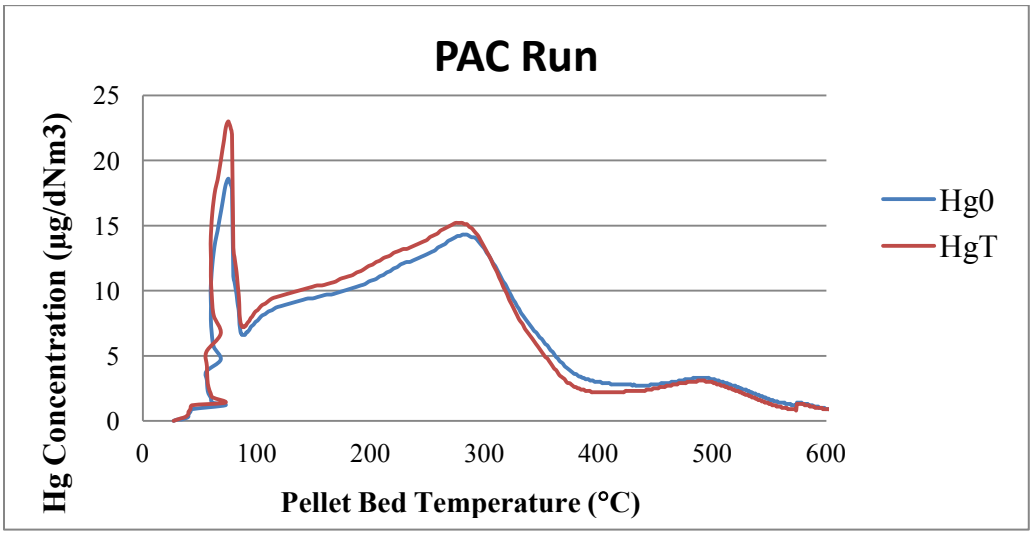

Figure 23 : Mercury release profile during heating of Minntac green balls with PAC additive

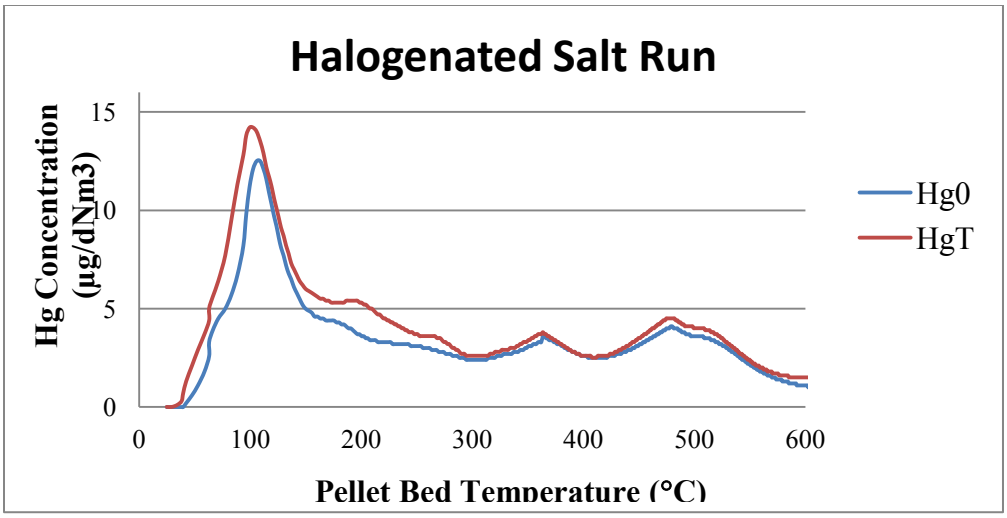

Figure 24 : Mercury release profile during heating of Minntac green balls with halogenated salts

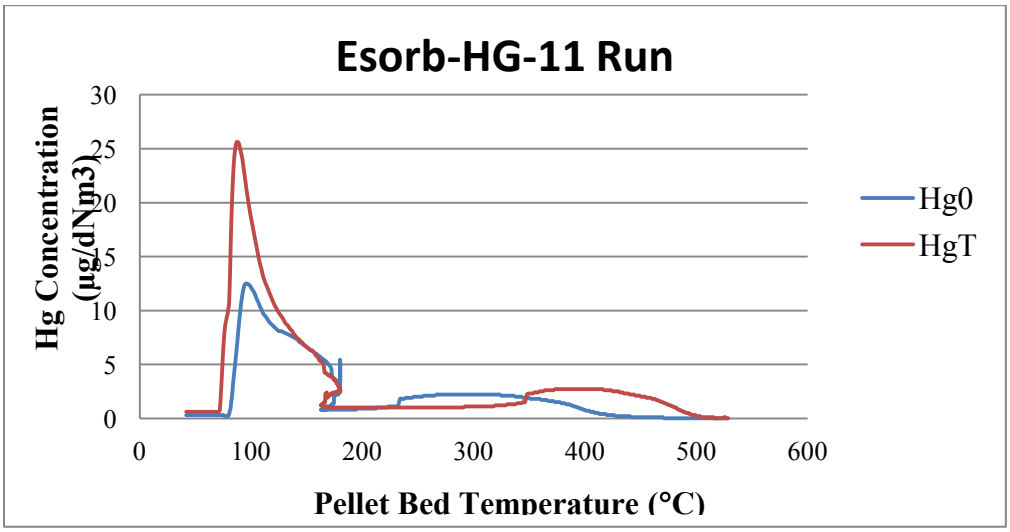

Figure 25 : Mercury release profile during heating of Minntac green balls with ESORB-HG-11

2. Additive Loading

From Section I, it is clear that ESORB-HG-11 is the most effective additive for mercury oxidation in the optimized equipment setup. Table 12 summarizes the results obtained from Minntac green ball testing with different additive loading. Mixed addition technique was used to form the green balls used in this testing. These tests used two different batches of green balls obtained in October, 2011 and February, 2012. There was a concern over "aging" of the green ball formulation and hence similar tests were performed on the green balls obtained in February, 2012. The two tests performed gave similar results; hence, data generated in February, 2012 is reported in this section. The results from October, 2011 are reported in Appendix A.

Results presented in Table 12 with the exception of 0.05% are performed with a flow rate of 7.5 lpm. Sodium Thiosulfate ($Na_2S_2O_3$) was added to the elemental impinger solution to neutralize the effect of released bromine in the flue gases and also to minimize oxidation, as well as analyzer and sampling line maintenance.

Table 12 : Results from Minntac green ball testing – Additive loading

	Additive Loading	Loading Ratio	Percent Oxidation	
Additive	(wt.%)	(mg/kg)	Runs (%)	Average
ESORB-HG-11	0	0	7 26.7	16.9
ESORB-HG-11	0.05	500	39.7 33	36.4
ESORB-HG-11	0.1	1000	54.7 35.3	45
ESORB-HG-11	0.2	2000	46.9 67	57
ESORB-HG-11	0.3	3000	50.1 46.5	48.3
ESORB-HG-11	0.5	5000	50.6	46.5

During the baseline runs, a large peak was observed between 100°C to 400°C. This leads us to a conclusion that most of the mercury release takes place between 100°C to 400°C. Second peak was observed between 500°C and 600°C which is in agreement with the previous work reported. (11, 12)

Figure 26 is a plot of mercury concentration (μg/dNm^3) versus pellet bed temperature (°C). As mentioned in section 3.4.1, the reactor is preheated before the green balls are placed, hence, the first peak observed in the Figure 26 can be due to the mercury release from the outer surface of the green ball which is directly exposed to the heat. As the heating of green ball bed progresses, green balls slowly release mercury which will probably led to the second peak. As mentioned in Table 12, first baseline run showed a very little oxidation of 7.0% and the second run gave 26.7% oxidation. Hence, average oxidation for baseline is 16.9 %.

The first ESORB-HG-11 test was with the 0.05 wt% loading, Figure 27. During this run, most of the mercury release occurred before the bed reached 400°C, with little or no oxidation observed after 200°C for the first run and 300°C for the second run. The average oxidation observed for both runs was 36.4%, and increase from the baseline average of 16.9%.

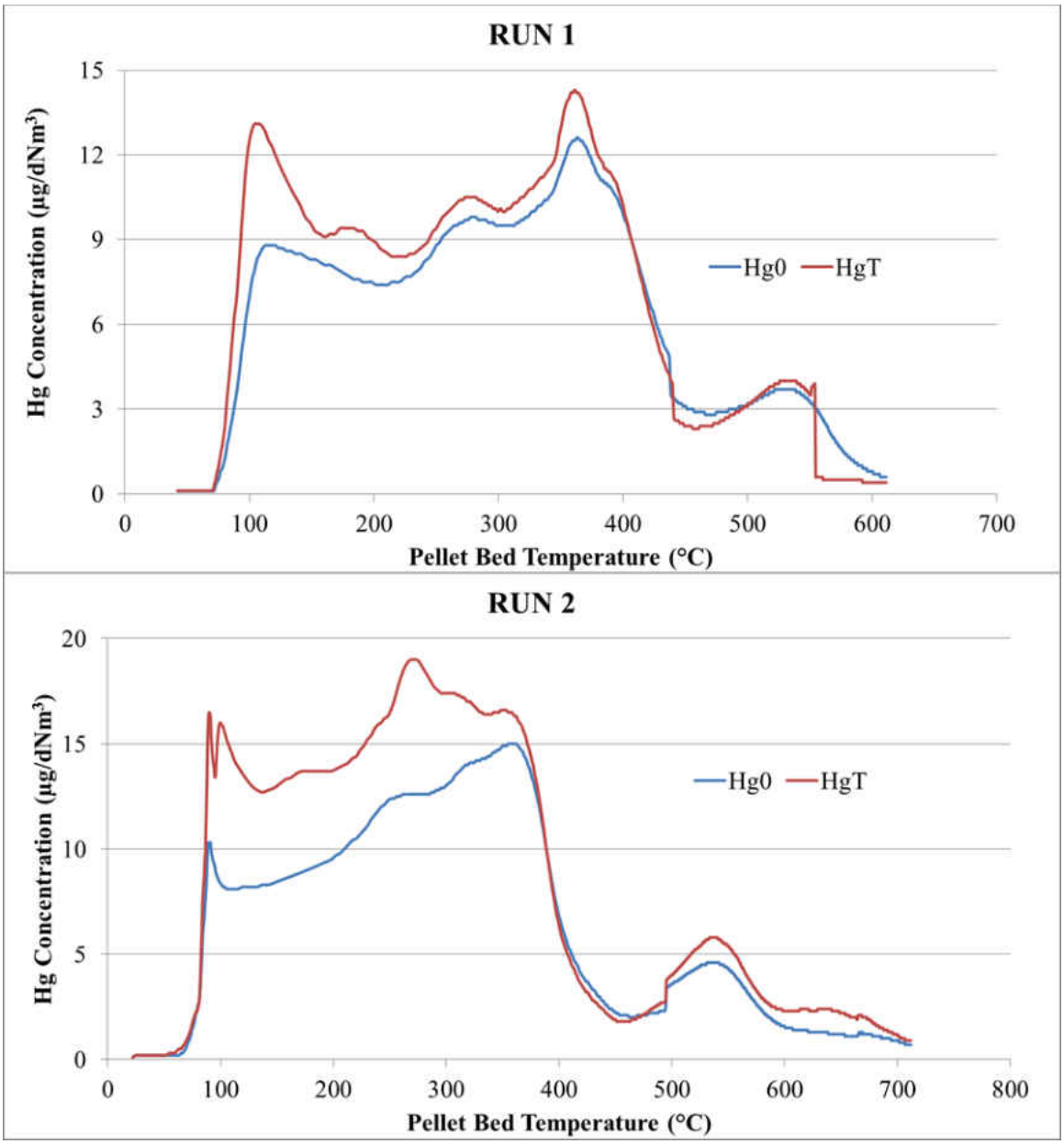

Figure 26 : Mercury release profiles during heating of baseline (additive free) green balls

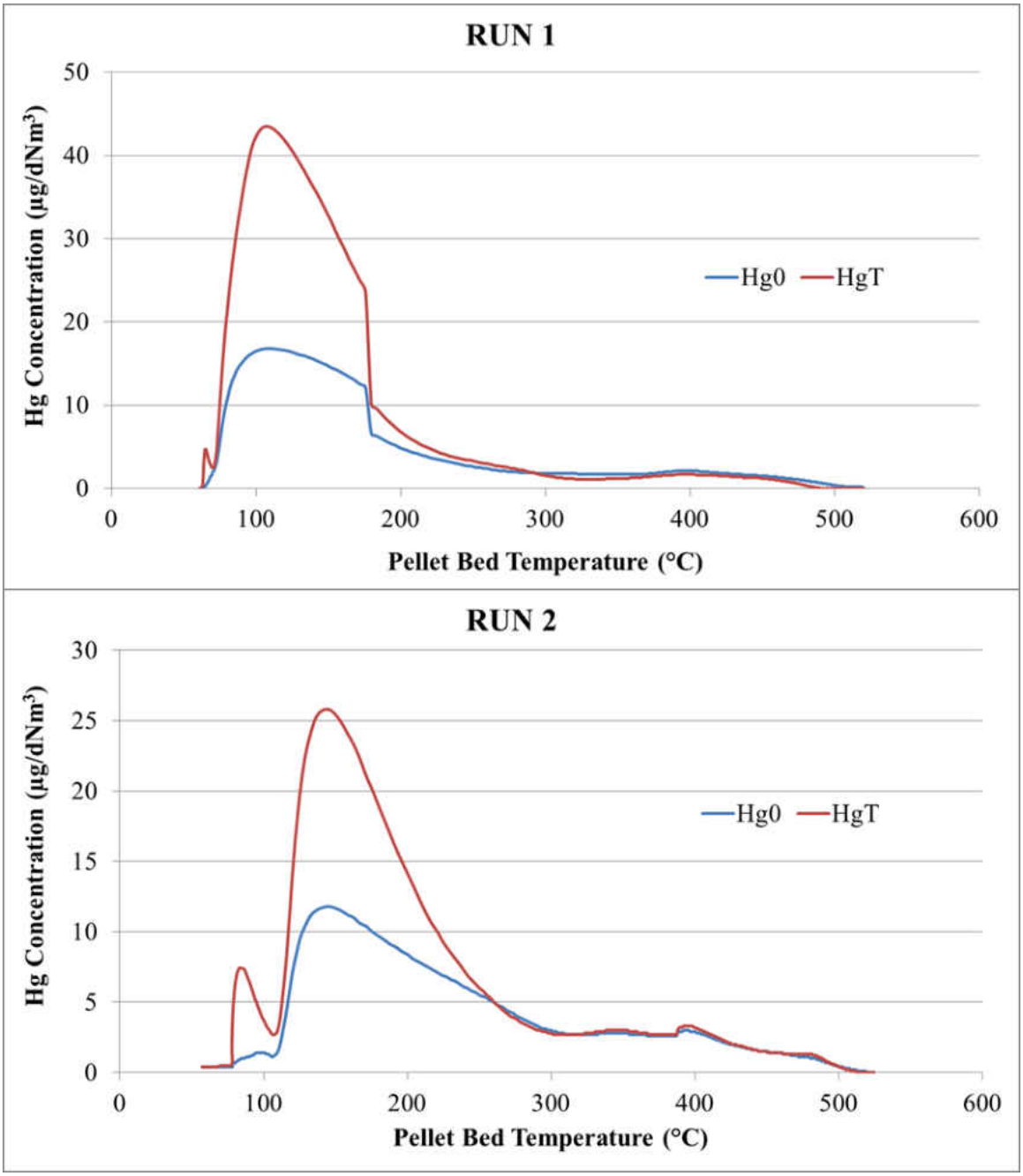

Figure 27: Mercury release profiles during heating with 0.05g ESORB-HG-11 in green balls

Figure 28 presents the results for 0.1 wt% loading of ESORB-HG-11, the enhanced activated carbon used to improve oxidation. Most of the mercury is also seen to be released oxidized within the 100°C to 400°C temperature range just like with the 0.05wt% loading. No prominent peak or oxidation is observed between the 500°C and 600°C as was the case with the baseline. Similar results are also observed in Figures 29, 30 and 31 of ESORB-HG-11 loadings of 0.2, 0.3 and 0.5 wt% respectively.

Increasing the loading rate beyond 0.1 wt% did not result in any significant increase in oxidation as shown in Table 12. Hence, the oxidation could either be no longer mass limited or some phenomena such as bromine volatilization, reduces the effectiveness of the additive.

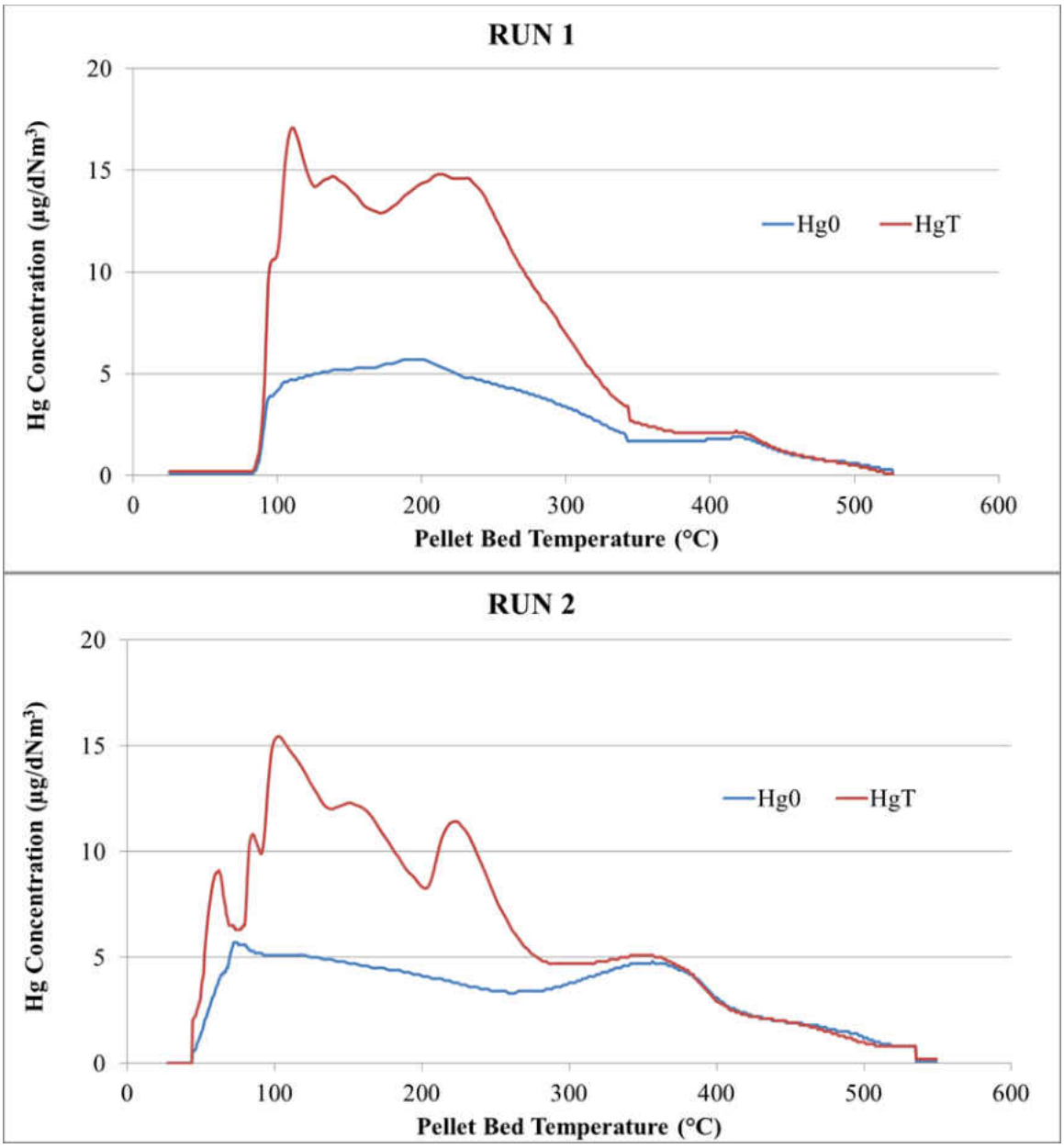

Figure 28: Mercury release profiles during heating with 0.1 g ESORB-HG-11 in green balls

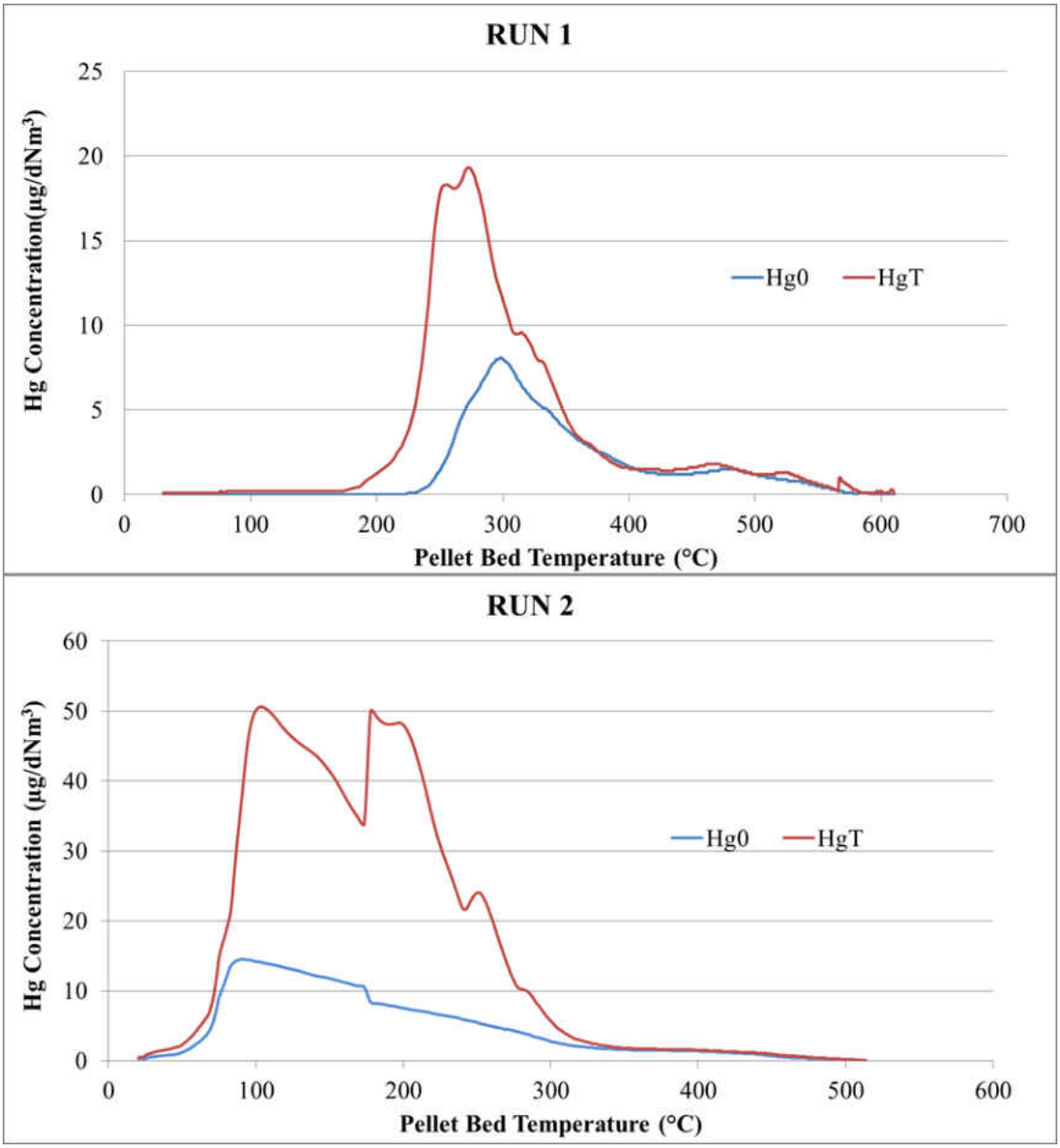

Figure 29: Mercury release profiles during heating with 0.2 g ESORB-HG-11 in green balls

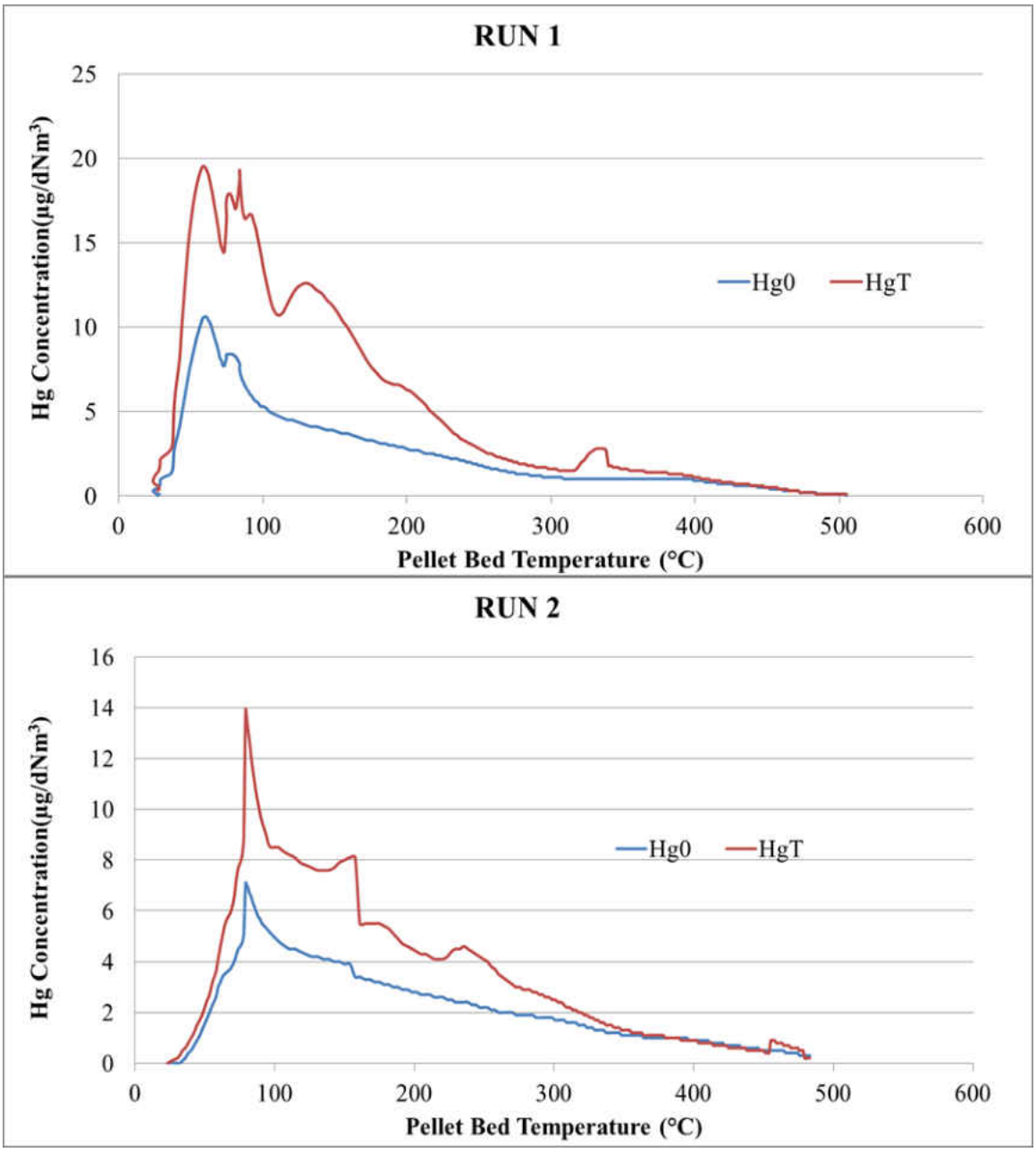

Figure 30: Mercury release profile during heating with 0.3 g ESORB-HG-11 in green balls

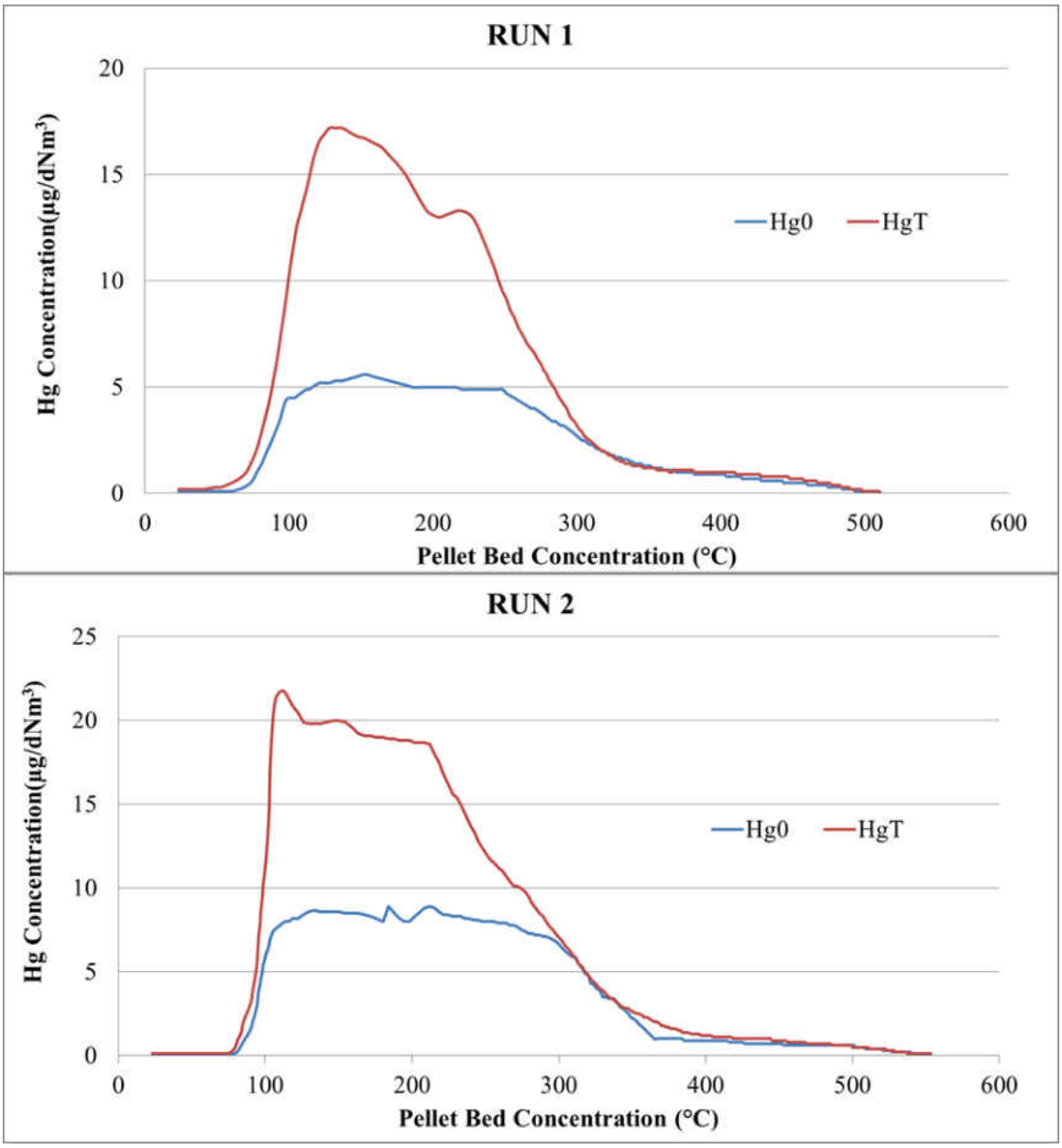

Figure 31: Mercury release profiles during heating with 0.5 g ESORB-HG-11 in green balls

During the mixed sampling tests, it is evident that there is some degree of oxidation observed when the baseline runs are compared to the ESORB-HG-11 runs. An average baseline oxidation of 16.9% is observed which roughly doubles to 36.4% for the 0.05wt% sample and then stabilizes at an average oxidation of 49.2% for higher loadings of ESORB-HG-11 runs. The increase in oxidation from the baseline averages is

consistent with results of successful runs performed during earlier Phase I testing of Minntac green balls. The temperature profile during heating will be investigated in more detail during Phase 2 to observe any consistent trends or changes due to the addition of carbon to the green balls.

3. Surface Tests

Surface tests for Minntac green balls was carried out with a procedure explained in section 3.4.2 . Surface tests showed inconsistent results when compared to mixed tests. Table 13 summarizes the results obtained for Minntac surface tests. These tests were carried out after the equipment was optimized but failed to show significant mercury oxidation (< 40%). After careful review of method of production of green balls at various taconite facilities, it was concluded that surface testing will not be a feasible method to scale up at a plant site and hence the method was not further investigated.

Figure 32 is a plot of mercury concentration versus pellet bed temperature (°C) during heating of surface coated Minntac green balls. From the plot, it is clear that the oxidation level of elemental mercury is not significant.

Table 13: Minntac Surface Test Results

	Additive Loading	Loading Ratio	Hg° Curve Area	Hg^{T} Curve Area	Oxidation
Run	(wt.%)	(mg/kg)	(ng)	(ng)	(%)
1	0.2	2000	126	189	33.5
2	0.2	2000	154	212	27.2
3	0.2	2000	1325	1555	14.8

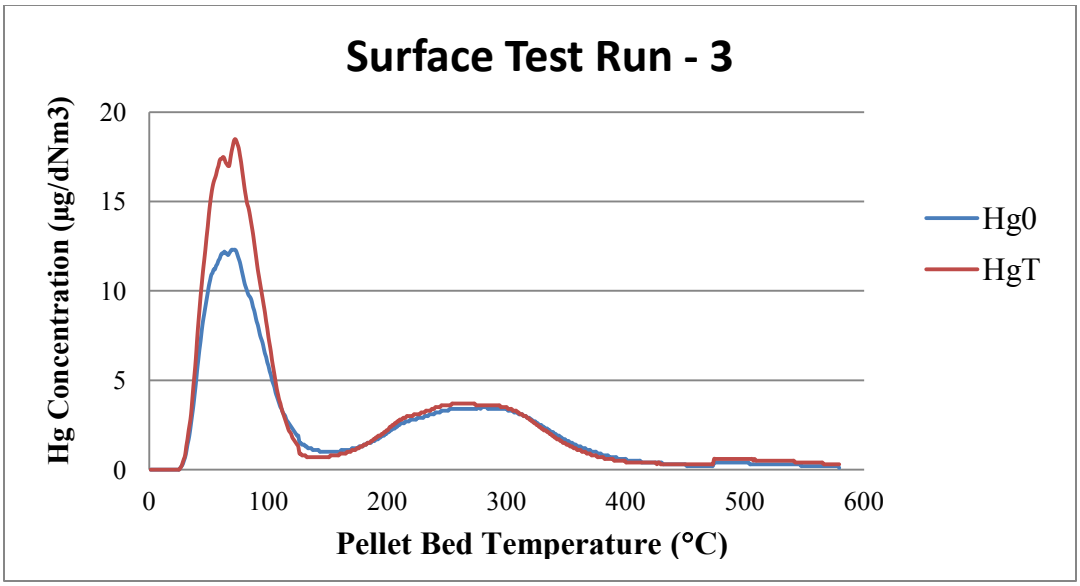

Figure 32 : Mercury release profile during heating of surface coated Minntac green balls

II. Utac Results

In Phase I, Utac green ball testing was done in two steps, mixed addition and surface addition. Results for mixed addition are presented in Table 14 and results from surface addition are presented in Table 15.

Table 14 includes the results of mixed addition with different additives which includes ESORB-HG-11, Powdered Activated Carbon (PAC) and halogenated salts. First run mentioned in the table is a baseline run in which green balls are produced as per the procedure in section 3.4.2 of this thesis without any additive. Comparing the baseline run to with additives runs, it is clear that none of the additives have significant effect on the elemental mercury level. After referring to numerous resources, it was found that Utac green ball formation process is susceptible to aging and hence the testing was postponed till Phase II without any solid conclusion. The effect of additives will be examined when a fresh batch of green balls will be obtained in Phase II.

Table 14 : Mixed Addition Results

	Additive Loading	Loading Ratio	Hg^0 Curve Area	Hg^T Curve Area	Oxidation
Additive	(wt.%)	(mg/kg)	(ng)	(ng)	(%)
None	0	0	1538	1932	20.4
ESORB-HG-11	0.1	1000	914	1331	31.3
PAC	0.1	1000	913	1206	24.3
NH_4Br	0.01	100	943	1314	28.2

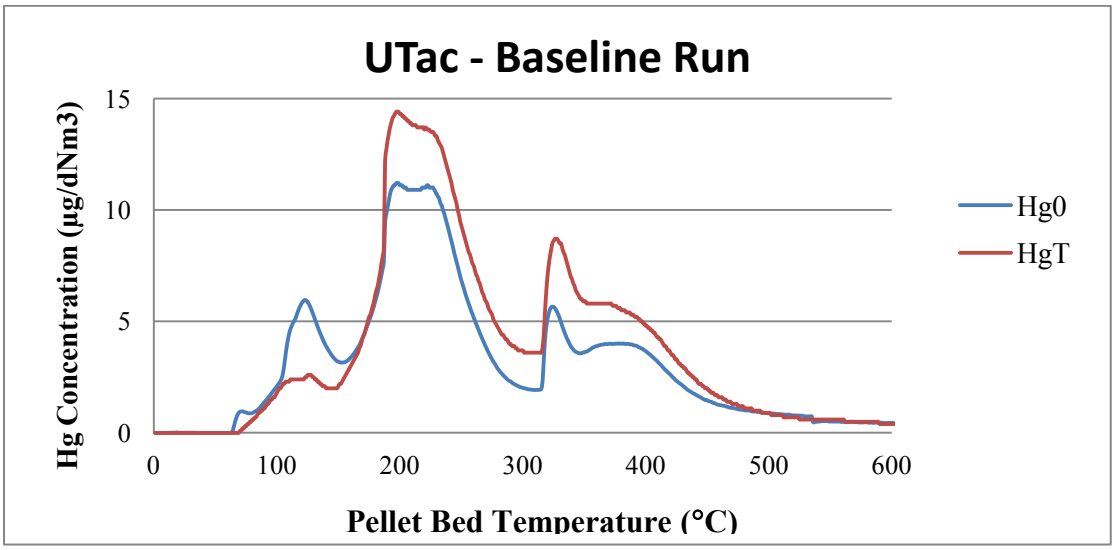

Figure 33 : Mercury release profile from Utac green balls with no additive (Baseline)

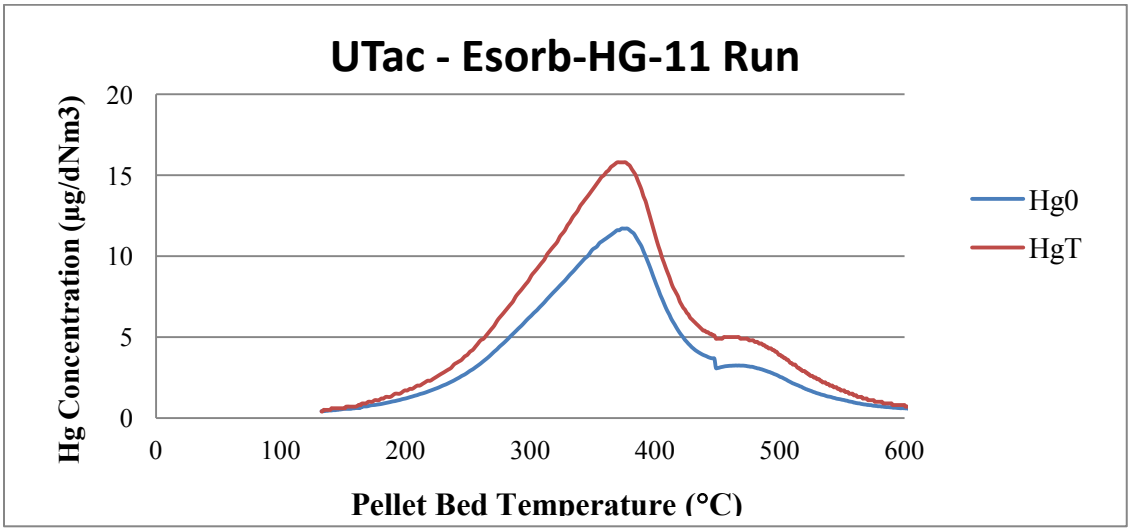

Figure 34 : Mercury release profile from Utac green balls with ESORB-HG-11 additive

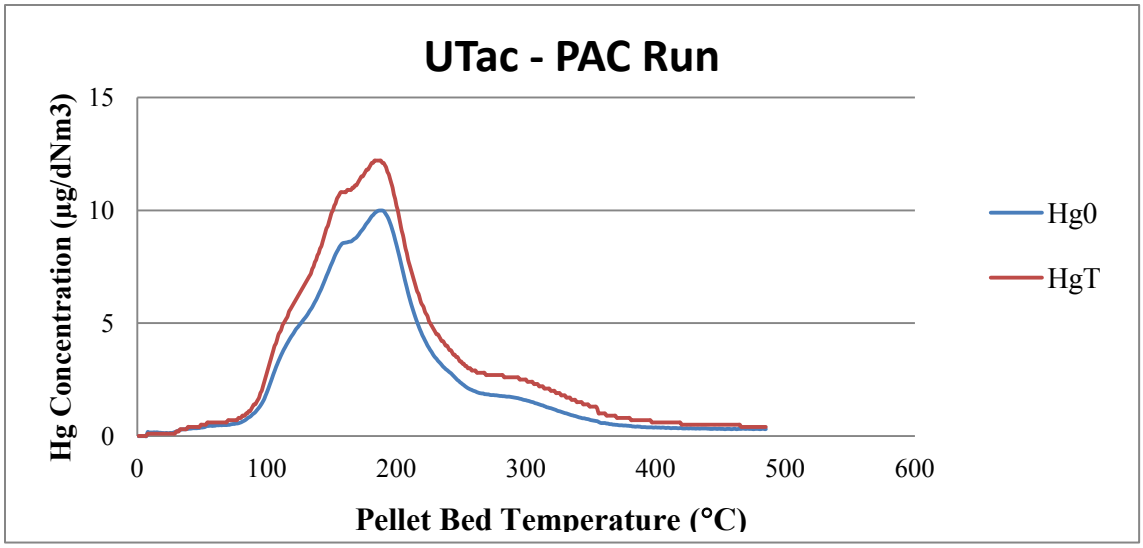

Figure 35 : Mercury release profile from Utac green balls with PAC additive

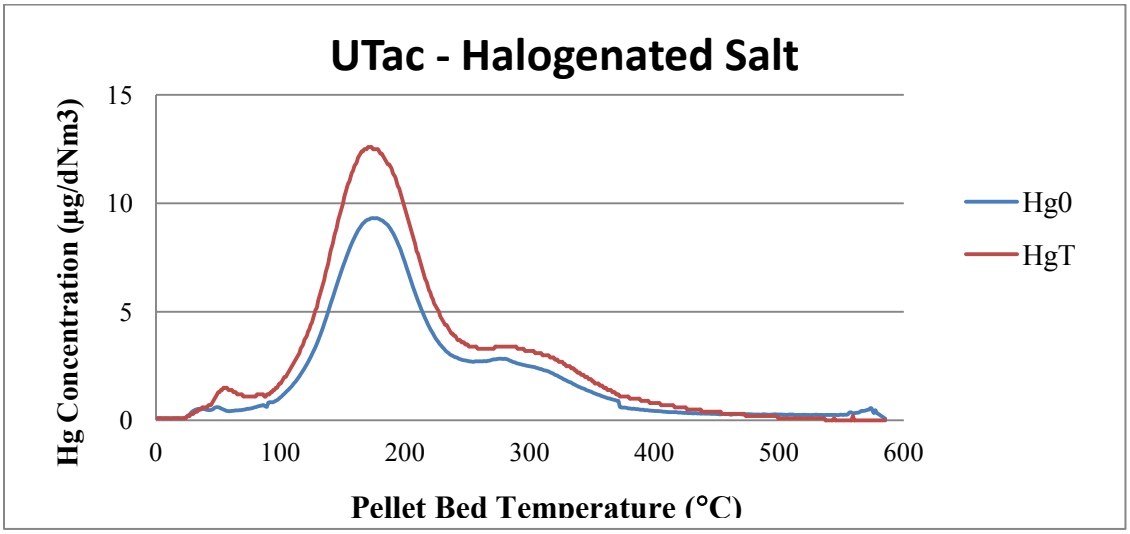

Figure 36 : Mercury release profile from Utac green balls with PAC additive

Table 15 : Surface Addition Results

	Additive Loading	Loading Ratio	Hg^0 Curve Area	Hg^T Curve Area	Oxidation
Additive	(wt.%)	(mg/kg)	(ng)	(ng)	(%)
ESORB-HG-11	0.1	1000	122	146	16.4
ESORB-HG-11	0.1	1000	218	401	45.6

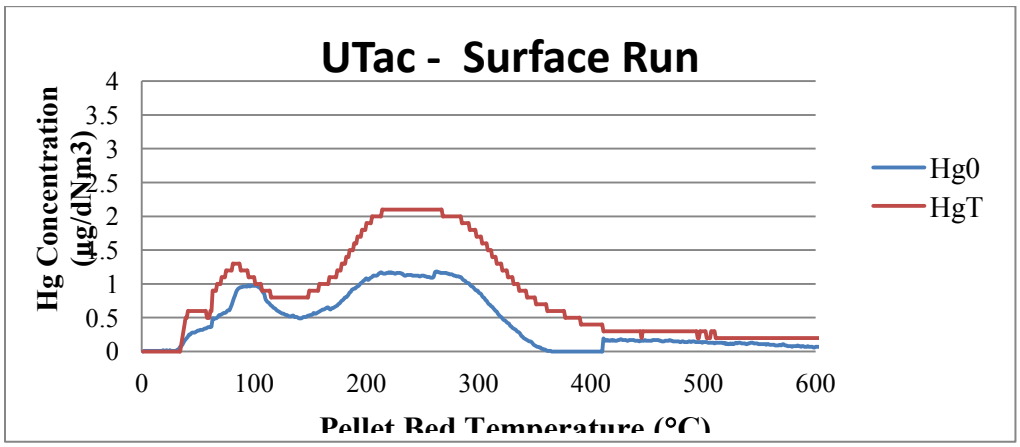

Figure 37 : Mercury release profile from Utac green balls with surface addition method

3.7 Conclusion – Preliminary Analysis (Phase I)

In Phase I, the mercury oxidation potential of different additives was established with the help of two different methods namely carbon addition to the flue gas and carbon addition to the green ball feed. It was clear from carbon addition to flue gas experiments that it will not be a feasible method due to lack of residence time of carbon in the reactor assembly.

Hence, it was crucial to evaluate the carbon addition to green ball method. This testing was carried out with two plants. Minntac tests involving mixed green balls with ESORB-HG-11 consistently gave good results by showing oxidation levels greater that 40 percent. This confirms that the proposed technology is a viable way to oxidize mercury and in turn to capture mercury in scrubber. The testing involved 5 different loadings of ESORB-HG-11 giving a ratio of distribution of 500,1000,2000,3000 and 5000 mg/kg. The attached figure (Figure 38) is a graph of average percent mercury oxidation versus weight percent of ESORB-HG-11. It is evident from the graph that increasing amount of ESORB-HG-11 does not produce a significant effect. It gives a limited benefit within the range ± 5 percent. Reasons for the limited increase in the performance at higher additive ratios could be due to either diffusion or kinetic limitations in the green balls. Hence, it was decided that in Phase II testing will focus on baseline, 0.1 percent and 0.5 percent of loading.

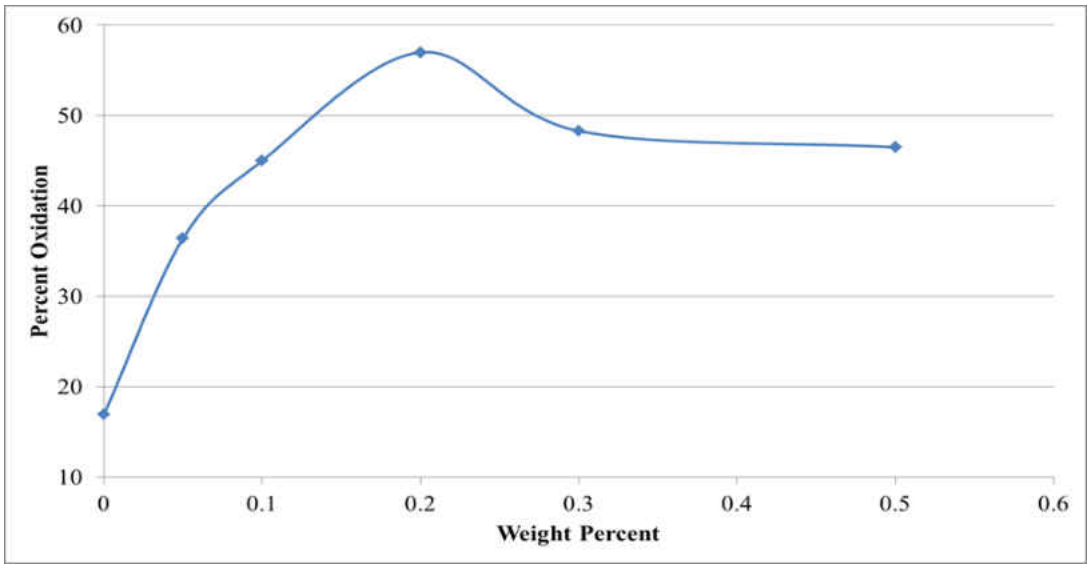

Figure 38 : Percent oxidation observed as a function of additive loading

Surface tests on the other hand were not conclusive since all the data obtained from these experiments yield low mercury concentration values. These tests were not investigated in detail as it was established that Utac samples can have a problem of "aging" and also forming technique was not relevant to field testing. PAC was also not tested extensively since it was established that PAC is effective in an environment where halogens are present in the flue gas. However, halogenated salts on the other hand, did not establish any appreciable oxidation levels unlike what was observed in the literature. This can lead us to a conclusion that the reductions observed during field testing can be due to the gas phase oxidation of mercury or mercury measurement bias.

In the lab scale apparatus the results show that mercury oxidation takes place on the surface of green ball or carbon. Hence, there is little or no gas phase oxidation in the lab scale setup taking place, however; gas phase oxidation may be observed during field testing in scale up of this technology.

The main goal of the Phase I tests was to determine if the technology proposed, ESORB-HG-11 (additive) incorporation into the green ball formulation has a potential to show significant mercury oxidation (> 40%). This was confirmed with Minntac mixed sample tests carried out with optimized testing equipment.

It is important to note that the temperatures used to plot the mercury concentration graphs are pellet core temperatures. Pellet core temperature is measured by inserting a thermocouple in the green ball. However, initially the thermocouple was inserted into the pellet bed and the temperature of the pellet bed was measured. There is a significant difference in the pellet core temperature and pellet bed temperature with respect to time. Pellet bed temperature increases rapidly in the initial heating of green balls and mercury release mostly takes place around 200° C up to 500°C. In case of pellet core temperature, mercury release starts around 100° C and continues up to 450° C.

CHAPTER IV

PHASE II

ANALYSIS OF MERCURY OXIDATION POTENTIAL OF ESORB-HG-11

In Phase I, research was focused on establishing the potential and optimum loading of ESORB-HG-11 to oxidize mercury released from green balls. Phase II will be focused on laboratory scale work performed to establish the oxidation potential of ESORB-HG-11 with 0.1 and 0.5 weight percent loading in green ball formulation for five different taconite plant sites. The extensive study was carried out for five different plants which includes United Steel's Minntac and Keetac, United taconite (Utac), Arcelor Mittal and Hibtac. The green ball formulation was obtained from all the five plants with the required raw material. Green balls were produced at Colerain Mineral Research Laboratory (CMRL). Preparation was done based on a batch balling procedure established by CMRL.

CMRL is an established testing facility for iron ore related bench and pilot scale experiments. Several different tests related to the taconite processing are performed by CMRL and the batch balling procedure is known and accepted by the taconite industry. The first step in batch balling test was to obtain concentrates from all the five plants and performing a moisture test. Minntac provided a filter cake that was received as slurry which needed to be pressure filtered to meet with facility's standard moisture content. Table 16 gives the test matrix for Phase II testing.

4.1 Test Matrix

Table 16 : Phase II Test Matrix

No.	Plant	Additive Level (%)			Replicate(%)
1	Arcelor Mittal	0	0.1	0.5	0.1
2	Hibtac - Standard Pellet	0	0.1	0.5	0.5
3	Hibtac - High Compression Pellet	0	0.1	0.5	0
4	Keetac	0	0.1	0.5	0.1
5	Minntac	0	0.1	0.5	0
6	Utac	0	0.1	0.5	0.5

Green balls were produced for all the facilities. For each facility, a batch was prepared containing no additive, 0.1 weigh percent additive and 0.5 weight percent additive. A replicate of baseline, 0.1 weight percent or 0.5 weight percent was prepared for each plant in the sequence mentioned in Table 16. This gave us a total of 4 batches per plant except Hibtac. Hibtac produces two different types of green balls depending upon the formulation. Hence, for Hibtac, two different sets of batches were prepared. In total, 24 batches of green balls were prepared and tested in Phase II.

Batch Balling Procedure

1. Almost all the taconite obtained from plants is used on an “as received” basis. The only parameter that is adjusted is the moisture content. The moisture content should be between 9.0 % and 9.5 %.
2. All the taconite ore is passed through a shredder to ensure that all chunks are broken apart.
3. For each batch an amount of binder is weighed out. The amount and binder type are dependent on the plant being tested.
4. The desired amount of carbon is then added to the binder and mixed. (Refer figure 40)
5. Some of the binder/carbon mix is sprinkled onto the ore, and then the result is mixed by hand. More binder/carbon is added and mixed in until of the binder/carbon is used up.
6. The ore/additive mix is passed through the shredder again to mix it more and to ensure all larger clumps are broken up.
    a. Note: This mixing technique has been used multiple times over the past ten years to blend small amounts of additive. No difference between this technique and the intensive mixers used in plants has ever been determined. Furthermore lab scales intensive mixtures then “micro-ball” which effects green ball development.
7. Some of the resulting mix (around 300 grams) is then placed in the balling tire, where a machine spins it. Water is sprinkled at this time, and small balls of taconite/additive called “seed balls” are produced.

8. The newly produced seed balls are fed through a series of meshes to eliminate balls that are too big or too small. Seed balls are specified to be -3 to +4 Mesh. Normally 170g to 250g of seed balls are produced for one batch of green balls. (Refer figure 41)
9. Place the seed balls into the bailing tire and spin them again. (Refer figure 39) Pour the taconite/additive mix on top of the spinning seed balls to create green balls. Using water and a sprayer, make sure that the balls in the balling tire are adequately wet.
    a. From when the first seed balls are added to when the green balls are formed should take 3 minutes
10. After the green balls are formed, they are allowed to roll in the bailing tire for another minute.
11. The green balls are removed and again fed through the mesh. This time the acceptable size is -1/2" + 3/8". (Refer figure 42)

After the green balls were formed following the above procedure, approximately 200-300 grams of green balls were placed in oven to determine moisture content. 10 grams of green balls from each batch was subjected to 18" wet drop test. Ten dried green balls from the moisture content test were then subjected to dry compressive strength test. The results from these physical tests are attached in table 17.

Figure 39 : Batch Balling Tire Assembly

Figure 40 : Taconite ore with binder and carbon additive

Figure 41 : Green Ball Seeds

Figure 42 : Sieved Green Balls

Table 17 : NRRI Physical Tests Data

UND - Batch Balling Test Results

Test #	Iron Ore Concentrate	Description	Binder	Additive (s)	UND Carbon Additive, %	Green Ball Quality			Green Ball Sizing, %		
						Moist, %	18" Drop	Dry Comp	+1/2"	-1/2" +7/16"	-7/16" +3/8"
B12576	Arcelor-Mittal Minorca	Fluxed	Bentonite	Limestone-Dolomite	0.0	9.8	7.5	7.8	0.5	44.0	55.6
B12577	Arcelor-Mittal Minorca	Fluxed	Bentonite	Limestone-Dolomite	0.1	9.9	8.2	9.0	1.1	48.4	50.5
B12578	Arcelor-Mittal Minorca	Fluxed	Bentonite	Limestone-Dolomite	0.5	9.8	7.2	7.1	1.8	55.8	42.4
B12579	Arcelor-Mittal Minorca	Fluxed	Bentonite	Limestone-Dolomite	0.1	9.7	7.1	7.9	7.3	64.2	28.5
Std Deviation						*0.1*	*0.5*	*0.8*			
B12580	Keewatin Taconite	Std	Bentonite	--	0.0	9.4	4.8	6.8	11.7	49.2	39.0
B12581	Keewatin Taconite	Std	Bentonite	--	0.1	9.5	4.9	5.6	6.8	46.4	46.8
B12582	Keewatin Taconite	Std	Bentonite	--	0.5	9.2	4.5	3.1	14.8	43.2	42.0
B12583	Keewatin Taconite	Std	Bentonite	--	0.1	9.5	5.7	5.7	7.7	52.2	40.1
Std Deviation						*0.1*	*0.5*	*1.6*			
B12584	Hibbing Taconite	Std Pellet	Bentonite	Low Level Limestone	0.0	9.7	6.5	8.8	1.8	46.9	51.2
B12585	Hibbing Taconite	Std Pellet	Bentonite	Low Level Limestone	0.1	9.6	6.3	8.4	3.5	51.3	45.2
B12586	Hibbing Taconite	Std Pellet	Bentonite	Low Level Limestone	0.5	9.5	6.2	3.9	10.2	47.1	42.7
B12587	Hibbing Taconite	Std Pellet	Bentonite	Low Level Limestone	0.5	9.6	6.0	4.3	4.6	46.4	49.0
Std Deviation						*0.1*	*0.2*	*2.6*			
B12588	Hibbing Taconite	High Comp	Bentonite	Low Level Limestone	0.0	9.6	6.8	7.2	2.8	52.4	44.8
B12589	Hibbing Taconite	High Comp	Bentonite	Low Level Limestone	0.1	9.7	6.1	9.0	1.7	35.0	63.3
B12590	Hibbing Taconite	High Comp	Bentonite	Low Level Limestone	0.5	9.6	6.3	7.9	6.1	57.1	36.7
B12591	Hibbing Taconite	High Comp	Bentonite	Low Level Limestone	0.0	9.5	6.5	8.8	2.9	48.6	48.5
Std Deviation						*0.1*	*0.3*	*0.8*			
B12592	Minntac	Fluxed	Bentonite	Limestone-Dolomite	0.0	9.5	6.8	8.6	0.3	33.6	66.0
B12593	Minntac	Fluxed	Bentonite	Limestone-Dolomite	0.1	9.6	6.5	8.1	0.7	47.2	52.1
B12594	Minntac	Fluxed	Bentonite	Limestone-Dolomite	0.5	9.2	5.9	6.0	3.3	54.7	42.0
B12595	Minntac	Fluxed	Bentonite	Limestone-Dolomite	0.0	9.2	6.2	8.8	0.5	37.4	62.1
Std Deviation						*0.2*	*0.4*	*1.3*			
B12596	United Taconite	Std	Organic	Low Level Limestone	0.0	9.9	5	2.1	25.2	40.1	34.6
B12597	United Taconite	Std	Organic	Low Level Limestone	0.1	10.1	5.5	2.8	7.6	50.5	41.9
B12598	United Taconite	Std	Organic	Low Level Limestone	0.5	10.2	5.9	3.1	11.4	49.2	39.3
B12599	United Taconite	Std	Organic	Low Level Limestone	0.5	9.7	5.5	2.6	12.1	39.5	48.4
Std Deviation						*0.2*	*0.4*	*0.4*			

4.2 Results and Discussion – CMRL Testing

Results from CMRL testing are summarized in Table 17. Green ball formulation is a very important step in taconite processing. Data in the Table 17 shows that the addition of the carbon based additive into the green ball formulation does not have a significant effect on the physical properties at both high (0.5 weight percent) and low level. (0.1 weigh percent) Additive show no significant influence when compared to baseline in moisture content, 18" wet drop test or dry compression strength measurement.

The standard green ball prepared for Hibtac and Keetac show a slight decrease in the dry compression strength at high dosage level. (0.5 weight percent) It should be noted that both the facilities have slightly coarser particle size distribution as compared to other plants due to their relative location in Mesabi Iron Range and they also have slightly different transition of silica into the ore body. It should be also noted that relative green ball size distribution is slight larger (+1/2" size fraction) in case of high dosage level. (0.5 weight percent)

4.3 Experimental Procedure

Pellet Testing Equipment

The bench scale apparatus is illustrated in Figures 43 and 44. It consists of a tube furnace, reaction vessel, a gas metering system, gas conditioning, mercury pretreatment system, and mercury analyzer. The procedure for testing involves placing approximately 100 grams of green balls into the reaction vessel and heating the green balls up to 700 °C. During the heating process, air passes through the vessel at 7.5 lpm and flows through heated PFA tubing to a pretreatment system and then directly to the analyzer for an elemental mercury determination.

Most of the conditions for Phase II testing were similar to that of Phase I. However, in Phase I, equipment was optimized in the initial runs where flow rates and mass of green balls used for experiments was varied. In Phase II, all the conditions were kept similar for all the sixty experiments. As shown in Figure 44 and 45, a wet pre-treatment unit was used to condition the flue gas before it enters the Horiba mercury analyzer. It consisted of two parallel sets of impingers (4 impingers in total). The first impinger contains a 150 ml of 10 weight percent potassium chloride (KCl) and 0.8 weight percent of Sodium Thiosulfate ($Na_2S_2O_3$) solution that captures the oxidized mercury in order to obtain only elemental mercury concentration, while the second impinger sits in an ice bath and traps all moisture present in the gas sample before analysis by the mercury analyzer. The second impinger train is for conditioning the total mercury stream. Here, the first impinger contains 150 ml of 0.8 weight percent stannous chloride ($SnCl_2$) solution and 20 weight percent of Sodium Hydroxide (NaOH). The

$SnCl_2$ reduces the oxidized mercury in order to obtain a total mercury measurement of the flue gas.

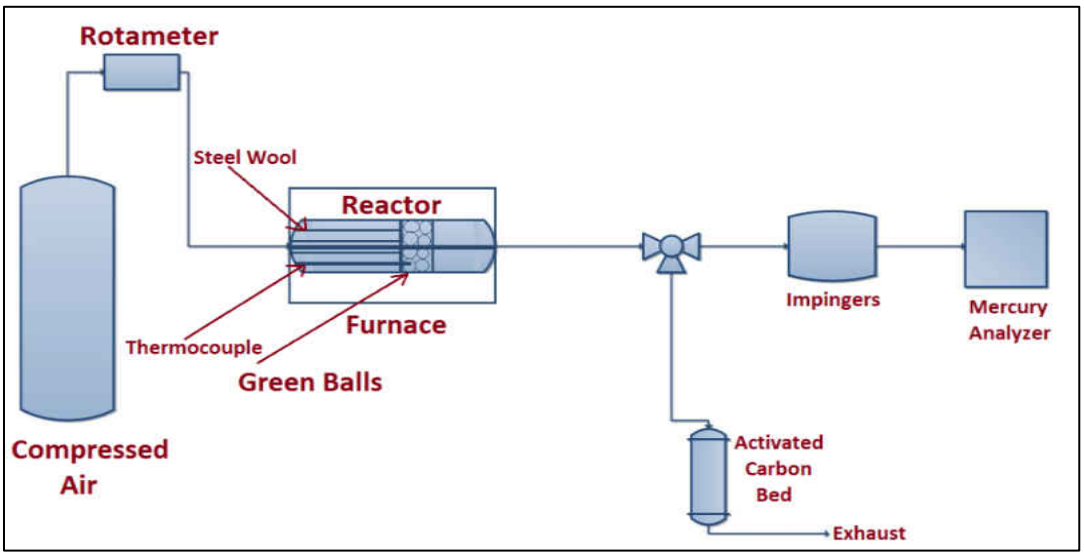

Figure 43 : Schematic of testing equipment – Phase II

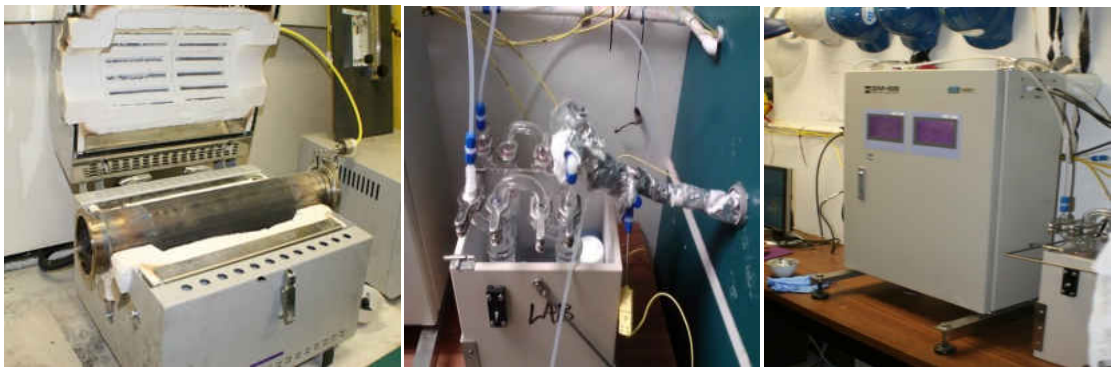

Figure 44 : Pictures showing reactor vessel, Wet-chemistry impinger train, Horiba DM-6B mercury analyzer.

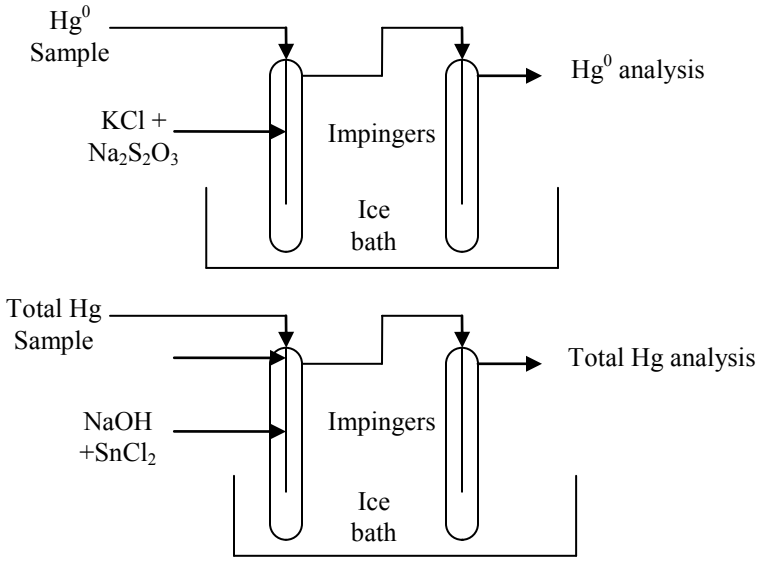

Figure 45 : Schematic diagram of impinger train – Phase II

Table 18 summarizes the test matrix developed for Phase II testing. All the batches produced at CMRL were tested in triplicates with the exception of batches which have been replicated.

Table 18 : Test Matrix for Phase II testing

Plant	Pellet Type	Additive Loading (weight percent)	Number of Runs
Minntac	Standard	0 (Baseline)	2
		0(Baseline Replicate)	2
		0.1	3
		0.5	3
Keetac	Standard	0 (Baseline)	3
		0.1	2
		0.1 (Replicate)	2
		0.5	3
Arcelor Mittal	Standard	0 (Baseline)	3
		0.1	2
		0.1 (Replicate)	2
		0.5	3
Utac	Standard	0 (Baseline)	3
		0.1	3
		0.5	2
		0.5(Replicate)	2
Hibtac	Standard	0 (Baseline)	3
		0.1	3
		0.5	2
		0.5(Replicate)	2
Hibtac	High Compression Pellet	0 (Baseline)	2
		0(Baseline Replicate)	2
		0.1	3
		0.5	3

Continuous Mercury Monitors system was measuring elemental (Hg^0) and total mercury (Hg^T) continuously. Difference between elemental and total mercury is assumed to be oxidized mercury. From previous studies, it was shown that oxidized mercury gets captured into scrubber systems; hence the percent mercury oxidation was used as an estimate for percent mercury reduction in emissions.

Oxidation formula used to calculate the percent oxidation is as follows:

$$\% \text{ Hg Oxidation} = \frac{\{Hg^T - Hg^0\}}{Hg^T} * 100$$

Where,

Hg^T = Total mercury emission during the run

Hg^0 = Elemental Mercury emission during the run

(Hg^0 and Hg^T are measured with the help of Horiba DM-6B Cold Vapor Atomic Absorption Spectroscopy CMM)

The mercury reduction potential of the technology/additive is determined by following formula:

$$\text{Reduction Potential} = \frac{Hg[2] - Hg[1]}{100 - Hg[1]} * 100$$

Where,

Hg [2] is the average mercury oxidation obtained for runs with 0.1/0.5 weight percent of ESORB-HG-11.

Hg[1] is the average mercury oxidation obtained for baseline runs of the respective facility and formulation.

4.4 Results and Discussion – Phase II Testing

In Phase II, testing was extensively carried out with five different plants and six different formulation techniques. Results in this section are subsequently divided into six different parts. Ten runs were carried out for each formulation including the replicated runs. Some graphs are added to the discussion section for illustration purposes while others can be found in Appendix B.

I. Minntac Results

Table 19 summarizes the results obtained from Minntac green ball testing. Minntac testing consisted of 10 runs which include 2 runs for baseline batch, 2 runs for replicated baseline batch, 3 runs for batch with 0.1 weight percent loading and 3 runs for batch with 0.5 weigh percent loading. All the batches were prepared at CMRL and were tested at similar condition with a flow rate of 7.5 lpm. Percent oxidation for baseline runs and replicated baseline runs showed a good agreement averaging to 22.31% and 25.73% respectively. Good agreement for replicated batch confirms the reliability of the batch balling procedure as well as the testing equipment.

Experiments with 0.1 weight percent loading showed a close agreement in results averaging to 62 percent. 0.5 weight percent loading gave 63 percent of average oxidation which is very close to 62 percent from 0.1 weight percent loading. Hence, 0.5 weight percent loading did not show a significant effect when compared to 0.1 weight percent loading. The data confirms that the results obtained during Phase I testing, which refers to a conclusion of 0.1 weight percent optimum loading, was proved to be correct. All the additive runs showed more than 50 percent oxidation which is a significant number.

Figure 46, 47 and 48 are the mercury release profiles from Minntac green ball with 0, 0.1 and 0.5 weight percent loading respectively. It is clear from this plot that the given additive is working efficiently and there is no significant difference between 0.1 and 0.5 weight percent loading. To better understand the effect of temperature on the mercury release from green balls from Minntac, a plot of cumulative mass of mercury evolved per mass of green ball versus the pellet core temperature was made in figures 49 and 50. The release profiles from the duplicated and triplicated runs were similar and hence only one representative run was used for this plot. Also, run with similar mercury values were selected for these plots to avoid normalization of the results. The ratio of cumulative mass of mercury evolved and the mass of green balls used was plotted against the pellet core temperature. The plotted curve shows the rate at which mercury is released as a function of temperature.

Table 19 : Minntac Test Results – Phase II

Additive Loading (weight percent)	Percent Oxidation	Average Percent Oxidation	Percent Reduction	Average Percent Reduction
0 (Baseline)	17.28%	22.31%	N/A	N/A
0 (Baseline)	27.35%			
0 (Baseline Replicate)	26.78%	25.73%	N/A	N/A
0 (Baseline Replicate)	24.68%			
0.1	64.23%	61.60%	52.92%	49.46%
0.1	53.45%		38.74%	
0.1	67.12%		56.73%	
0.5	68.03%	62.94%	57.92%	51.23%
0.5	61.20%		48.94%	
0.5	59.60%		46.82%	

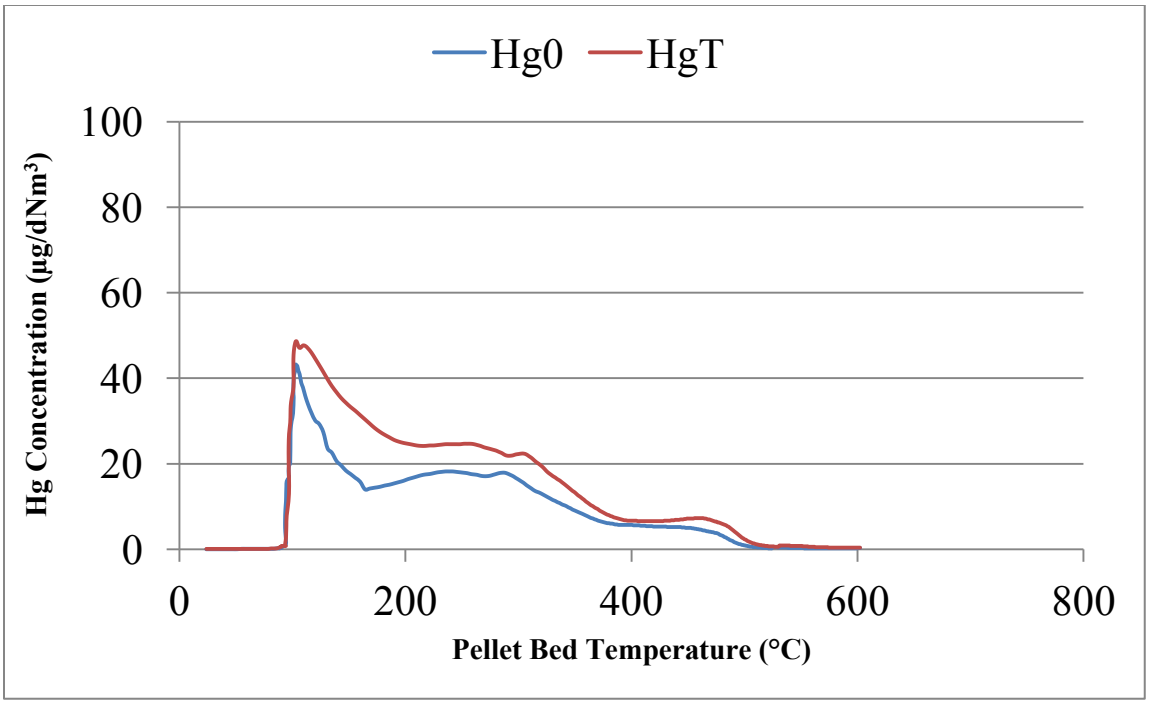

Figure 46 : Mercury release profile for Minntac green ball baseline run -1

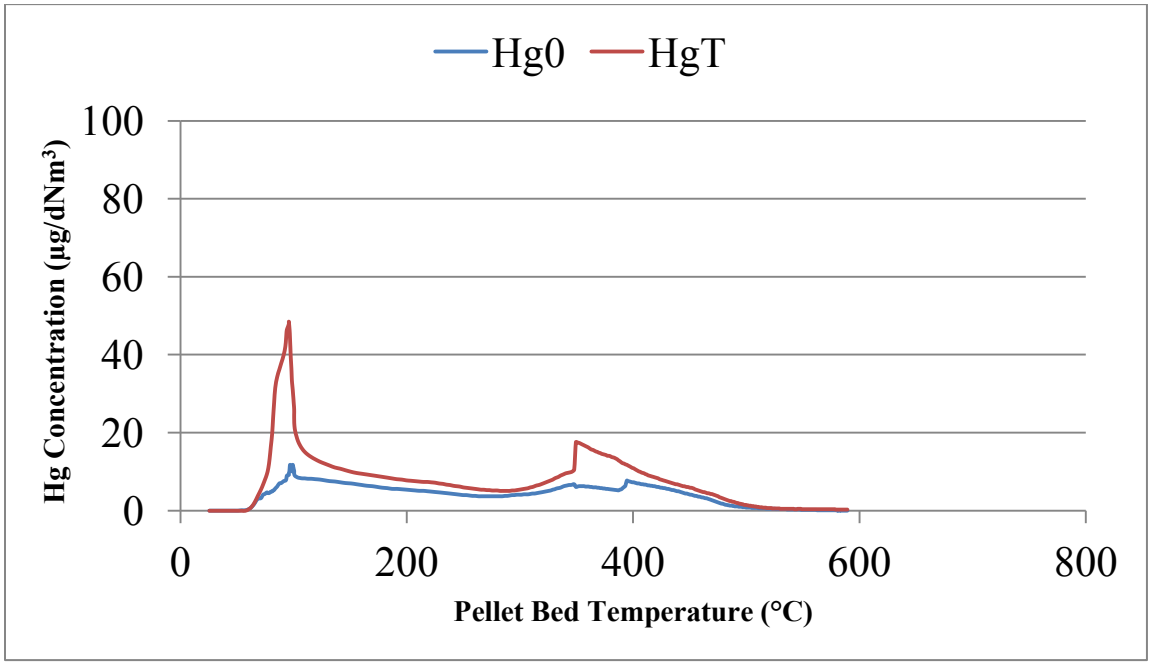

Figure 47 : Mercury release profile for Minntac green ball with 0.1 weight percent ESORB-HG-11-1

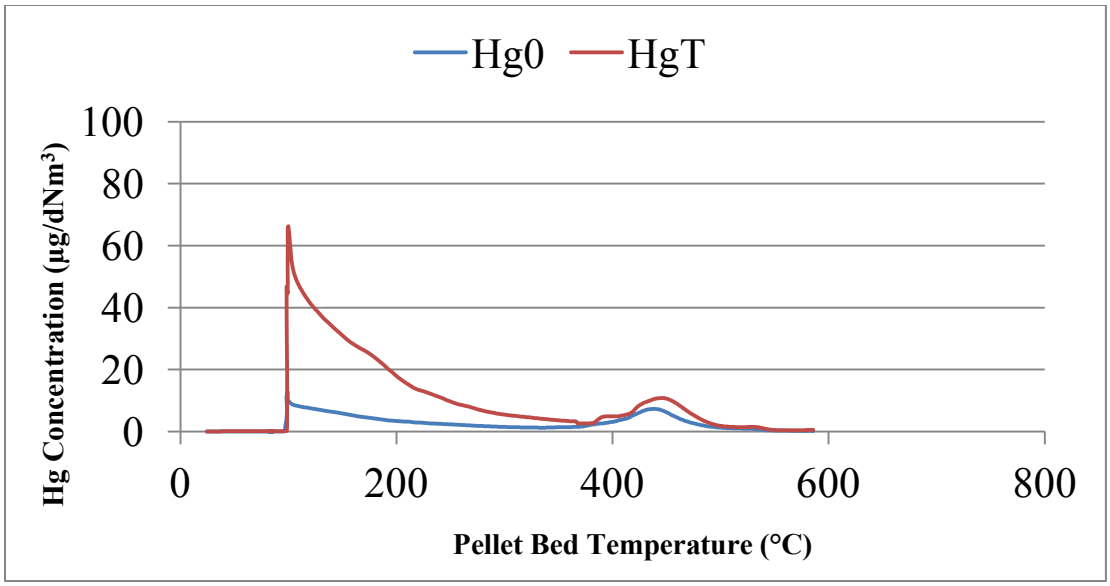

Figure 48 : Mercury release profile for Minntac green ball with 0.5 weight percent ESORB-HG-11 -1

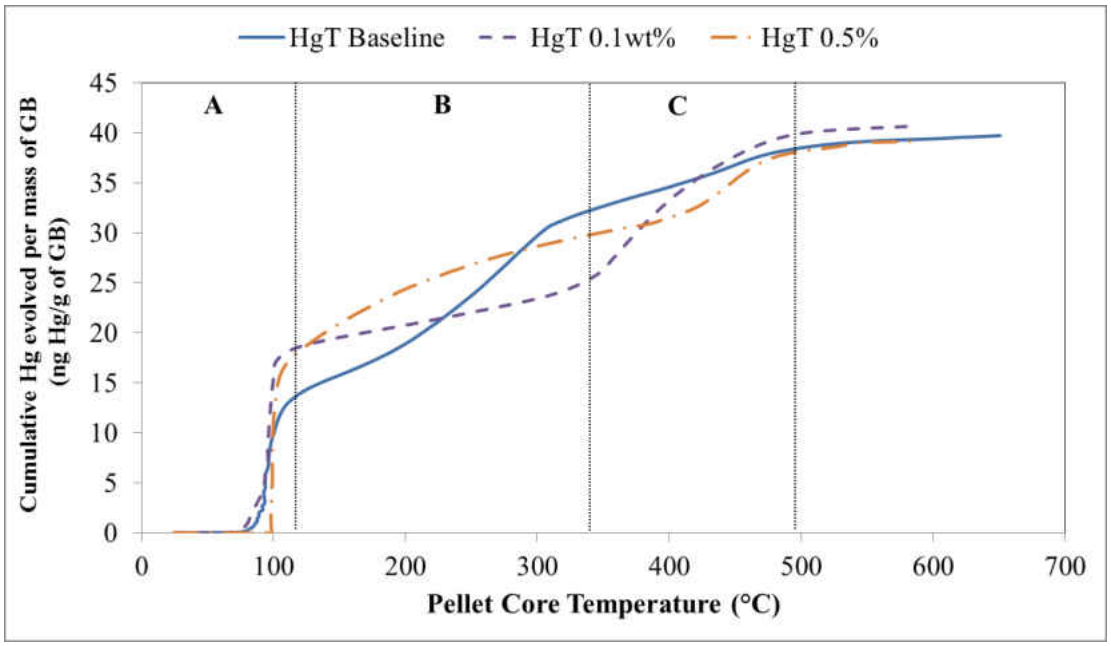

Figure 49 : Minntac cumulative mercury release profile for total mercury for baseline, 0.1 weight percent and 0.5 weight percent as a function of pellet bed temperature

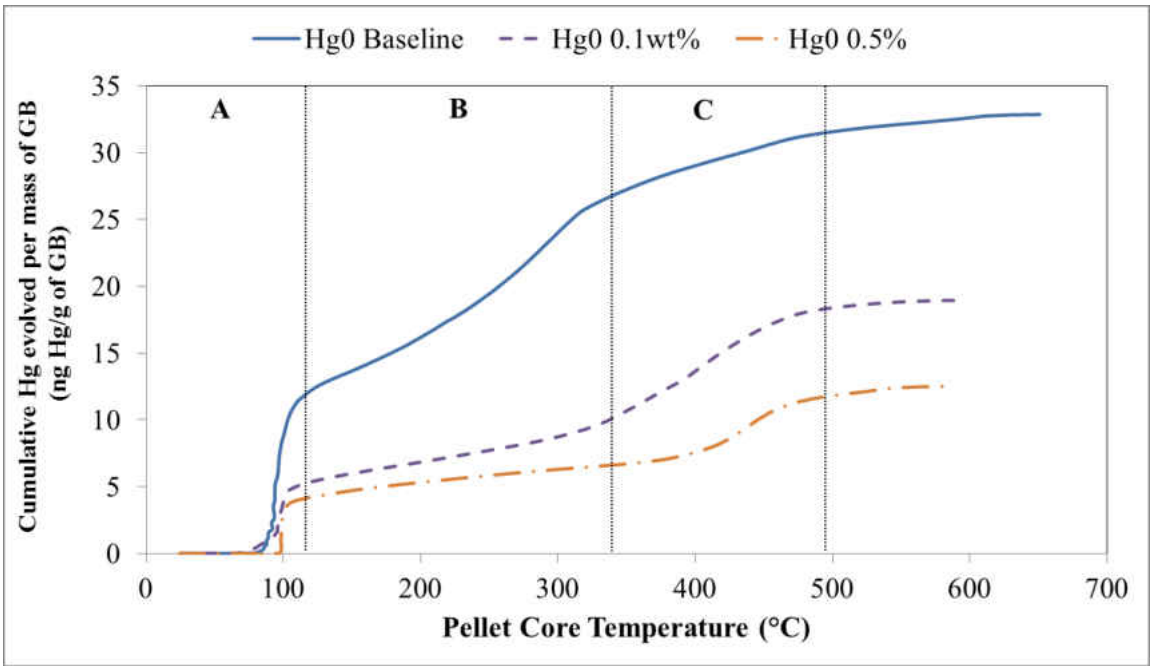

Figure 50 : Minntac cumulative mercury release profile for elemental mercury for baseline, 0.1 weight percent and 0.5 weight percent as a function of pellet bed temperature

Figure 49 and 50 denotes the cumulative plots generated to understand the mercury release behavior. These plots are divided into three different regions namely A, B and C. Region A corresponds to the initial zone where the pellet is gaining heat from the surrounding and slowly releases mercury from its surface. In this region, green balls are inserted into the reactor which is maintained at 250°C and heating up with a ramp rate of 20°C/min. Hence, the temperature of the surface of green ball is believed to be around 300°C. In the figures 49 and 50, we see a steep slope mercury release.

Since the furnace ramp rate is 20°C/min, green balls are rapidly gaining heat and the curve appears to flatten in region B which can be associated with the fact that most of the mercury release from the surface has already took place. Flatter curve can also suggest that the mercury release is taking place from deeper within the pellet as it is

gradually heating up. After careful observation, it can be also concluded that baseline curves are steeper in region B as compared to the 0.1 or 0.5 weight percent loadings.

Region C is the final heating zone where mercury is coming out from the pellet core. In this region, the trend has been observed to be reversed where 0.1 or 0.5 weight percent loading graphs are steeper and baseline curve appear to flatten out. This phenomenon is possibly due to the oxidation effect of ESORB-HG-11. The oxidation phenomenon with the help of ESORB-HG-11 believes to have a capture step followed by oxidation step. In capture step, ESORB-HG-11 captures the mercury on the carbon surface where as in oxidation step it gets oxidized by the bromine atoms present at the active sites. Hence, in region B, ESORB-HG-11 is capturing the mercury and hence the curve flattens out. In region C, pellet temperature is believed to be at least 350°C, a temperature where carbon starts to get burned off and cannot hold mercury anymore. Hence, all the captured mercury gets released from carbon in higher temperature range which is region C. Also from all the Minntac runs, it can be concluded that most of the mercury release takes place between 100°C – 500 °C and carbon does not exhibit any oxidation capacity after 400°C. This trend is consistent with all the Minntac runs. Graphs displaying the trends can be found in Appendix B. The highest mercury oxidation level was observed to be 68 percent which in turn gave us the average mercury reduction of 51 percent.

Also, it is important to note here that the temperature used for plots is the pellet core temperature. The pellet core temperature is measured by inserting a thermocouple into the green ball. This suggest that the surface of green ball is at a higher temperature and mercury release starts around 150° C for pellet surface temperature.

II. Keetac Results

The results obtained from Keetac green ball testing are summarized in Table 20. In the Keetac set, 10 experiments were performed at random which includes triplicates for baseline, triplicates for 0.5 weight percent loading and duplicates of 0.1 weight percent and its replicated batch. First run in the baseline section gave an -0.4% of oxidation and hence it was not considered for averaging the baseline runs. Baseline runs gave an average oxidation of 15.10%. This level is lower than the observed baseline oxidation levels of Minntac, Utac and Arcelor Mittal. 0.1 weight percent showed an average oxidation of 43.70% and its replicated batch gave an average oxidation of 47.85%. Close agreement of 0.1 and its weight percent shows that the equipment and batch balling procedure are reliable.

Additive loading of 0.5 percent gave an average oxidation level of 52.33% which is slightly higher than 0.1 weight percent loading. However, the difference is negligible and hence it can be concluded that the higher loading of additive does not have any significant effect on the oxidation level. A percentage release analysis of Keetac was not performed since the plots from different experiments were not conclusive. There was a lesser similarity between the runs of particular loading and hence, they were not reported. Keetac results are in agreement with other plants which proves that the additive is effective for mercury oxidation.

Table 20 : Keetac Test Results – Phase II

Additive Loading (weight percent)	Percent Oxidation	Average Percent Oxidation	Percent Reduction	Average Percent Reduction
0 (Baseline)	-0.40%	15.10%	N/A	N/A
0 (Baseline)	16.90%			
0 (Baseline)	13.30%			
0.1	43.60%	43.70%	59.29%	34.00%
0.1	43.80%		41.00%	
0.1 (Replicate)	44.20%	47.85%	41.57%	46.79%
0.1 (Replicate)	51.50%		52.00%	
0.5	51.50%	52.33%	52.00%	53.19%
0.5	46.50%		44.86%	
0.5	59.00%		62.71%	

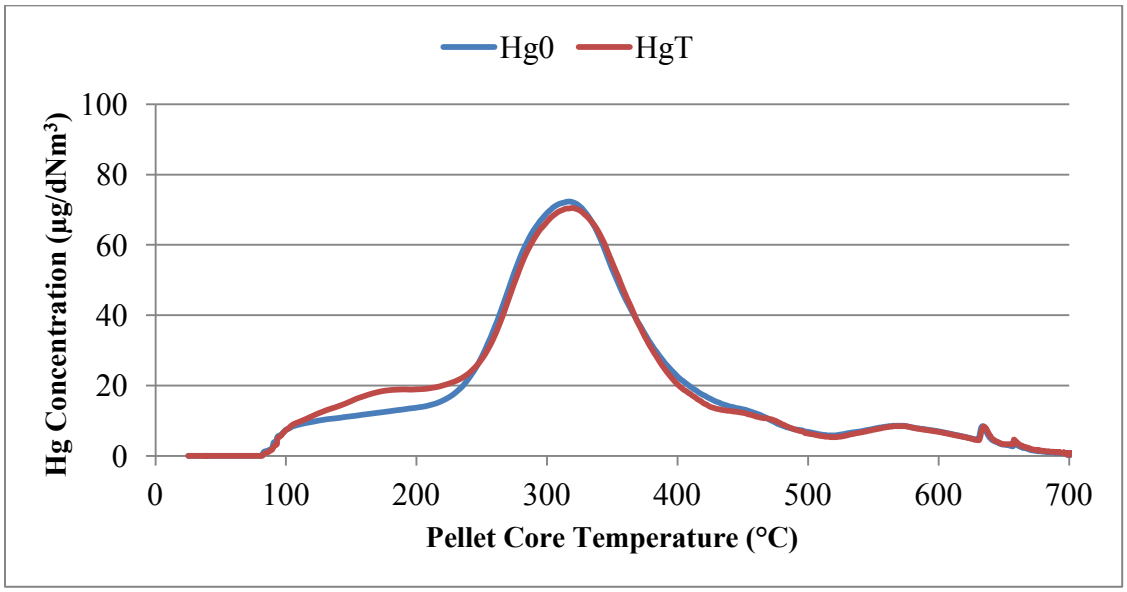

Figure 51 : Mercury release profile from Keetac green ball baseline -1

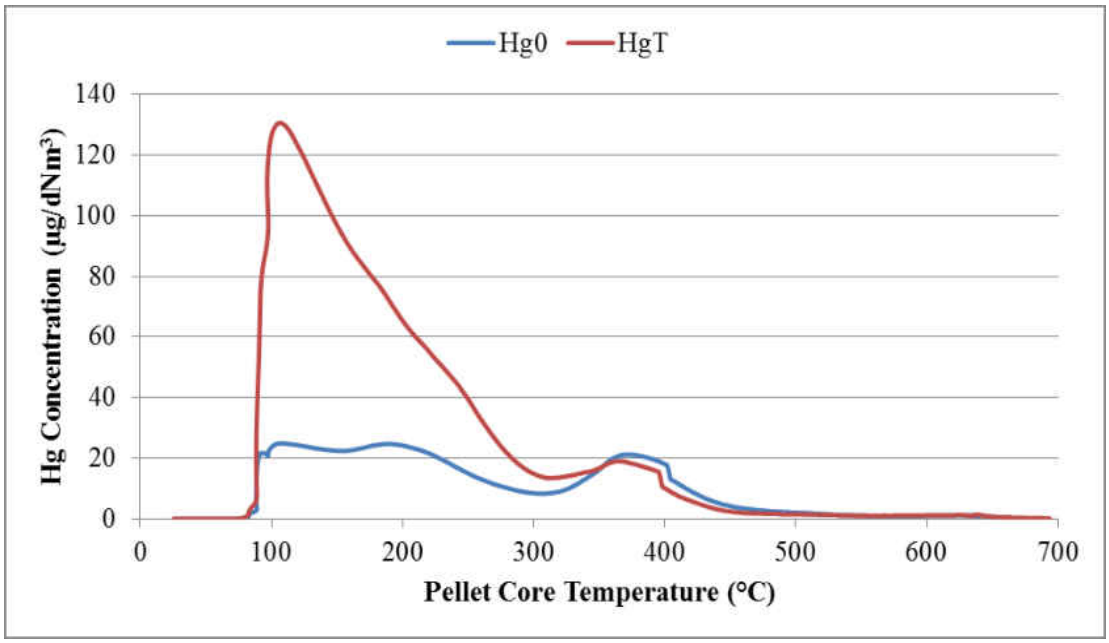

Figure 52 : Mercury release profile from Keetac green ball with 0.1 weight percent of ESORB-HG-11 -1

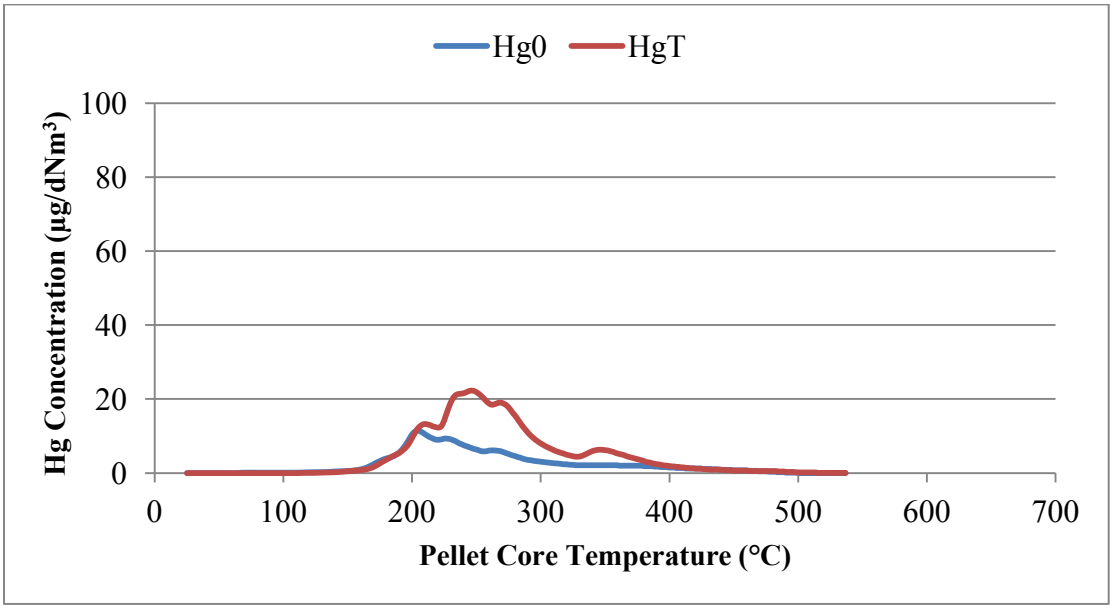

Figure 53 : Mercury release profile from Keetac green ball with 0.5 weight percent of ESORB-HG-11 -1

III. Arcelor Mittal Results

Results from Arcelor Mittal tests are summarized in Table 21. Ten experiments were carried out in the Arcelor Mittal set which includes triplicates for baseline, triplicates for 0.5 weight percent loading and duplicates for 0.1 weight percent and its replicated batch. Average percent oxidation for baseline was found to be 19.87%. Higher oxidation levels were observed for 0.1 and 0.5 weight percent loading. For 0.1 weight percent loading, an average oxidation level of 56.90% was observed. The replicated batch of 0.1 percent gave an oxidation level of 48.20%. Close agreement in these two levels prove the reliability of the batch balling procedure and the testing equipment. For 0.5 percent, oxidation level of 53.30% was observed which is in close accordance with 0.1 weigh percent loading. Hence, higher amount of additive does not have any significant effect on the oxidation level.

Cumulative total mercury release profiles are shown in Figure 57 while cumulative elemental mercury release profiles are summarized in Figure 58. These diagrams are in accordance with Minntac profiles. In region A, the amount of mercury released from runs with additive are higher than that from the baseline runs. Careful observation from the plots reveals that in Region C (400-500°C), the slope for 0.1 weight percent and 0.5 weight percent increases. After careful review of all the plots, it is determined that more release and oxidation occurs at the beginning of the experiment which is at lower temperatures. These runs were performed randomly over a period of time and hence a possible cause was not fully determined.

Table 21 : Arcelor Mittal Test Results – Phase II

Additive Loading (weight percent)	Percent Oxidation	Average Percent Oxidation	Percent Reduction	Average Percent Reduction
0 (Baseline)	20.00%	19.87%	N/A	N/A
0 (Baseline)	20.80%			
0 (Baseline)	18.80%			
0.1	66.40%	56.90%	58.07%	34.00%
0.1	47.40%		34.36%	
0.1 (Replicate)	53.40%	48.20%	41.85%	35.36%
0.1 (Replicate)	43.00%		28.87%	
0.5	49.90%	53.30%	37.48%	41.72%
0.5	60.10%		50.21%	
0.5	49.90%		37.48%	

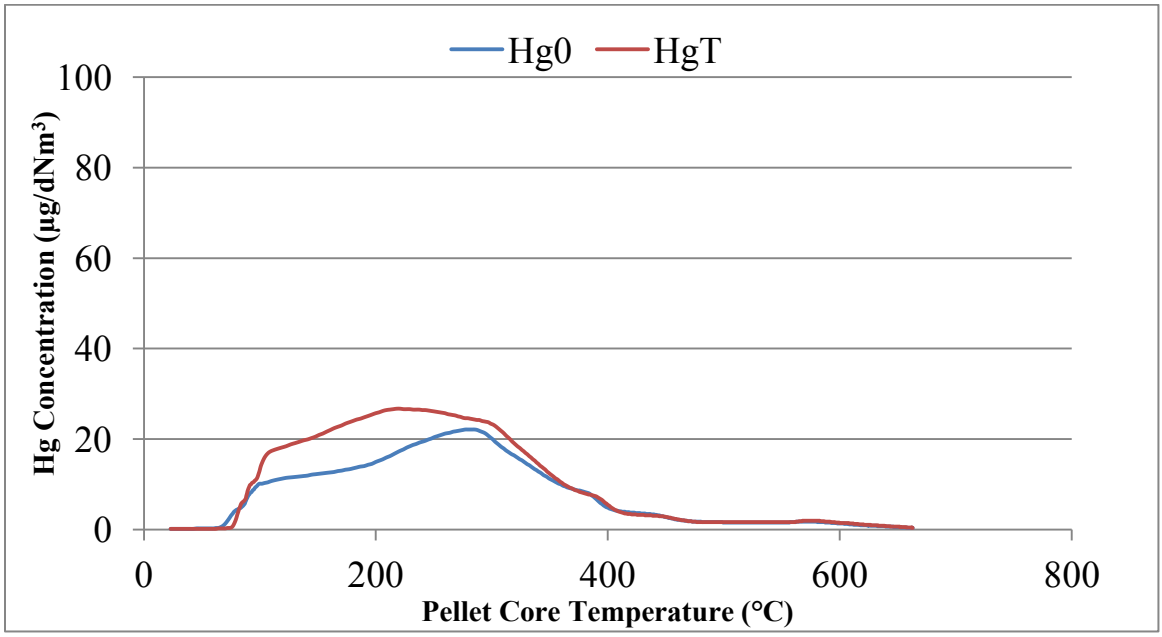

Figure 54: Mercury release profile from Arcelor Mittal green ball baseline -1

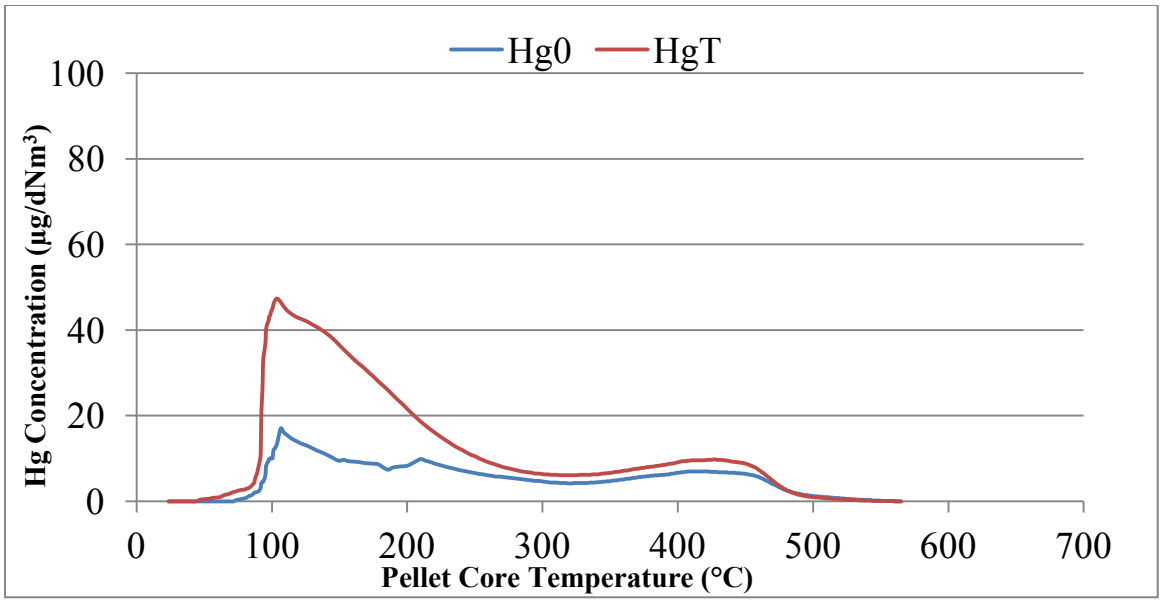

Figure 55 : Mercury release profile from Arcelor Mittal green ball with 0.1 wt% of ESORB-HG-11 -1

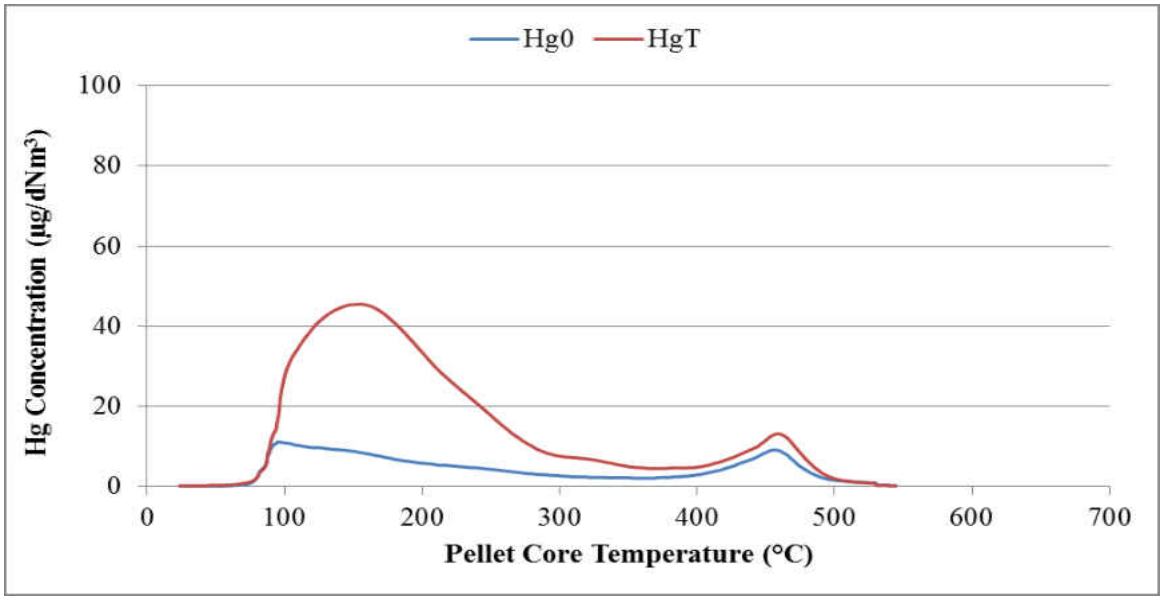

Figure 56 : Mercury release profile from Arcelor Mittal green ball with 0.5 wt% of ESORB-HG-11 -1

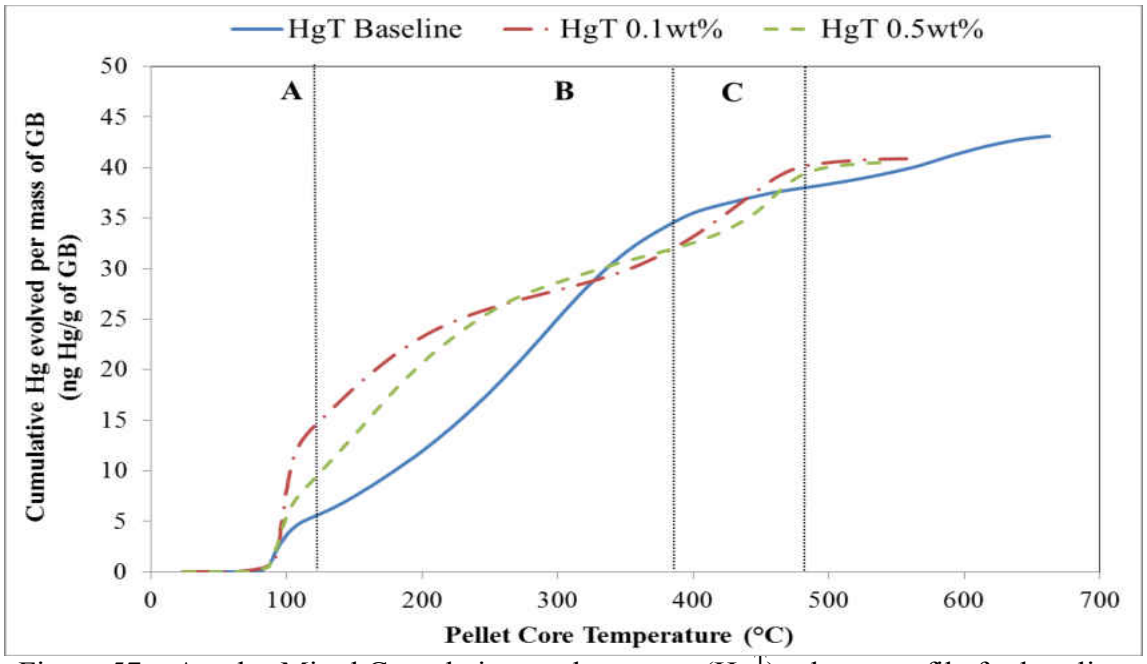

Figure 57 : Arcelor Mittal Cumulative total mercury (Hg^T) release profile for baseline, 0.1wt% and 0.5wt%; as a function of temperature.

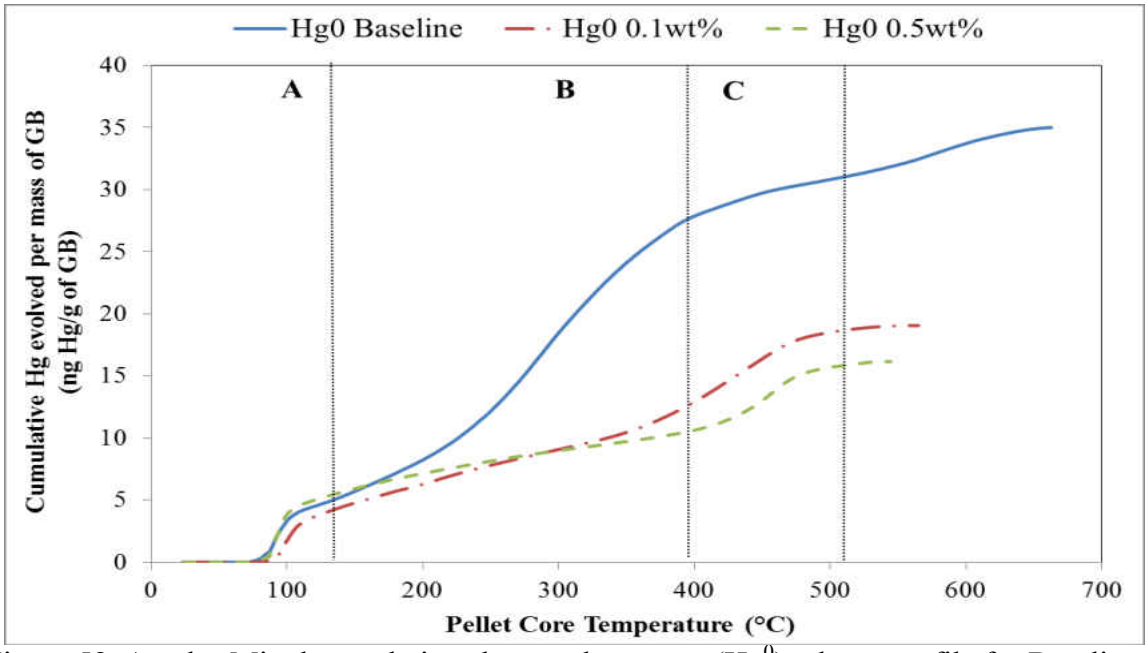

Figure 58. Arcelor Mittal cumulative elemental mercury (Hg^0) release profile for Baseline, 0.1wt% and 0.5wt%.

IV. Utac Results

Results obtained from Utac green ball testing are summarized in Table 22. In total, 10 runs were performed with Utac green balls. However, results from one run (0.1 weight percent carbon loading) were discarded during quality control assessment tests after the experiment. It was found that the reactor had some leakage issues which were fixed before the testing proceeded. Hence, in total there were triplicates of baseline, and duplicates from all other batches. 0.5 weight percent had a replicated batch which was duplicated during the runs.

Results from baseline were in close agreement with average being 21.67%. Additive loading of 0.1 weight percent gave an oxidation level of 36.8% where-as 0.5 weight percent loading gave 34.20% and 37.15% respectively. Hence, oxidation percentage ranges over 34 to 37 % and also shows 16 to 19% average percent reduction. Clearly, this is not a significant oxidation level. Figures 59, 60, 61 illustrate the mercury concentration obtained versus pellet bed temperature. It is clear from these graphs that lower oxidation levels are observed in case of Utac green balls. The possible reason for lower oxidation level could not be established during Utac green ball testing. Also, the cumulative percentage plots are not included due to the variation in the data. There was very less similarity observed in the cumulative plots and hence it was hard to get to a solid conclusion. Consequently, it was impossible to plot one run which can be representative of the other runs.

Table 22 : Utac Test Results – Phase II

Additive Loading (weight percent)	Percent Oxidation	Average Percent Oxidation	Percent Reduction	Average Percent Reduction
0 (Baseline)	25.70%	21.67%	N/A	N/A
0 (Baseline)	19.70%			
0 (Baseline)	19.60%			
0.1	32.90%	36.80%	14.34%	19.32%
0.1	40.70%		24.30%	
0.5	33.90%	34.20%	15.62%	16.00%
0.5	34.50%		16.38%	
0.5 (Replicate)	28.10%	37.15%	8.21%	19.77%
0.5 (Replicate)	46.20%		31.32%	

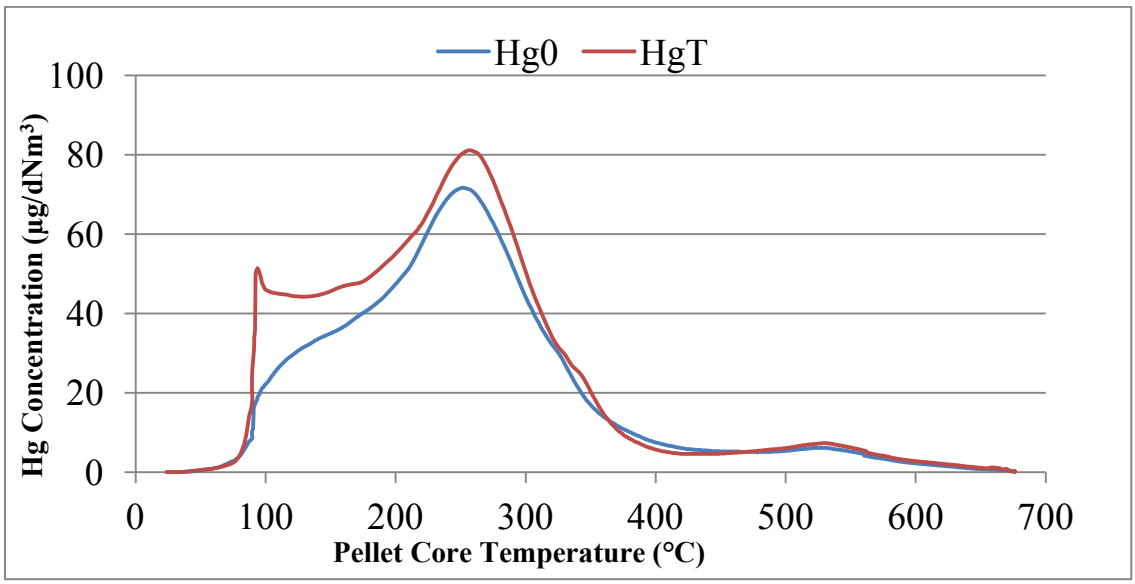

Figure 59 : Mercury release profile from Utac green ball baseline -1

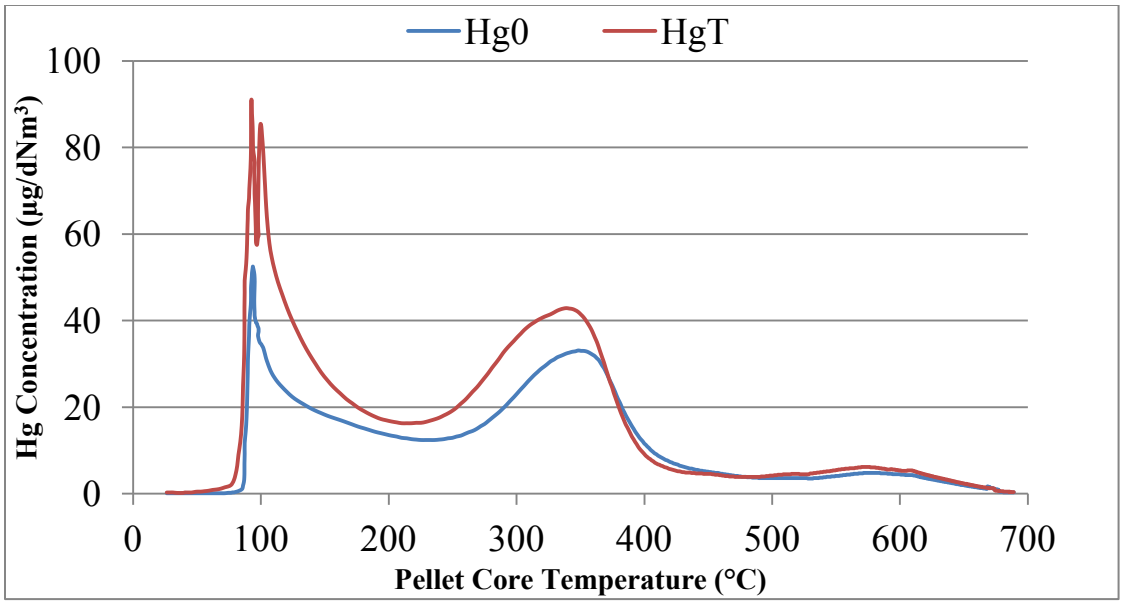

Figure 60 : Mercury release profile from Utac green ball with 0.1 wt% of ESORB-HG-11 -1

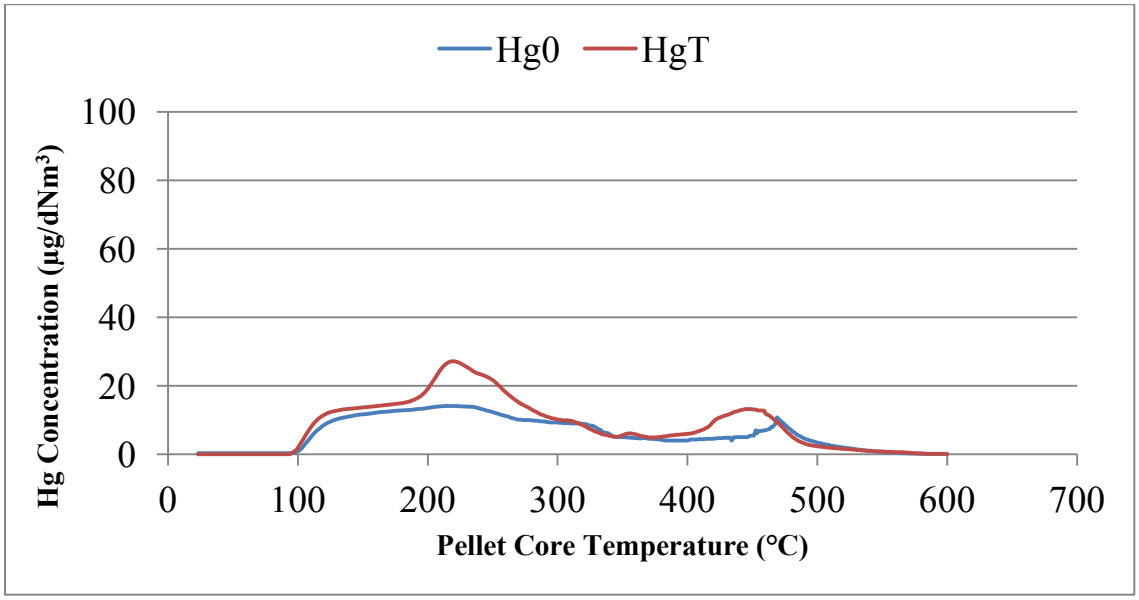

Figure 61 : Mercury release profile from Utac green ball with 0.5 wt% of ESORB-HG-11 -1

V. Hibtac – Standard Pellet Results

Hibtac tests were divided into two sets. First set includes testing of standard composition of pellets and second set includes the testing of high compression pellet. First formulation was evaluated with 10 runs which include triplicates of baseline and 0.1 weight percent loading of additive. Testing was also carried out in duplicates of 0.5 weight percent and its replicated batch.

Results from baseline testing gave the average baseline oxidation percent as 14.03%. 0.1 weight percent loading gave an oxidation level of 54.57% which in accordance with other plants. 0.5 weight percent loading gave an oxidation level of 60.90% where as the replicated batch gave an oxidation percentage of 56.75%. The close agreement between the experiment and its replicates proves the reliability of the batch balling procedure and testing equipment. The ESORB-HG-11 reduction potential was determined to be 47.15% and 52.15%. A percent analysis was not carried out on Hibtac standard pellet results since the release profiles were dissimilar in nature. However, results showed that the additive is a good solution to reduce mercury emissions.

Table 23 : Hibtac – Standard Pellet Results Test Results – Phase II

Additive Loading (weight percent)	Percent Oxidation	Average Percent Oxidation	Percent Reduction	Average Percent Reduction
0 (Baseline)	12.50	14.03	N/A	N/A
0 (Baseline)	21.60			
0 (Baseline)	8.00			
0.1	52.70	54.57	44.98	47.15
0.1	58.80		52.07	
0.1	52.20		44.40	
0.5	44.10	60.90	34.97	54.52
0.5	77.70		74.06	
0.5 (Replicate)	44.70	56.75	35.67	49.69
0.5 (Replicate)	68.80		63.71	

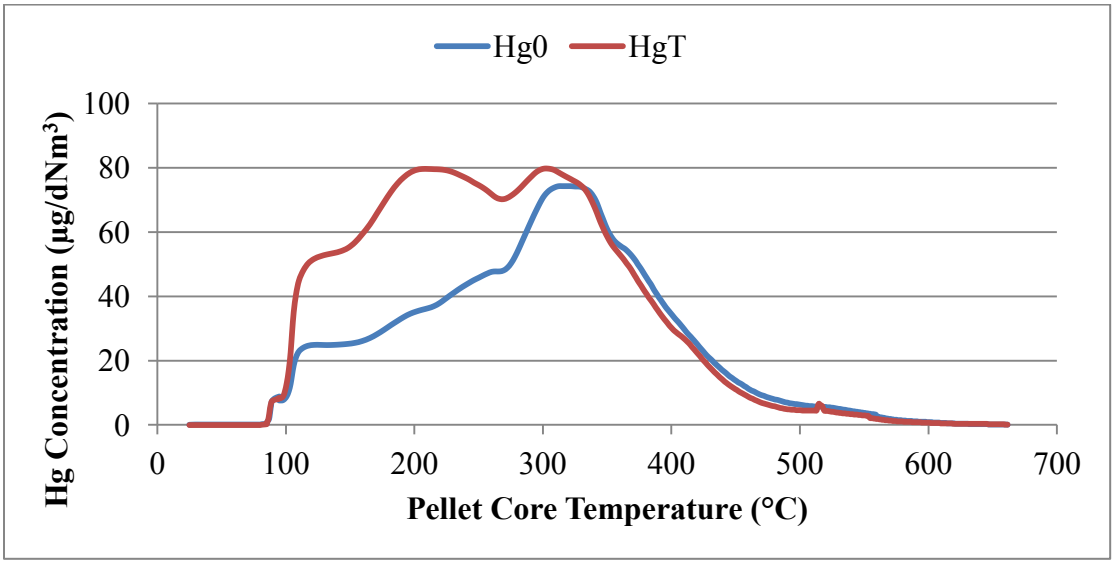

Figure 62: Mercury release profile from Hibtac – Standard green ball baseline -1

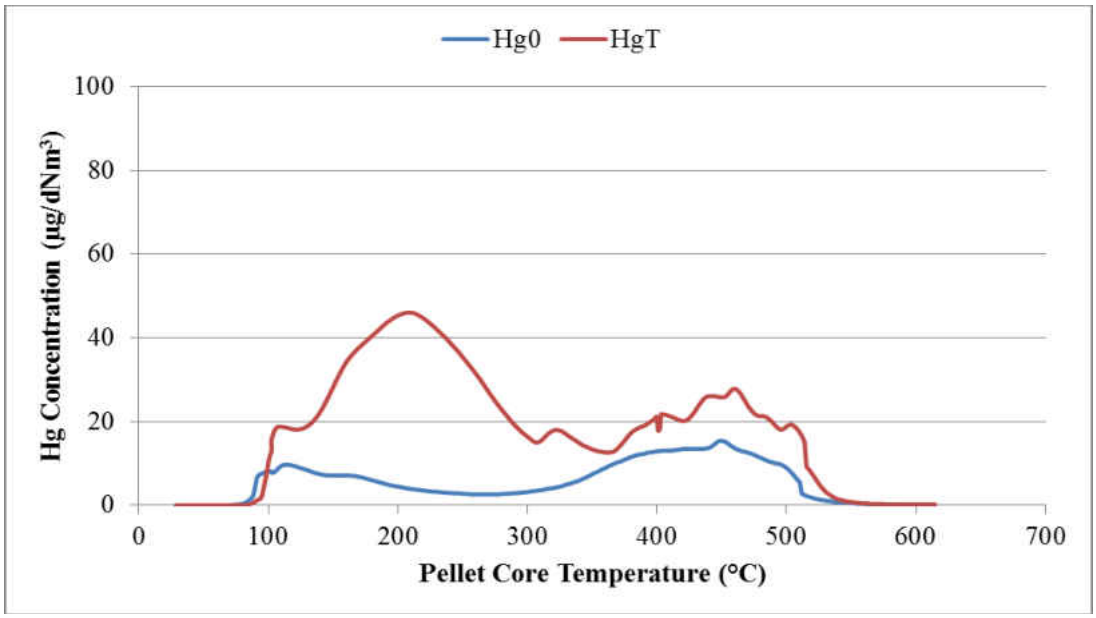

Figure 63 : Mercury release profile from Hibtac – Standard green ball with 0.1 wt% of ESORB-HG-11 -1

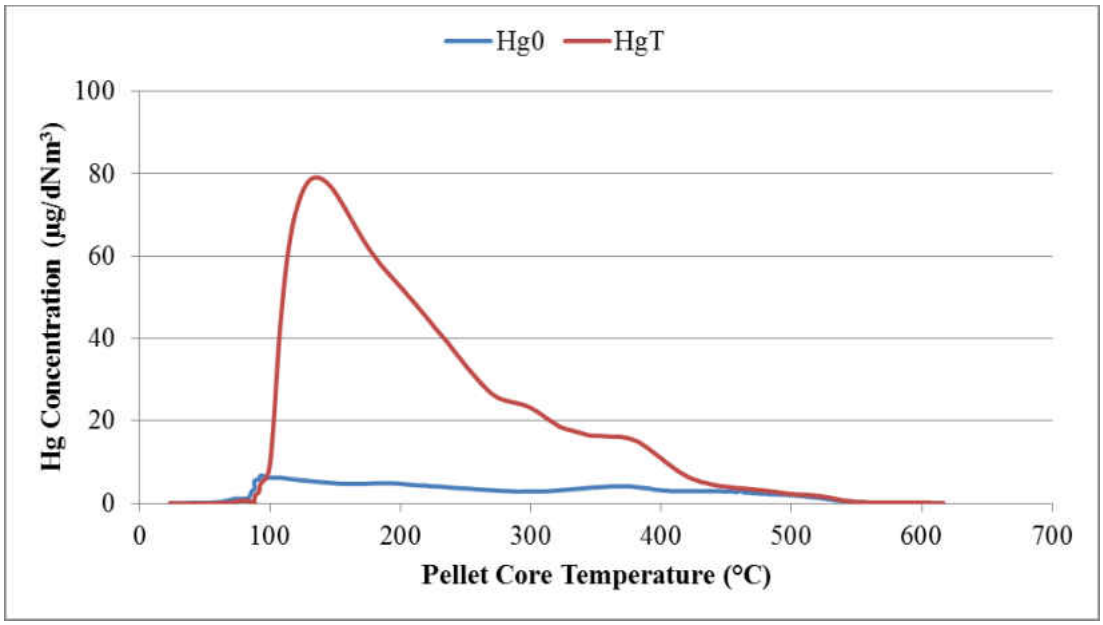

Figure 64 : Mercury release profile from Hibtac – Standard green ball with 0.5 wt% of ESORB-HG-11 -1

VI. Hibtac – High Compression Pellet Results

Results from the Hibtac high compression pellet tests are summarized in Table 24. Testing involved 10 runs of experiments which include triplicates of 0.1 weight percent and 0.5 weight percent and duplicates of baseline and its replicated batch. Average percent oxidation for baseline was calculated to be 10.10% which is lower than all other plants. 0.1 weight percent and 0.5 weigh percent gave 49.53% and 62.80% average oxidation. The mercury reduction was observed to be 39.67% and 55.53% respectively.

The observed release profiles of the experiments are mentioned in figures 65, 66 and 67. The release profiles for the runs were dissimilar and making a percentage graph was not feasible. However, results show very good agreement with other plants and hence it proves that additive was effective in oxidizing mercury.

Table 24 : High Compression Pellet Results Test Results – Phase II

Additive Loading (weight percent)	Percent Oxidation	Average Percent Oxidation	Percent Reduction	Average Percent Reduction
0 (Baseline)	15.10%	10.10%	N/A	N/A
0 (Baseline)	5.10%			
0(Baseline Replicate)	22.00%	22.60%	N/A	N/A
0(Baseline Replicate)	23.20%			
0.1	45.10%	49.53%	34.37%	39.67%
0.1	47.60%		37.36%	
0.1	55.90%		47.28%	
0.5	46.80%	62.80%	36.40%	55.53%
0.5	75.10%		70.23%	
0.5	66.50%		59.95%	

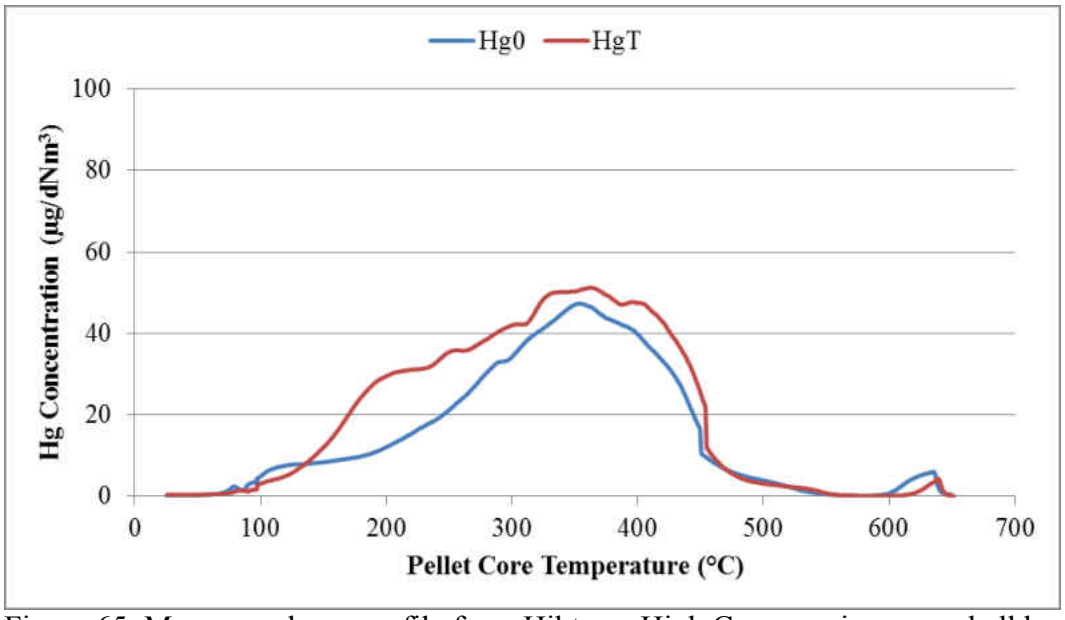

Figure 65: Mercury release profile from Hibtac – High Compression green ball baseline -1

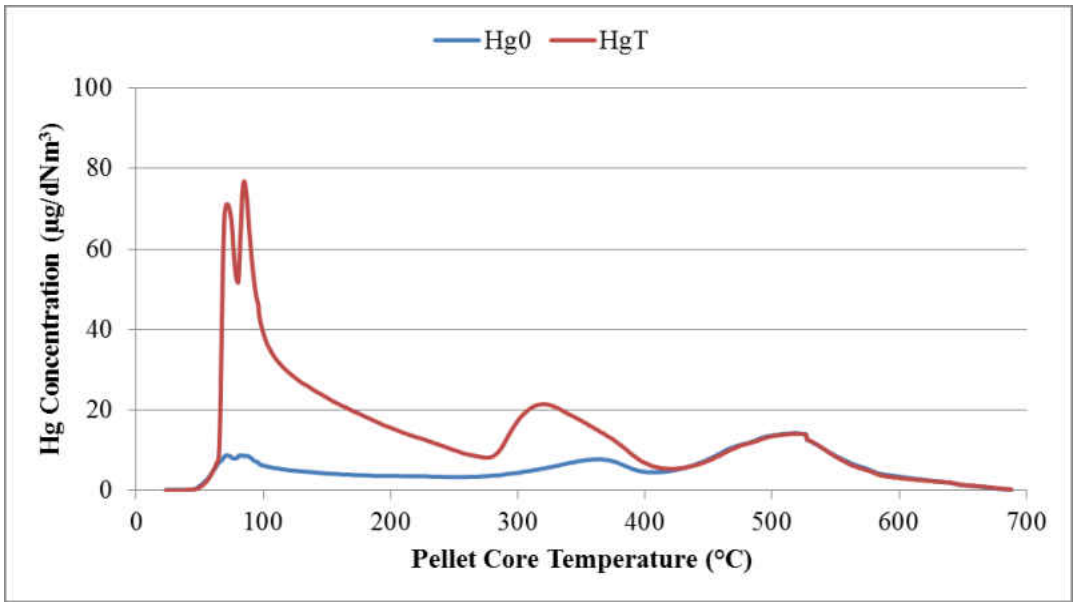

Figure 66 : Mercury release profile from Hibtac – High Compression green ball with 0.1 wt% of ESORB-HG-11 -1

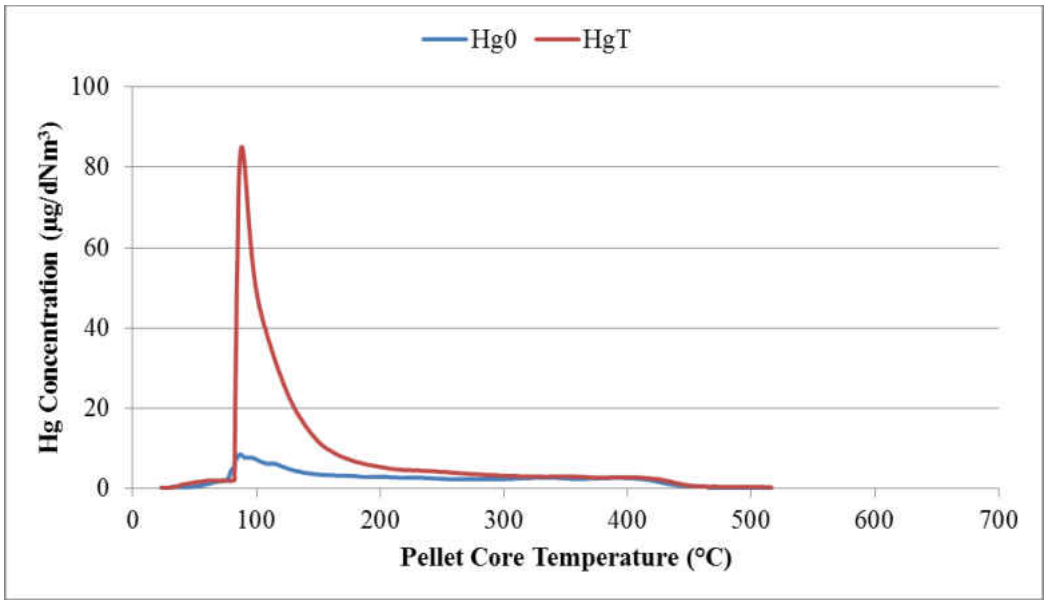

Figure 67 : Mercury release profile from Hibtac – High Compression green ball with 0.5 wt% of ESORB-HG-11 -1

4.5 Conclusion – Phase II

In Phase II, six different formulations of green balls were tested under similar conditions. This testing covers five taconite facilities operating on Mesabi Iron Range. All of them showed that the additive (ESORB-HG-11 - brominated activated carbon) has the ability to oxidize mercury when incorporated in the green ball and hence in turn, it can reduce the mercury emissions. All the green balls tested in Phase II were produced by Coleraine Minerals Research Laboratory (CMRL) of the Natural Resource Research Institute. Green balls were produced with the industry standard and formulation. Effect of addition of ESORB-HG-11 to green balls was studied in physical tests like moisture content, wet drop number and dry compressive strength. Results from these tests shows that there is no significant effect of addition of ESORB-HG-11 with respect to baseline runs. Slight differences were observed with 0.5 weight percent loading which needs further investigation.

Green balls containing ESORB-HG-11 showed high potential of mercury oxidation. The oxidation levels of green balls were within 29 to 74 % except for green balls obtained from United Taconite. The oxidation levels are summarized into the Figure 68. Baseline oxidation gave an average of 18 % with a standard deviation of 6% for all the plants. 0.1 weigh percent loading of ESORB-HG-11 gave reduction potential of 42% with a standard deviation of 9% and additive loading of 0.5 weigh percent gave reduction potential of 48% with a standard deviation of 13%. It is important to note that Utac data is not included in these calculations.

The close agreement in the results of all the plants shows that ESORB-HG-11 is an effective additive for mercury oxidation. The mercury oxidation is considered to occur on the surface of the pellet or the carbon. Gas phase oxidation is not considered significant in the lab scale testing. Hence, it can be easily concluded that there is higher potential of ESORB-HG-11 to reduce mercury emissions, if tested at the plant site. This claim can be supported by the previous studies. (1) Also, ESORB-HG-11 show good gas phase oxidation capabilities when added to flue gas at Minntac Line 3. [Taconite mercury emission control studies – Project 1 DNR]. After the review of all the results obtained in Phase I and Phase II, it was concluded that 0.1 weight percent of ESORB-HG-11 will be an optimum loading for full scale demonstration of the technology.

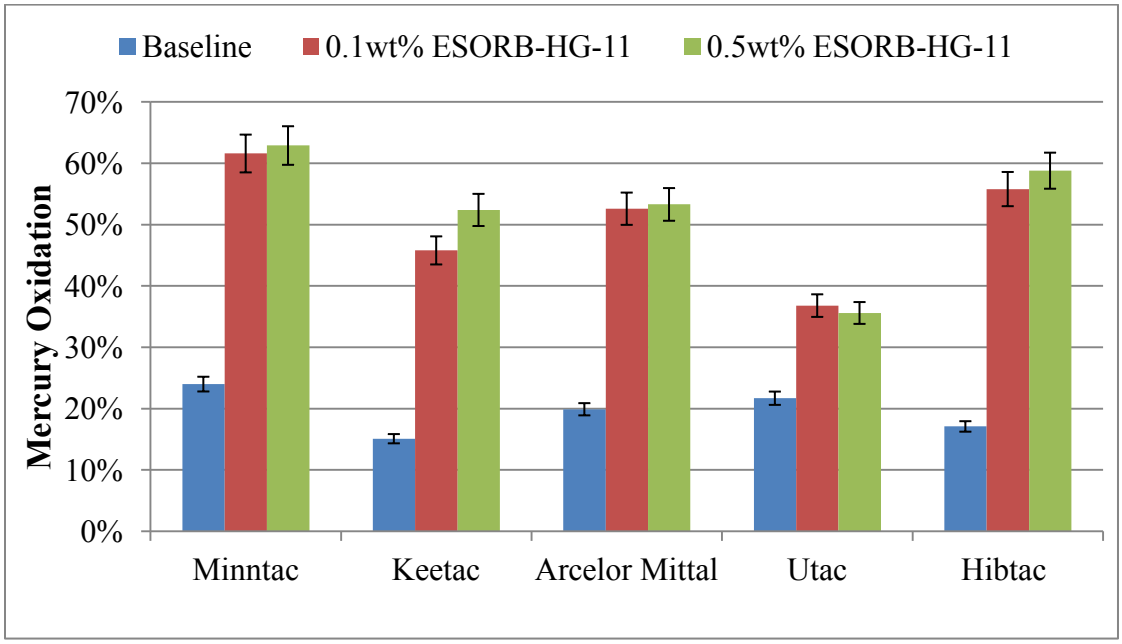

Figure 68 : Reduction potential of ESORB-HG-11 for 0.1 and 0.5 weight percent.

CHAPTER V

PHASE ANALYSIS

Phase analysis was performed to get a key insight into the transformation of magnetite to hematite and its effect on the mercury release. Techniques such as X-ray diffraction (XRD), Mössbauer analysis and Thermo Gravimetric Analysis/Differential Scanning Calorimetry (TGA/DSC) were used to gain a better understanding of the phase change. This chapter is broadly divided into two sections namely Phase I and Phase II.

Phase I testing involved the analysis of Minntac green balls collected in February, 2012. Phase II analysis was carried on the Utac, Minntac and Arcelor Mittal green ball samples prepared at CMRL in June, 2012.

Phase I

In Phase I, preliminary analysis was performed on the green balls (Unheated) and fired pellets (green balls heated at different temperatures). This study correlates the release and oxidation of mercury to the transformations of iron components in the taconite material. In order to understand the phase change of magnetite to hematite, XRD and Mössbauer spectroscopy analysis was carried out on three samples namely an unheated sample, sample heated at 400°C and sample heated at 700°C.

XRD Analysis

Figure 69 is the X-ray diffraction pattern obtained from the analysis of Minntac green balls at three different temperatures. It is a full spectra of identified phases excluding the non-magnetite and non-hematite phases. Secondary peaks were used to determine the intensities of magnetite and hematite peak due to the overlap of spectras at 35.5° position. However, at 33.2° position, hematite is clearly observed to be significant component. Baseline component gave the lowest intensity at 33.2° position whereas 700°C showed the highest intensity peak. This fact shows that with increasing temperature, magnetite concentration decreases and hematite concentration increases. This proves that magnetite is getting oxidized to hematite mostly between 400 °C and 700°C which is in accordance with the literature.

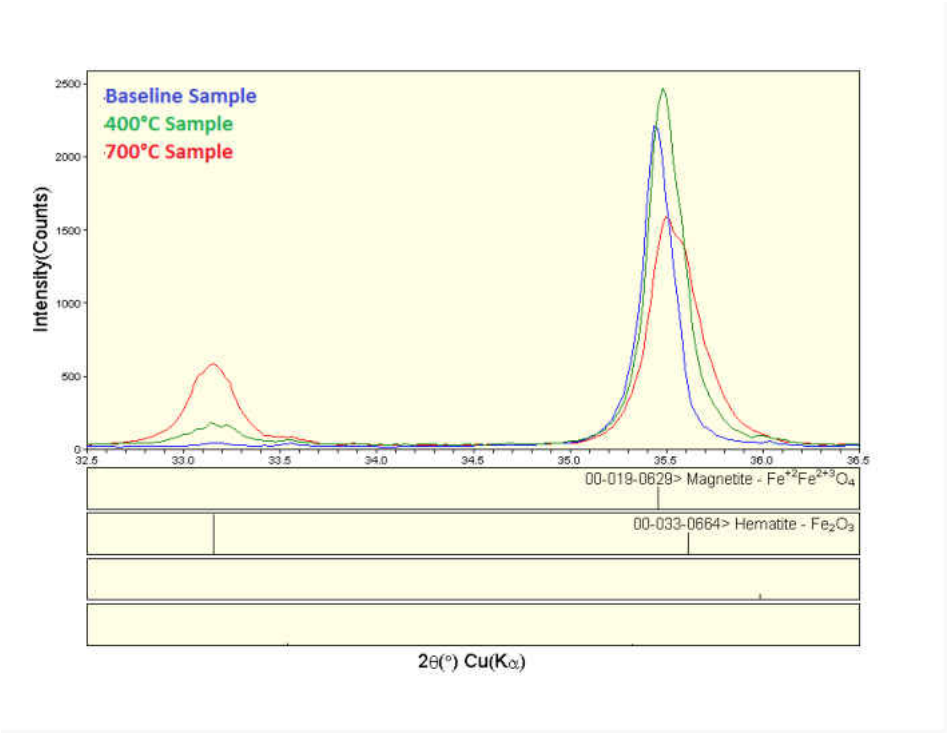

Figure 69: XRD Analysis of green balls fired at 400°C, 700°C and unheated sample

Mössbauer Analysis

Mössbauer Analysis was performed on three samples: baseline (pre-fired green ball), green ball fired at 400°C and green ball fired at 700°C to quantitatively determine the abundance of the forms of iron in the samples. The results from this test are summarized in Table 25. Figure 70 is the graphical representation of the results.

Magnetite A represents the octahedral sites while magnetite B represents the tetrahedral sites of magnetite. It clear from the results that the pre-fired green ball primarily has magnetite with an A/B ratio of 0.68. This value is very close to the value reported in the previous work, where Berndt et al. found a ratio of A/B as 0.72. (12) An unknown compound was observed in the pre-fired and 400°C samples which could not be attributed to any specific standard spectra. This compound is reported as unknown in the Table 25.

The sample from 400°C had higher ratio of A/B = 0.95. This leads us to the conclusion that the Fe ions on A site are undergoing an oxidation reaction at the higher temperature of 400°C. This could also indicate the formation of maghemite solid solution however; the spectra did not indicate the presence of maghemite conclusively. Spectra from 700°C sample shows a higher value of hematite as compared to other samples indicating that maghemite is converting to hematite around or before 700°C. It was concluded that to understand the complete mechanism of this conversion another sample of 1000°C needs to be evaluated. This sample was included in Phase II testing.

Table 25 : Mössbauer Analysis for Minntac Samples

I.D.	Temperature		
	25°C	400°C	700°C
Magnetite A	36	39	40
Magnetite B	53	41	33
Hematite	0	8	27
Unknown	11	12	0
Total	100	100	100

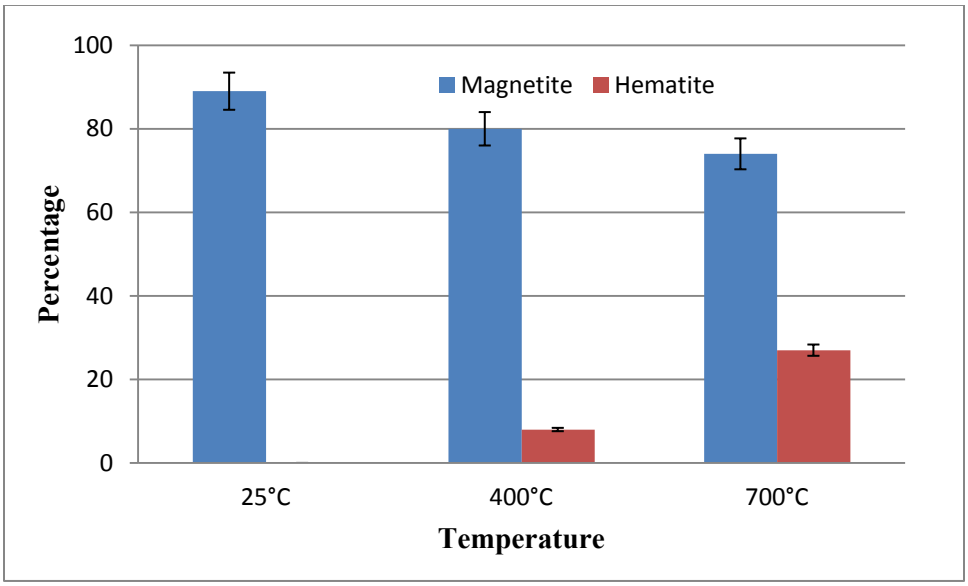

Figure 70 : Mössbauer Analysis for Minntac samples graphical representation

Phase II

In Phase I, it was concluded that magnetite gets oxidized to hematite with increase in temperature; however the completion temperature for this reaction was unknown. Hence, in Phase II, analysis was carried out on four different types of samples which includes pre-fired or unheated green ball, green ball fired at 400°C, green ball fired at 700°C and green ball fired at 1000°C. Test matrix for Phase II involves testing with four different formulations of green balls which includes Minntac baseline (no carbon), Minntac with 0.1 weigh percent additive, Utac with 0.1 weigh percent additive and Arcelor Mittal green ball with 0.1 weigh percent of additive.

In Phase II, XRD analysis, TGA analysis and Mössbauer Analysis were carried out on above mentioned samples to understand the temperatures at which oxidation of magnetite occurs. Mössbauer Analysis gave qualitative and quantitative information on the type of iron oxide (magnetite, maghemite or hematite) in the given sample with respective compositions. XRD is the qualitative analysis for compounds present in the different samples. TGA/DSC was used to provide the loss of mass as a function of temperature which gave us an insight into the oxidation temperature. These samples were also analyzed for their mercury content. Mercury content was analyzed with the help of EPA method 7471. Method 7471 – Mercury in Solid or Semisolid waste. The results are summarized in Table 26. The results obtained from these samples clearly indicate that most of the mercury release from green balls takes place before 400°C, which is in accordance with results obtained from the lab scale experiments mentioned in Chapter III and IV of this thesis.

Mercury Content Analysis

Table 26 : Mercury concentration in green balls heated to specific temperatures

	Minntac		Utac	Arcelor Mittal
Additive Loading	0	0.1	0.1	0.1
Temperature	Mercury Content(ng/g)			
25°C	6.6	25	26	5.7
400°C	N.D.	5.2	6.5	5.9
700°C	N.D.	5	N.D.	6.7
1000°C	N.D.	N.D.	N.D.	N.D.

N.D. = Not detect (Mercury concentration is below detection limits.)

Mössbauer Analysis

Mössbauer analysis results are summarized in Table 27, 28, 29 and 30 for Utac(0.1), Minntac(Baseline) , Minntac(0.1) and Arcelor Mittal (0.1), respectively. All of the results indicate that the 400°C sample has small quantities of hematite which gradually increases with temperature. All of the 1000°C samples did not have any magnetite concentration indicating that the oxidation reaction is complete and all the magnetite is been converted to the hematite. Graphical representation of all the results is summarized in Figure 71, 72, 73 and 74. It clear from the bar diagrams that magnetite concentration decreases with increase in temperature. The results also suggest that the oxidation of magnetite begins around 400°C and completes around 1000°C. Mössbauer analysis could not identify the presence of maghemite conclusively, however the data suggests the presence of maghemite in 400°C and 700°C sample. Maghemite is believed to play a role in the oxidation of mercury in taconite processes and hence it is important to understand the oxidation mechanism.

Table 27 : Mössbauer Analysis for Utac samples with 0.1 weight percent ESORB-HG-11

Temperature	I.D.	Percent Total
25°C	Magnetite A	37%
	Magnetite B	59%
	Unknown	4%
	Total	**100%**
400°C	Magnetite A	28%
	Magnetite B	47%
	Hematite	21%
	Unknown	4%
	Total	**100%**
700°C	Magnetite A	19%
	Magnetite B	20%
	Hematite	58%
	Unknown	3%
	Total	**100%**
1000°C	Hematite	93%

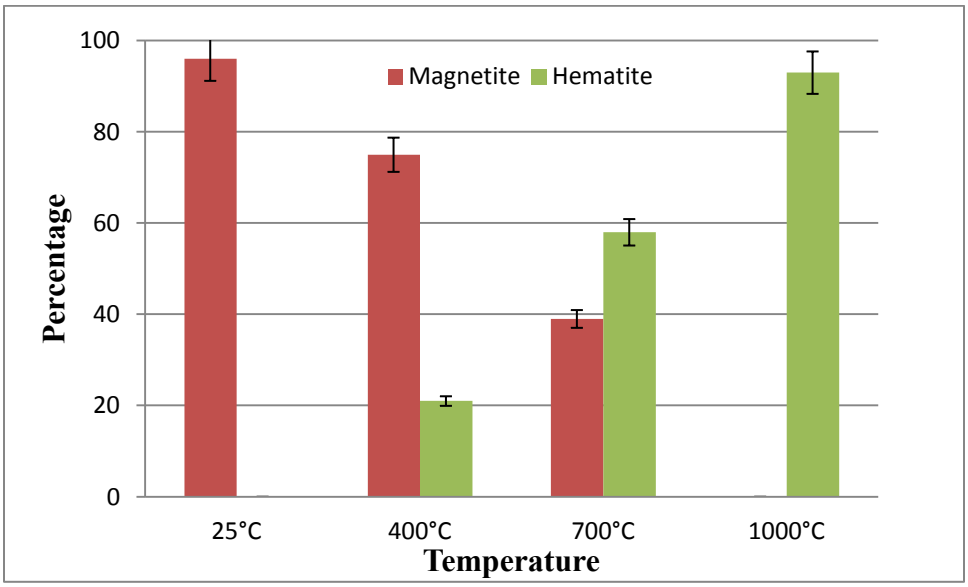

Figure 71 : Mössbauer Analysis for Utac samples with 0.1 weight percent ESORB-HG-11 graphical representation

Table 28 : Mössbauer Analysis for Minntac Baseline

Temperature	I.D.	Percent Total
25°C	Magnetite A	41%
	Magnetite B	56%
	Unknown	4%
	Total	**100%**
400°C	Magnetite A	28%
	Magnetite B	51%
	Hematite	13%
	Unknown	4%
	Total	**100%**
700°C	Magnetite A	28%
	Magnetite B	28%
	Hematite	45%
	Unknown	0%
	Total	**100%**
1000°C	Hematite	92%

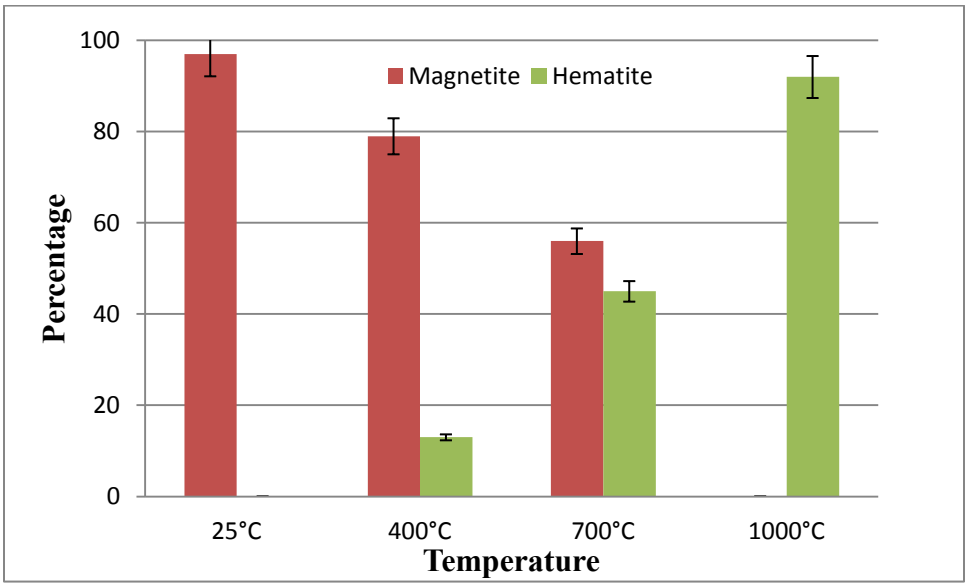

Figure 72 : Mössbauer Analysis for Minntac Baseline graphical representation

Table 29 : Mössbauer Analysis for Minntac samples with 0.1 weight percent ESORB-HG-11

Temperature	I.D.	Percent Total
25°C	Magnetite A	41%
	Magnetite B	56%
	Unknown	3%
	Total	**100%**
400°C	Magnetite A	31%
	Magnetite B	49%
	Hematite	17%
	Unknown	3%
	Total	**100%**
700°C	Magnetite A	28%
	Magnetite B	27%
	Hematite	44%
	Unknown	1%
	Total	**100%**
1000°C	Hematite	96%

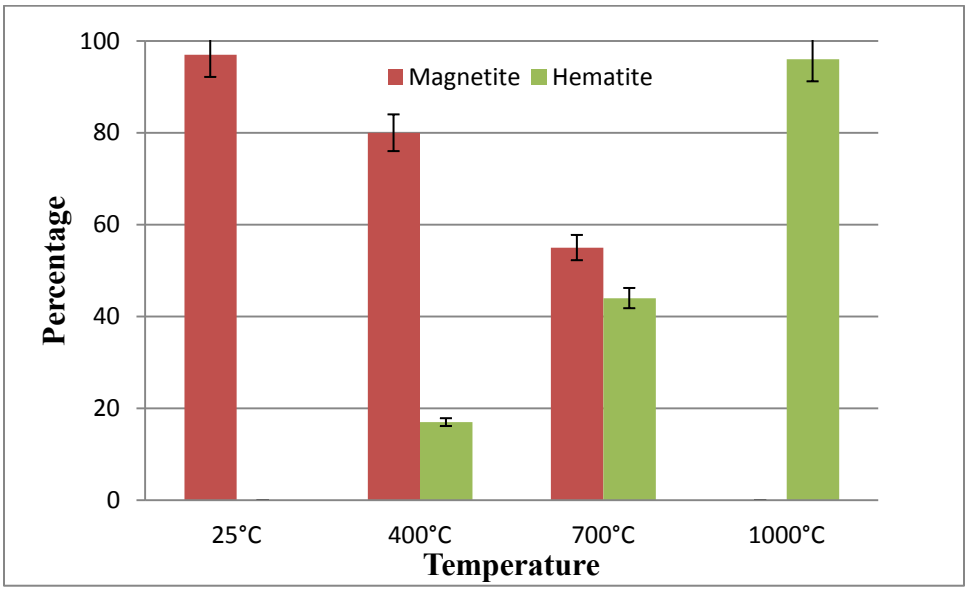

Figure 73 : Mössbauer Analysis for Minntac samples with 0.1 weight percent ESORB-HG-11 graphical representation

Table 30 : Mössbauer Analysis for Arcelor Mittal samples with 0.1 weight percent ESORB-HG-11

Temperature	I.D.	Percent Total
25°C	Magnetite A	39%
	Magnetite B	59%
	Unknown	3%
	Total	**100%**
400°C	Magnetite A	36%
	Magnetite B	49%
	Hematite	12%
	Unknown	2%
	Total	**100%**
700°C	Magnetite A	26%
	Magnetite B	31%
	Hematite	41%
	Unknown	2%
	Total	**100%**
1000°C	Hematite	91%

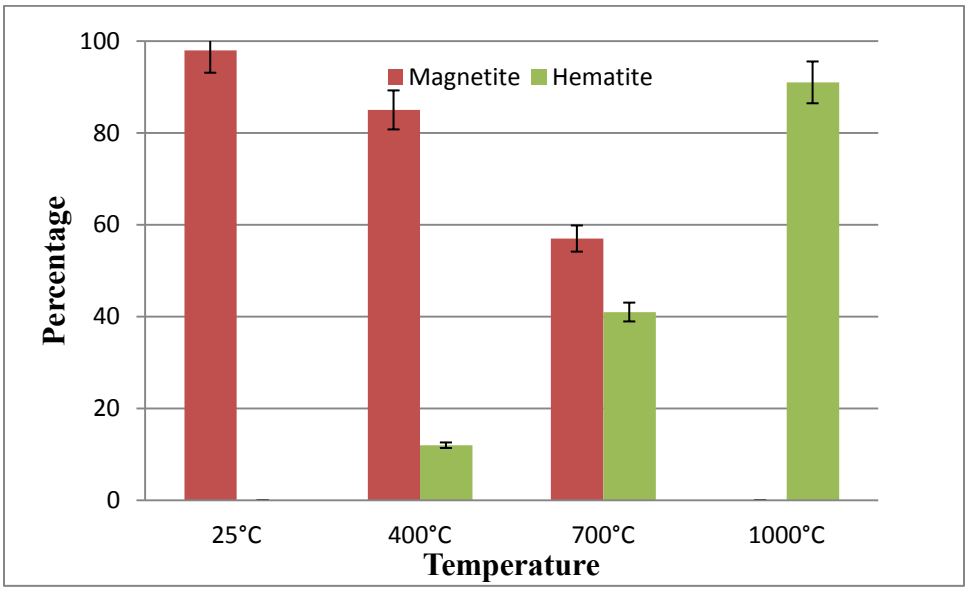

Figure 74 : Mössbauer Analysis for Arcelor Mittal samples with 0.1 weight percent ESORB-HG-11 Graphical representation

Thermo Gravimetric Analysis and Differential Scanning Calorimetry (TGA/DSC)

Results obtained from TGA/DSC are summarized in Figure 75, 76, 77 and 78. TGA/DSC consisted of heating the sample to 1100°C in air at a ramp rate of 20°C/min and held at 1100°C for approximately 10 mins. In all the obtained results, two significant drops are observed at the start of the experiment and around 700°C. The first drop was attributed to the loss of moisture from the green ball. The second drop was attributed to the calcinations of carbonated species (limestone or dolomite). A significant drop was not observed in Utac sample mostly likely due to the low level presence of limestone in the Utac green ball formulation.

Endotherms from the DSC are associated with the loss of moisture and decomposition of the carbonates. The heat flow is plotted against the temperature in the following diagrams. The basic principle of DSC is when the sample undergoes a physical transformation such as phase transitions, it will either liberate heat or it will absorb the heat. Hence, there will be a variation in the heat flow depending upon whether the process in endothermic or exothermic. The drop in the heat loss curve is attributed to process being endothermic and the gain of heat is attributed to exothermic reaction. It is clear from the graphs that conversion of magnetite to hematite is a exothermic reaction which is in accordance with the literature. (35) Also, the process of evaporation of moisture from green ball and the calcinations reactions are endothermic which is evident from the attached diagrams.

Heating the samples in nitrogen to 800°C followed by heating in air (Figure 76) showed a slight increase in mass between 350°C and 400°C. The similar type of profile is

observed in air samples. This confirms the results obtained from Mössbauer analysis which suggests the formation of hematite starts around 400°C.

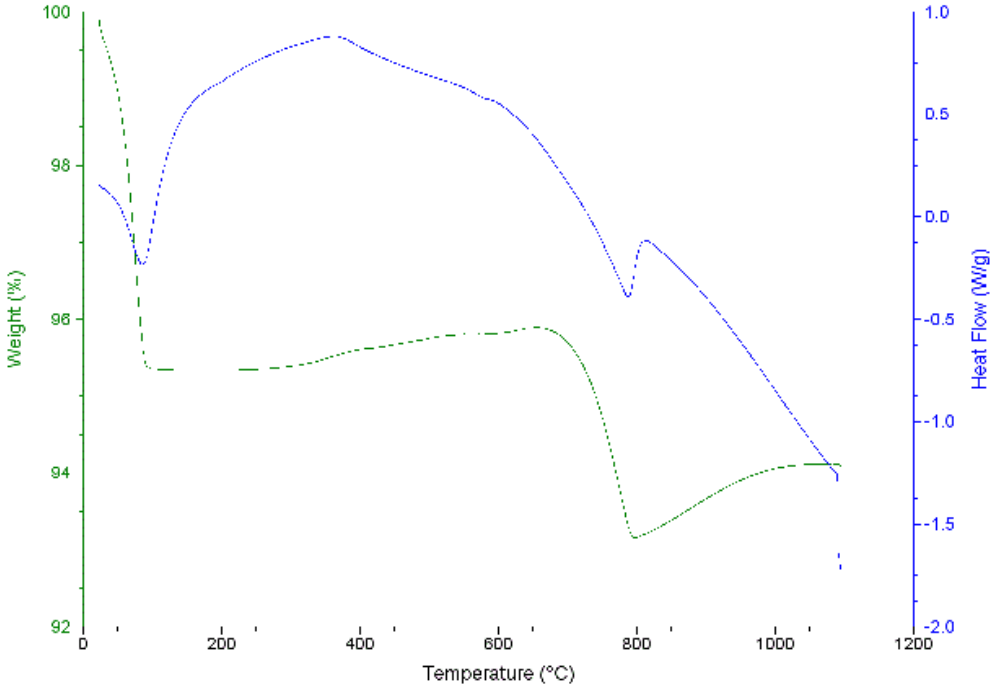

Figure 75 : TGA profile for Minntac green balls – baseline (air)

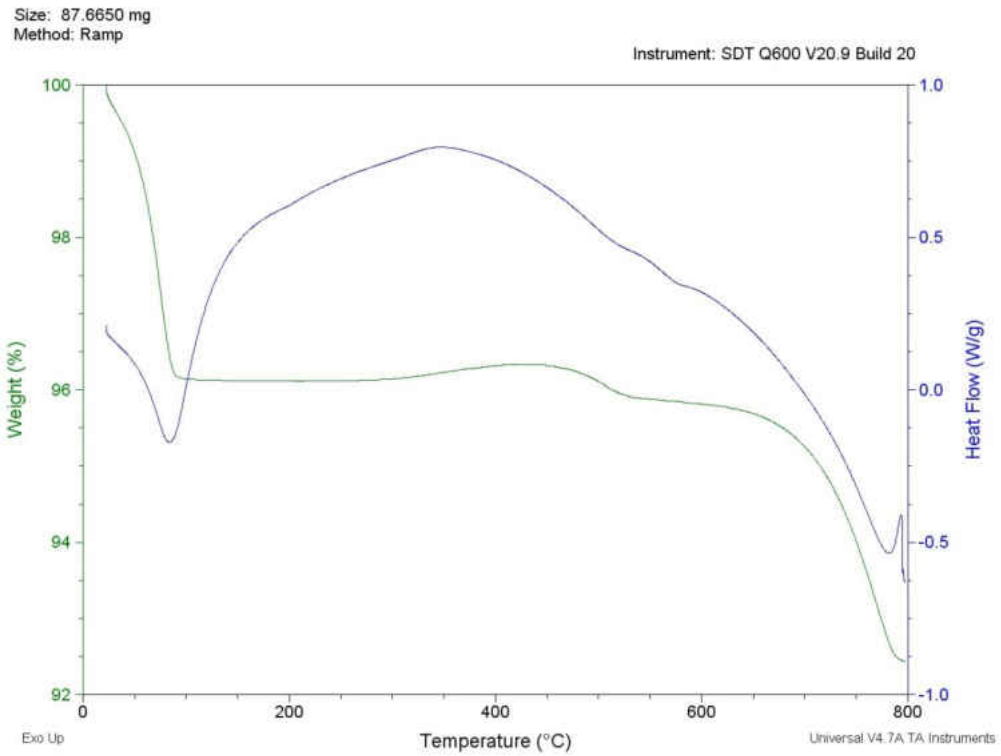

Figure 76 : TGA profile for Minntac green balls – baseline (Nitrogen)

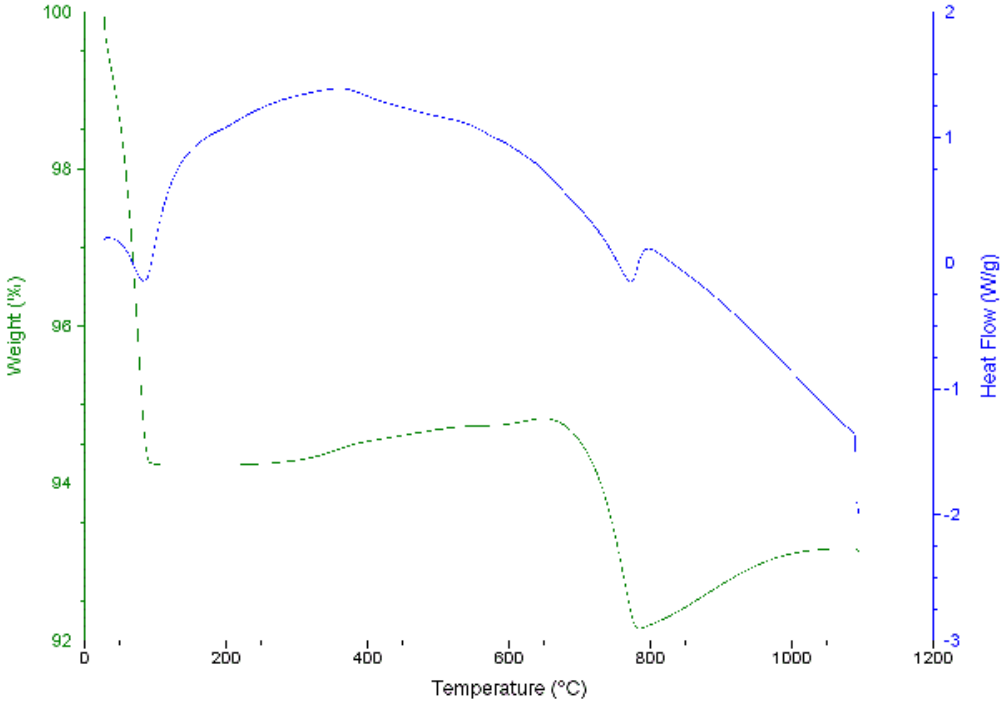

Figure 77 : TGA Profile for Minntac baseline with carbon in air

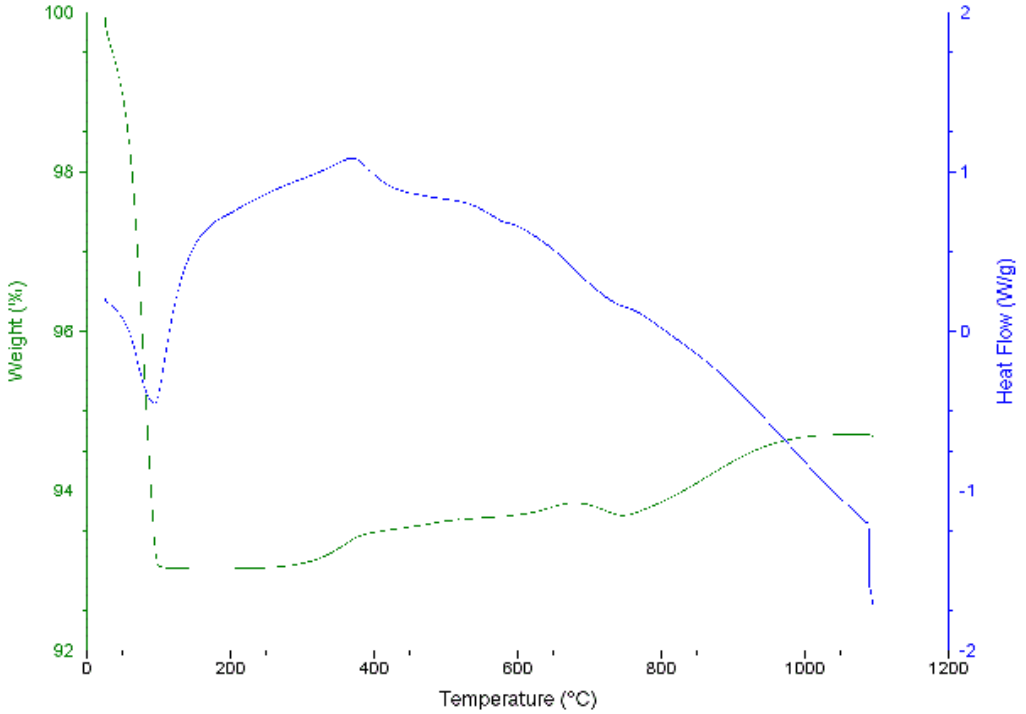

Figure 78 : TGA Profile for Utac baseline in air

XRD Analysis

Results from XRD analysis are summarized in Figure 79, 80, 81 and 82. All the results show an increase in hematite concentration with temperature which is in accordance with other analysis results.XRD results also confirmed the disappearance of carbonate species after 1000°C sample which confirms the validity of the results from TGA-DSC analysis.

Phase analysis proved the fact that oxidation of magnetite begins at 400°C. At this temperature, most of the mercury is released from the green balls. Mercury content of the green ball at 400°C is less than 25 percent of its original value. (Refer Table 26) and hence, this suggest that the mercury release from green balls takes place at a much lower temperature than 400°C and hence it is not a function of magnetite oxidation to hematite. However, previous work at the taconite plants suggested that the oxidation of magnetite to hematite plays a role in release of elemental mercury from green balls. (12) This difference can be due to the different process conditions used in lab scale apparatus as compared to the taconite processing plant. Air flow patterns at the plant are much more complex. Air from the higher temperature regions is re-circulated to heat up the lower temperature zones which mean that mercury released in the system re-contacts the green balls in colder zones. This can explain the difference in conclusions obtained at the lab scale experiments and field testing.

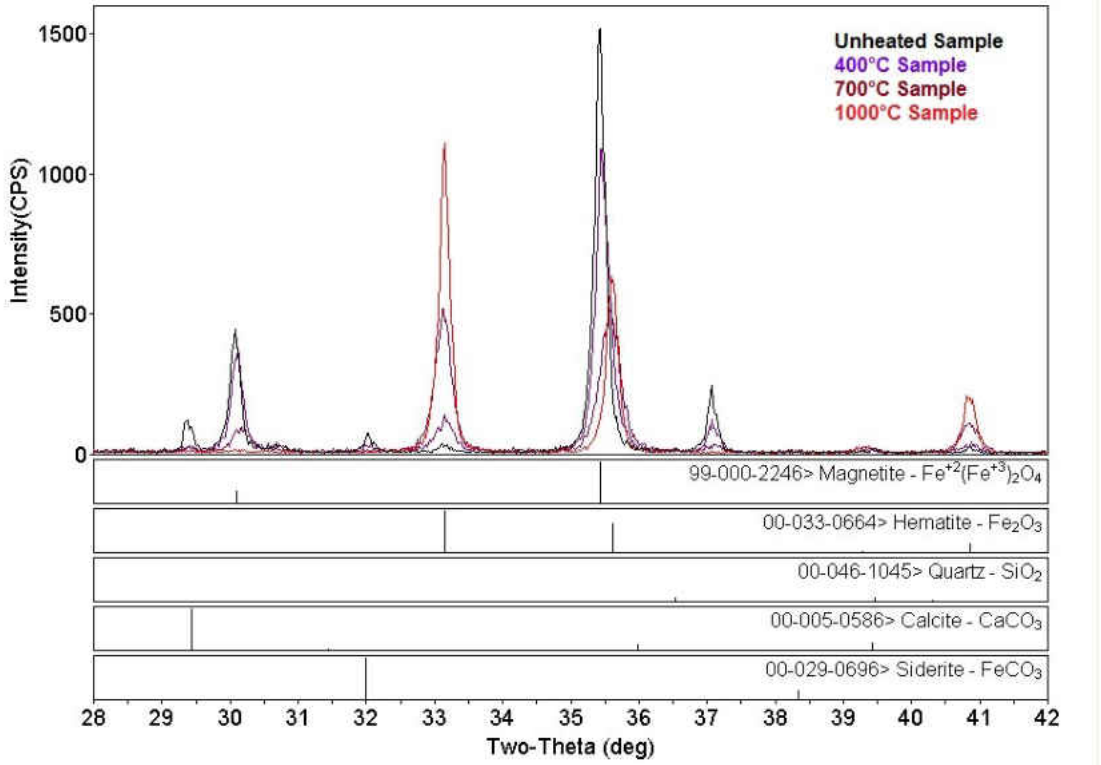

Figure 79 : XRD analysis for Utac samples with 0.1 weigh percent additive loading

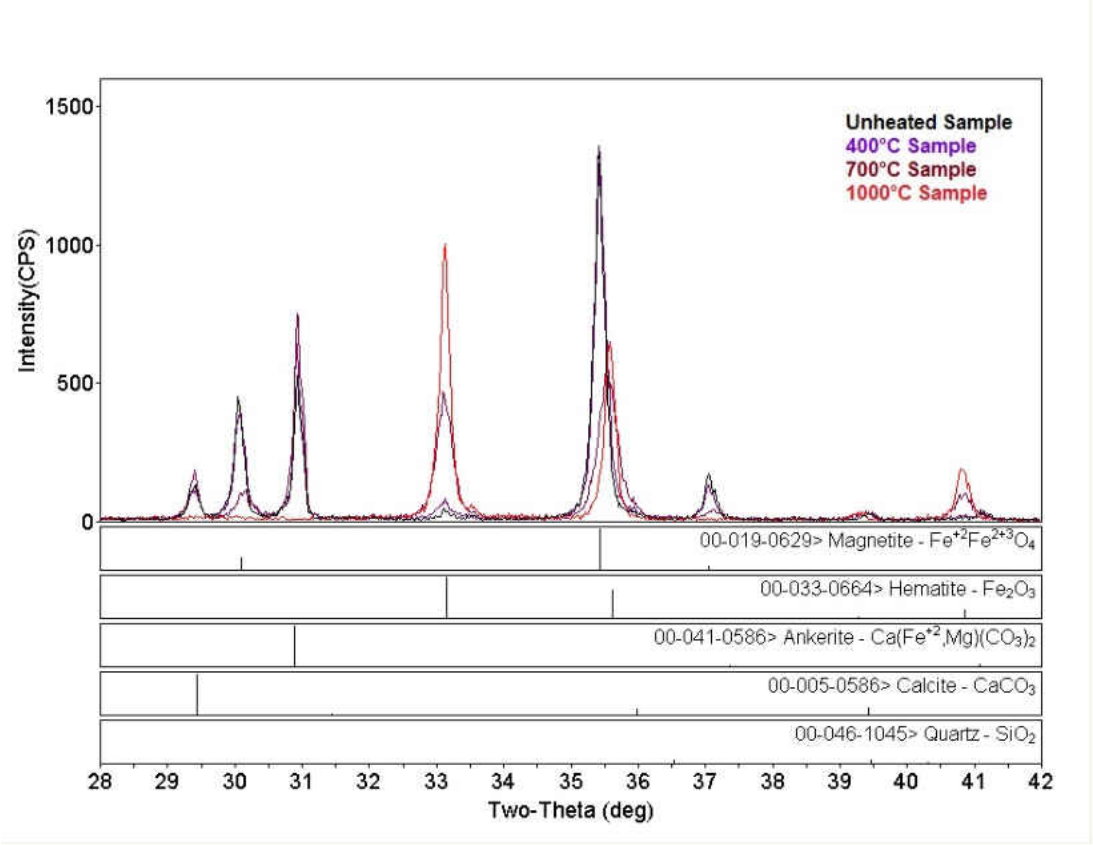

Figure 80 : XRD analysis for Minntac baseline samples

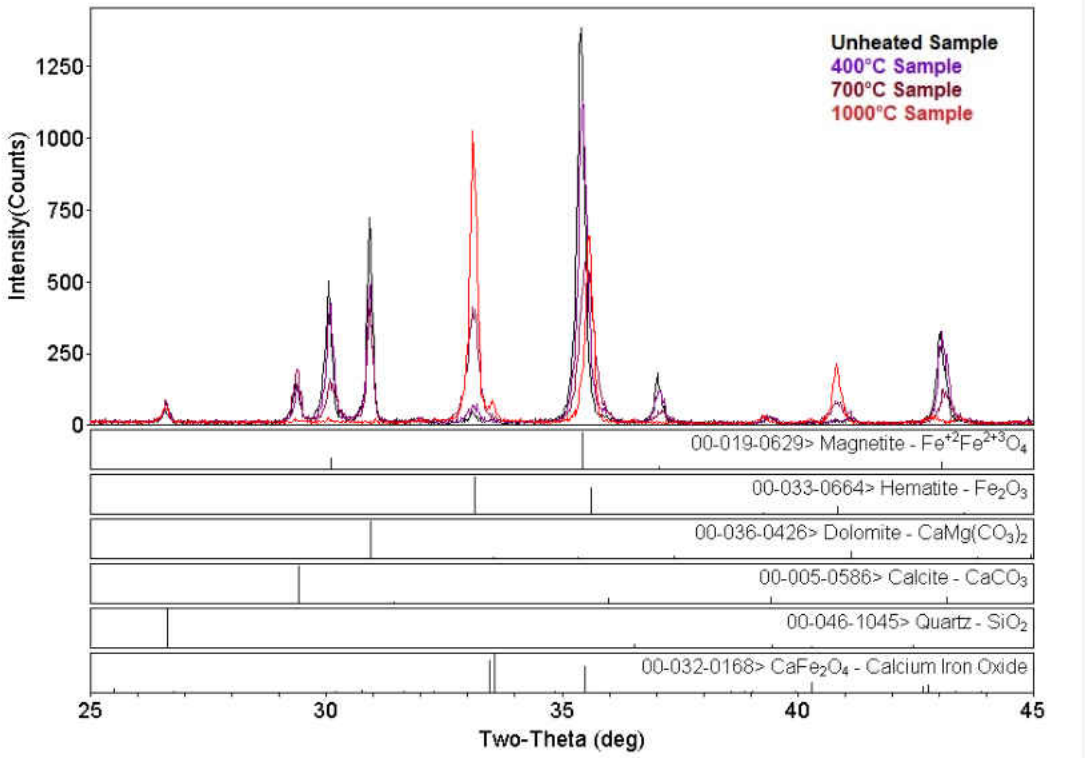

Figure 81 : XRD Analysis for Minntac samples with 0.1 weigh percent additive loading

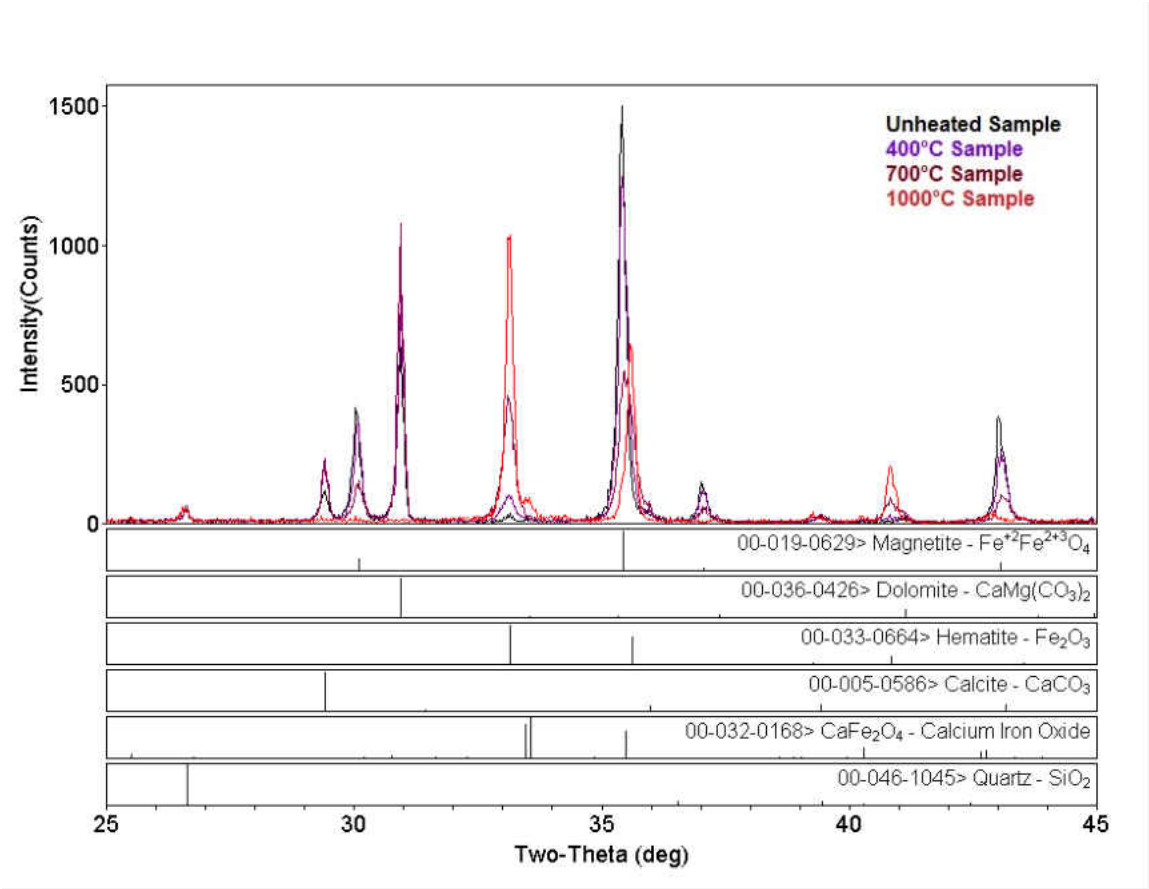

Figure 82 : XRD Analysis for Arcelor Mittal samples with 0.1 weigh percent additive loading

Scanning Electron Microscopy (SEM) analysis was carried out on samples to determine the propagation of magnetite to hematite when green ball is heated. Samples analyzed for SEM were ground to 200 mesh size and they were suspended in epoxy resin to enable polishing of the sample using diamond polishing wheel. Images obtained from SEM analysis did not show any observable difference on the surface of iron particles. It is proved from the analysis that the oxidation of magnetite to hematite occurs from the surface particle to core. This can explain the fact that magnetite gets oxidized and forms a layer of hematite on the surface. This could explain the reason behind the similarities observed in magnetite to hematite.

CHAPTER VI

CONCLUSIONS

A low corrosion method to increase mercury oxidation was evaluated on a lab scale setup by testing the green balls obtained from five different taconite facilities. It was found that ESORB-HG-11, a proprietary brominated activated carbon, when incorporated in green balls, has the potential to oxidize mercury and thus, improve its capture in scrubbers.

Testing was carried out in two phases: Phase I and Phase II. The experimental work performed in Phase I investigated the methods to incorporate additive into the green balls. It was found that the carbon addition to flue gas might not be a feasible method for ESORB-HG-11 addition. Hence, it was important to evaluate the carbon addition to green balls method. The testing covered green balls obtained from two different plants namely, Minntac and Utac. Phase I testing also involved evaluation of three different additives; out of which ESORB-HG-11 was found to be most effective. Hence, experiments were carried out for five different loadings of ESORB-HG-11 giving a ratio of 500, 1000, 2000, 3000 and 5000 mg/kg. It was evident from the results that increasing amount of ESORB-HG-11 does not produce any significant effect and hence, 0.1 percent was decided to be the optimum loading. In this section, surface tests were not conclusive since the surface experiments yielded low mercury concentration values. Also, an important observation was made from Phase I experiments which suggest that there is no or little

gas phase oxidation in the lab scale setup. Phase I experiments established the potential of ESORB-HG-11 additive.

Phase II research was focused on evaluating the effectiveness with two different loadings of 1000 and 5000 mg/kg of ESORB-HG-11 with six different green ball formulations obtained from five different taconite plants. All the green balls used in Phase II were prepared at Coleraine Mineral Research Laboratory (CMRL) with batch balling procedure and with industry standard and formulation. Physical tests results showed that there was no significant effect of ESORB-HG-11 addition when compared to baseline runs.

ESORB-HG-11 incorporated green balls showed a very high potential for mercury oxidation. Test results from these studies were carried out on five plants out of which four facilities showed best results with ESORB-HG-11 incorporation. The reduction potential for each plant is summarized in Table 31 below. Hg1 and Hg2 are averages obtained in the lab tests and Hg2 is estimated to be the minimum possible reduction expected from stack emissions during full scale work. There wasn't a significant difference in mercury oxidation level for 1000 and 5000 mg/kg loading; hence 1000 mg/kg was decided to be optimum loading. Hg2 is the average result from 1000 mg/kg for respective plant.

It is clear from the graphical representation that Utac green balls did not show appreciable decrease in the elemental mercury generation. However, all the other four plants showed higher reduction levels ranging between 36 to 49 %. Hence, it was found that ESORB-HG-11 had a significant effect on mercury oxidation when incorporated in green balls.

Table 31 : Reduction potential of ESORB-HG-11

Plant	Hg1 %		Hg2%		Reduction Potential	
	Average	Standard Deviation	Average	Standard Deviation	Value	Standard Deviation
Minntac	24	4.6	62	7.2	49	9.4
Keetac	15	2.5	46	3.8	36	4.5
Arcelor Mittal	20	1	53	10.2	41	12.7
Utac	22	3.5	37	5.5	19	7.1
Hibtac	15	7.2	52	5.1	43	6.5

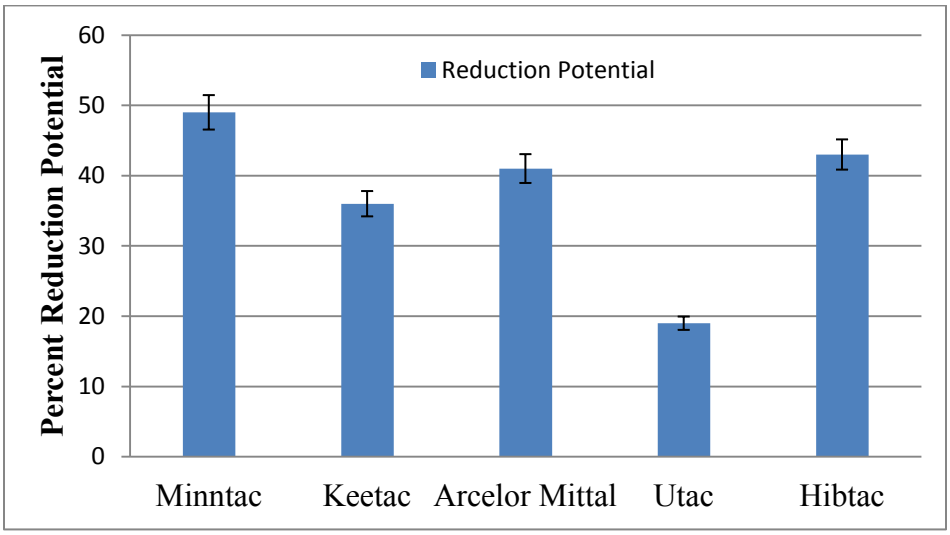

Figure 83 : Graphical representation of reduction potential of ESORB-HG-11

From Phase Analysis, it was proved that ESORB-HG-11 does not have any significant effect on the oxidation reaction of magnetite to hematite. All the results from Mössbauer analysis indicate that hematite is present in smaller quantities at 400°C which gradually increases with temperature. All of the 1000°C samples did not show any magnetite concentration proving that the oxidation reaction is complete. Results obtained from XRD and Mössbauer analysis also proved that conversion of magnetite to hematite is an exothermic reaction (TGA/DSC) which takes place between 200°C - 1000°C. TGA/DSC analysis shows that taconite ore gains negligible amount of mass during the

oxidation reaction. Mercury content analysis on samples show that most of the mercury is released before 400°C which leads us to the conclusion that, in this setup, mercury release is not related to the magnetite to hematite conversion.

Hence, this research has established the oxidation potential of ESORB-HG-11. Also, it is important to note that the no significant effect of addition of ESORB-HG-11 on the green ball quality was observed during green ball physical tests. Also, the gas phase oxidation was not considered as significant in the lab scale testing. This opens up the possibility of having higher reduction potential with actual field testing. Hence, it is highly recommended to scale up the technology to fit field scale testing.

CHAPTER VII

FUTURE WORK

It is important to study the effect of ESORB-HG-11 on the properties of the final product of taconite industries. It is highly recommended that fired pellet quality tests be carried out on ESORB-HG-11 incorporated green balls. If the data obtained from the fired pellet quality tests does not show any significant difference when compared to baseline (additive free) pellets, then full-scale testing of the technology is highly recommended. Gas phase oxidation was not considered to be significant in lab scale testing. Hence, the actual reduction potential of ESORB-HG-11 could be higher than that observed during lab scale testing.

Scanning Electron Microscopy (SEM) analysis of samples did not show any observable difference on the surface of the iron particles. Hence, it is highly recommended to perform a more detailed SEM analysis to show acceptable differences between magnetite and hematite structures.

In Phase II, green balls from all the plants with ESORB-HG-11 incorporation showed high level of reduction potential except Utac green balls. It is important to evaluate the reasons behind the additive being ineffective. Also, it is recommended that, research involving some other additives or other additive incorporation methods must be carried out to reduce the mercury emissions.

In phase analysis, surface characterization techniques were applied to four samples which includes Unheated or pre-firing sample, sample fired at 400°C, sample fired at 700°C and sample fired at 1000°C. It is highly recommended to carry out analysis with smaller temperature gap to get a better understanding of the phase conversion in green ball. It would be interesting to evaluate results from 100°C, 200°C, 300°C and so on.

Also, conclusions obtained from phase analysis and surface characterization suggested that the conversion of magnetite to hematite starts around 400°C and according to lab scale results (Refer Chapter IV) most of the mercury release takes place before 400°C. Hence, from the lab work, it can be concluded that the oxidation reaction does not have a significant effect on the mercury release. However, previous work at the taconite plants suggested that the oxidation of magnetite to hematite plays a vital role in release of elemental mercury from green balls. (12) This phenomenon needs to be investigated further with lab and field scale testing.

APPENDICES

APPENDIX A

Table 32 : Results for runs performed before final equipment optimization

Green Ball	Gas Flow rate	Temp.	Impinger	Additive	Loading	Oxidation	Average Oxidation
	(lpm)	(^{0}C)	Solution		(wt.%)	(%)	(%)
Minntac	5	700	KCl +$Na_2S_2O_3$	ESORB-HG-11	0.05	39.6 33.1	36.4
Minntac	5	700	KCl +$Na_2S_2O_3$	ESORB-HG-11	0.2	54.4 33.4	43.9
Minntac	5	700	KCl +$Na_2S_2O_3$	ESORB-HG-11	0.3	31	-
Minntac	5	700	KCl	-	0	39.6 39.8	39.7
Minntac	5	700	KCl	ESORB-HG-11	0.1	55.4 51.7	53.6
Minntac	5	700	KCl	ESORB-HG-11	0.2	45.7 65.2	55.4
Minntac	7.5	700	KCl	ESORB-HG-11	0.1	54	-

APPENDIX B

Mercury Release Profiles - Minntac

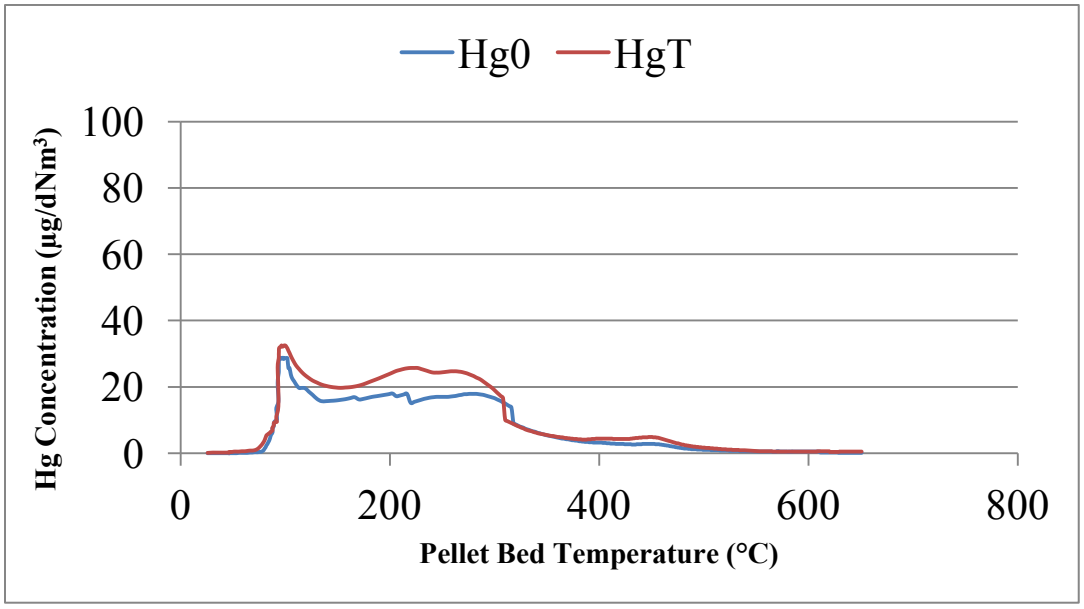

Figure 84 : Mercury release profile for Minntac green ball baseline - 2

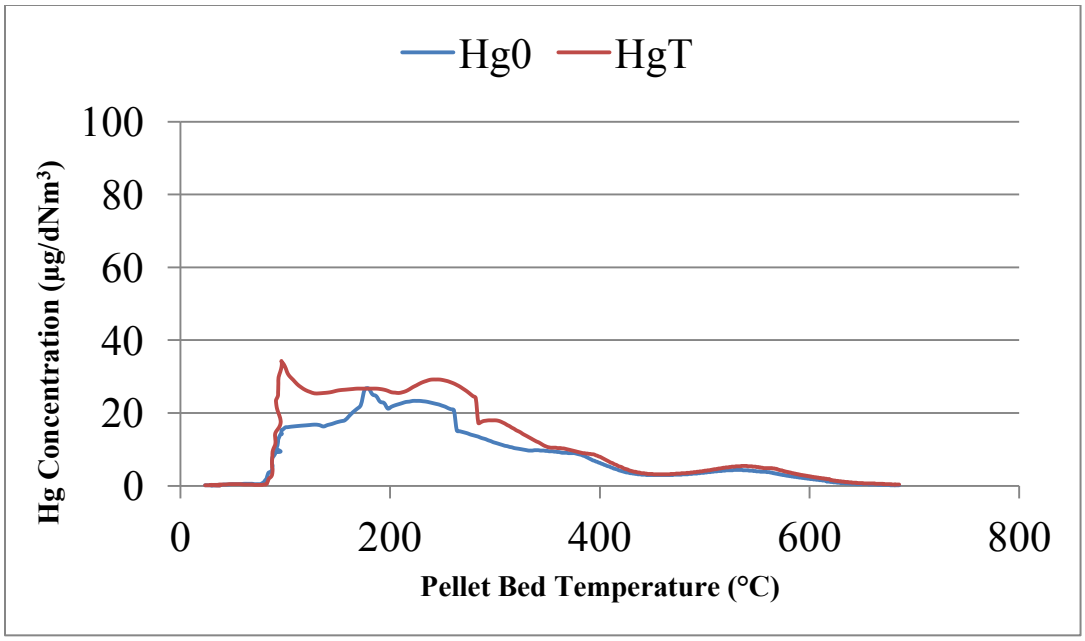

Figure 85 : Mercury release profile for Minntac green ball baseline – 3

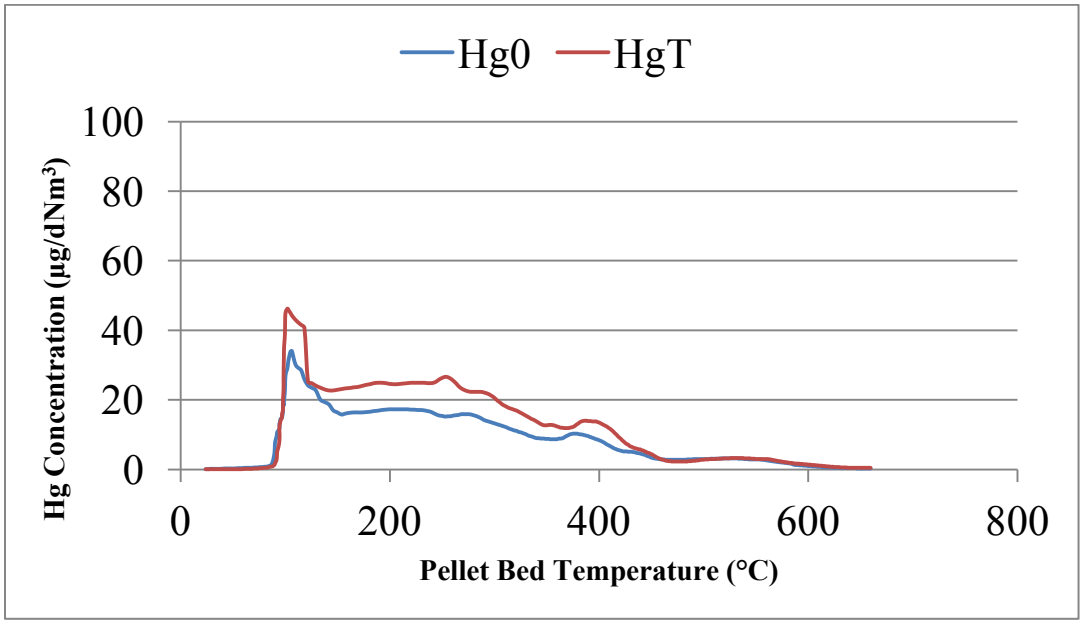

Figure 86 : Mercury release profile for Minntac green ball baseline – 4

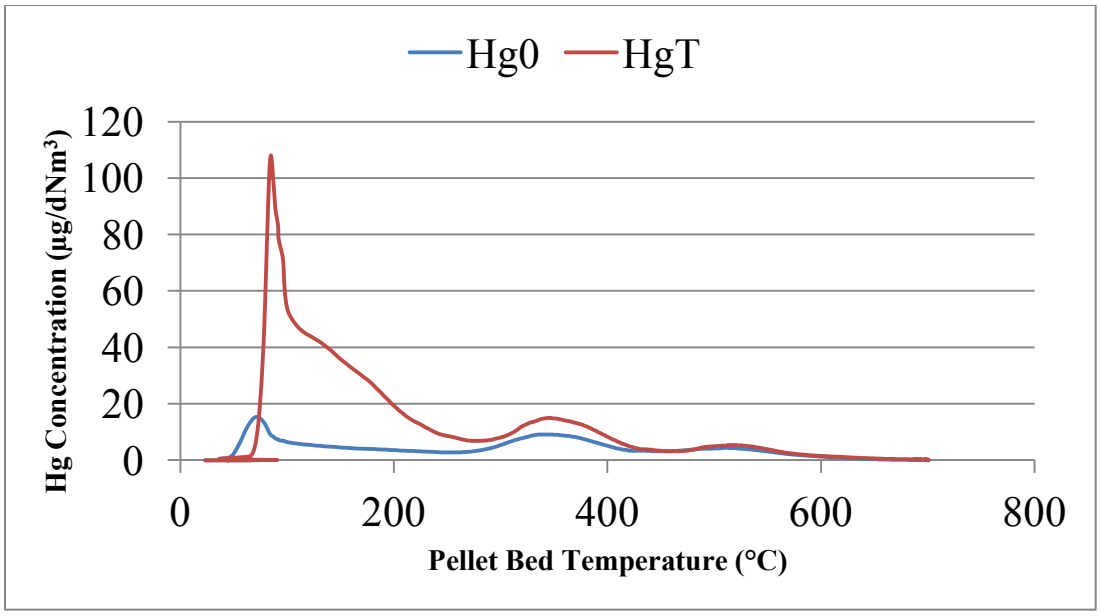

Figure 87 : Mercury release profile for Minntac green ball with 0.1 weight percent ESORB-HG-11 inside -2

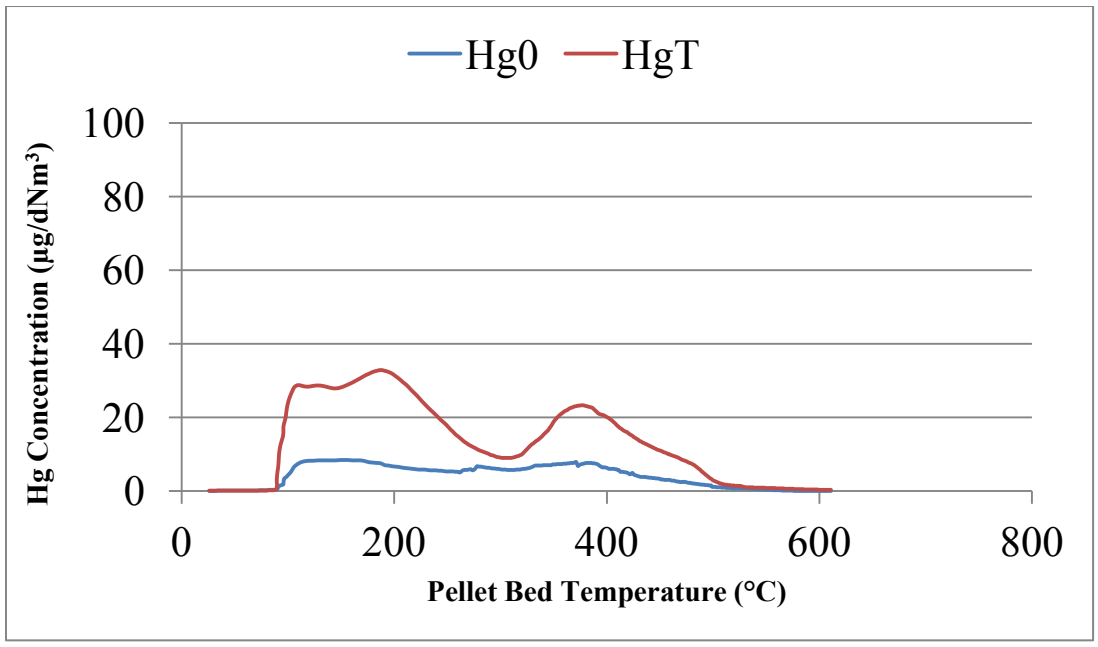

Figure 88 : Mercury release profile for Minntac green ball with 0.1 weight percent ESORB-HG-11 inside -3

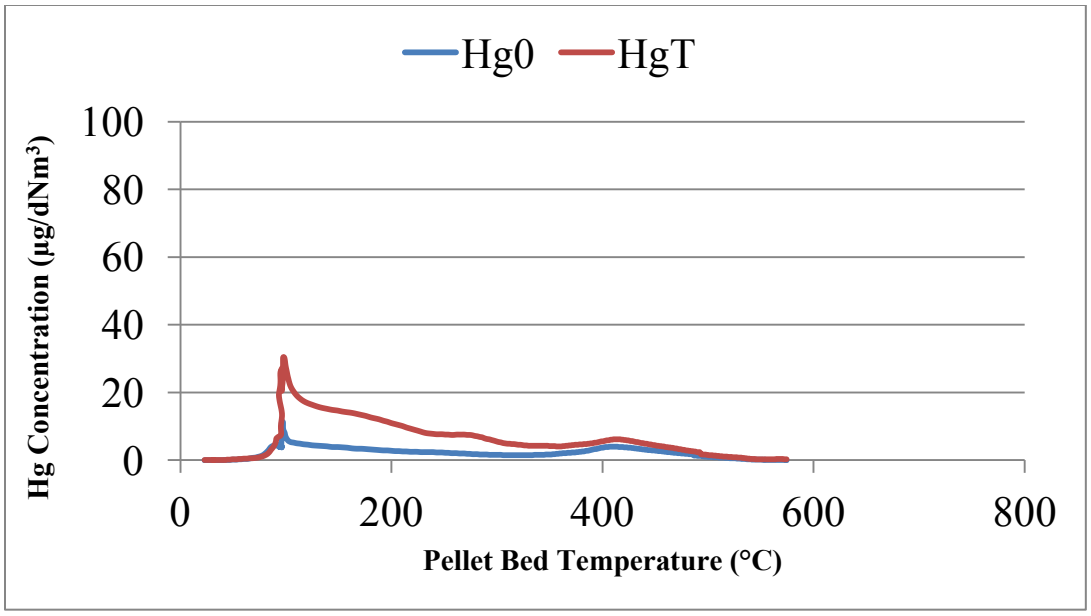

Figure 89 : Mercury release profile for Minntac green ball with 0.5 weight percent ESORB-HG-11 inside -2

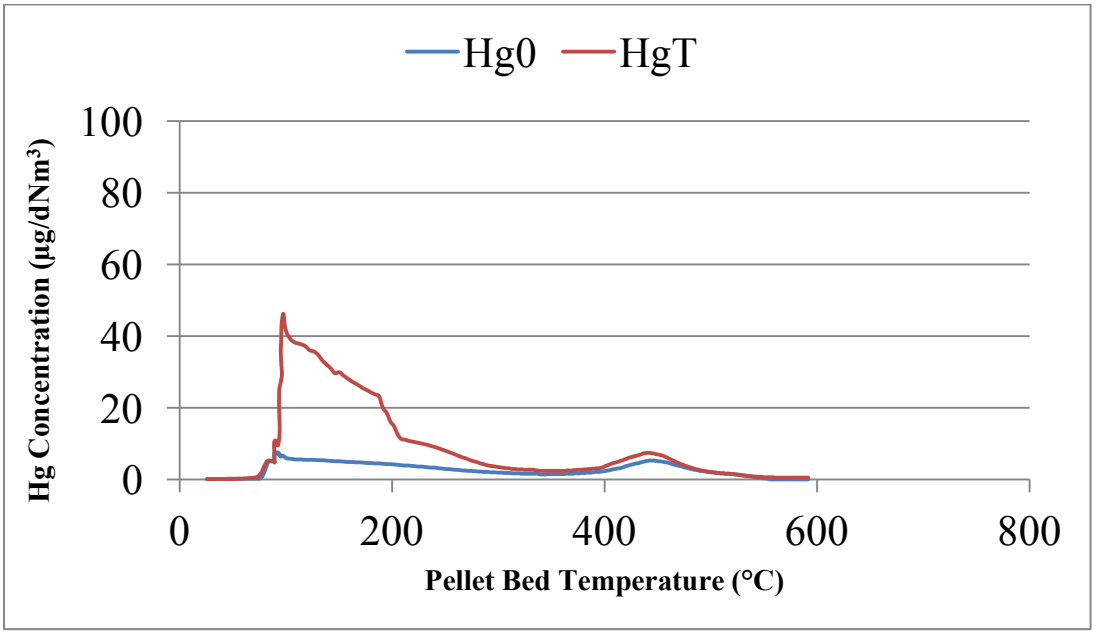

Figure 90 : Mercury release profile for Minntac green ball with 0.5 weight percent ESORB-HG-11 inside -3

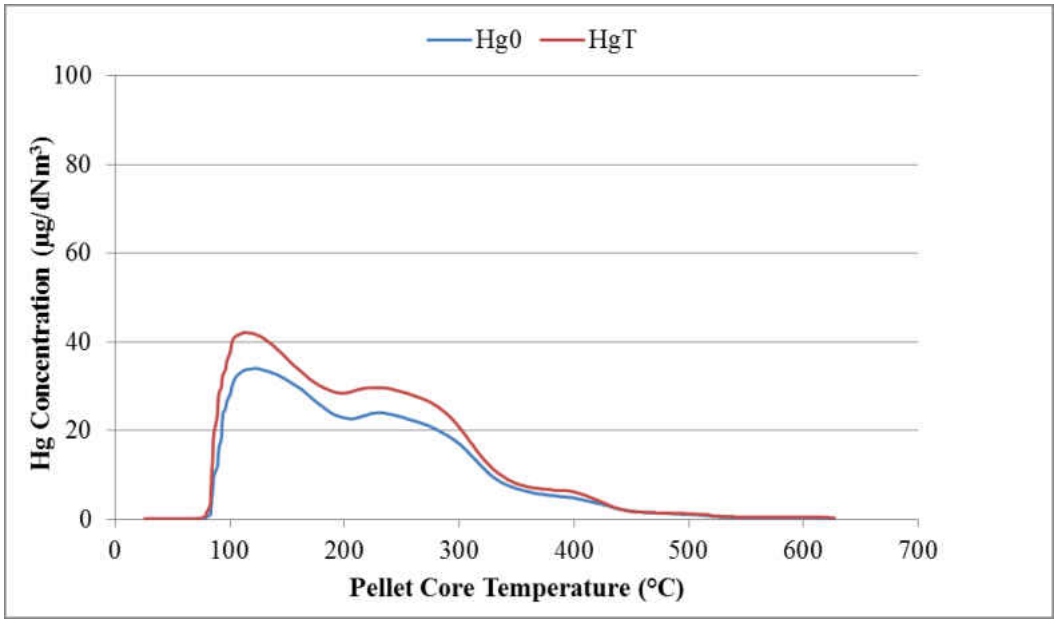

Figure 91 : Mercury release profile for Arcelor Mittal baseline run - 2

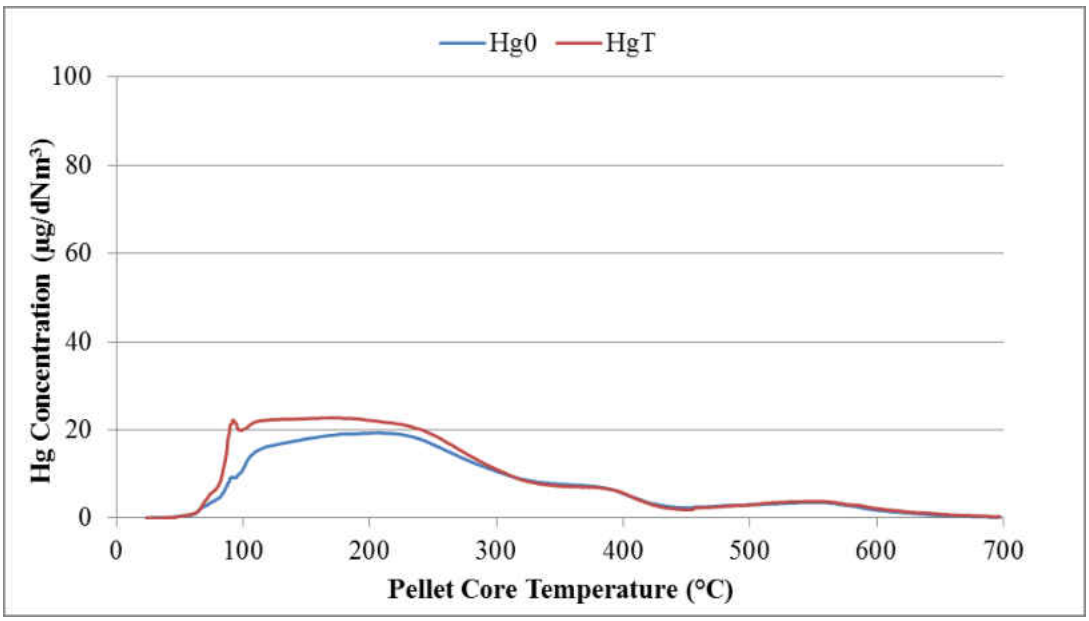

Figure 92 : Mercury release profile for Arcelor Mittal baseline run - 3

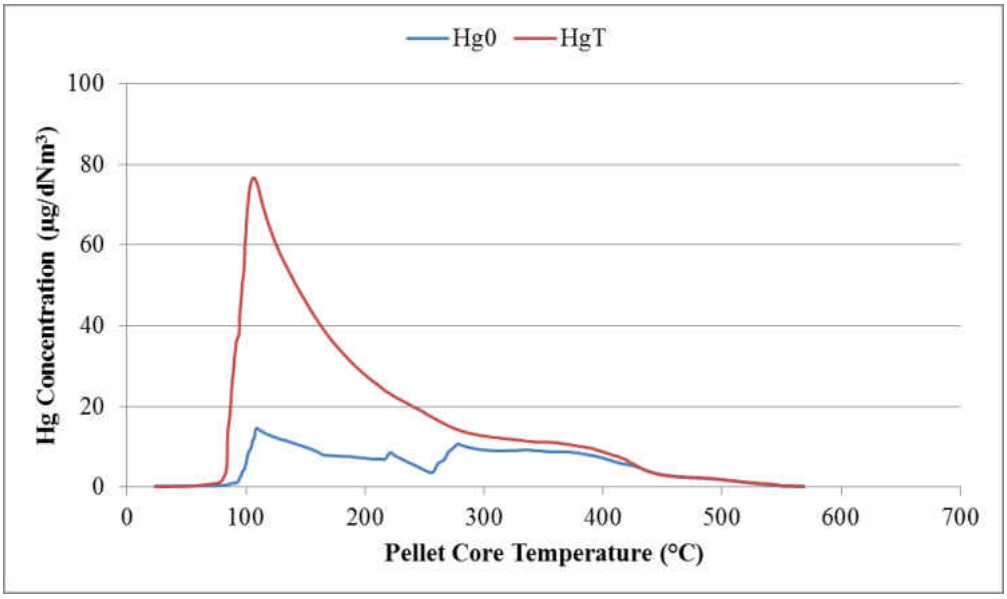

Figure 93 : Mercury release profile for Arcelor Mittal 0.1wt% loading run -2

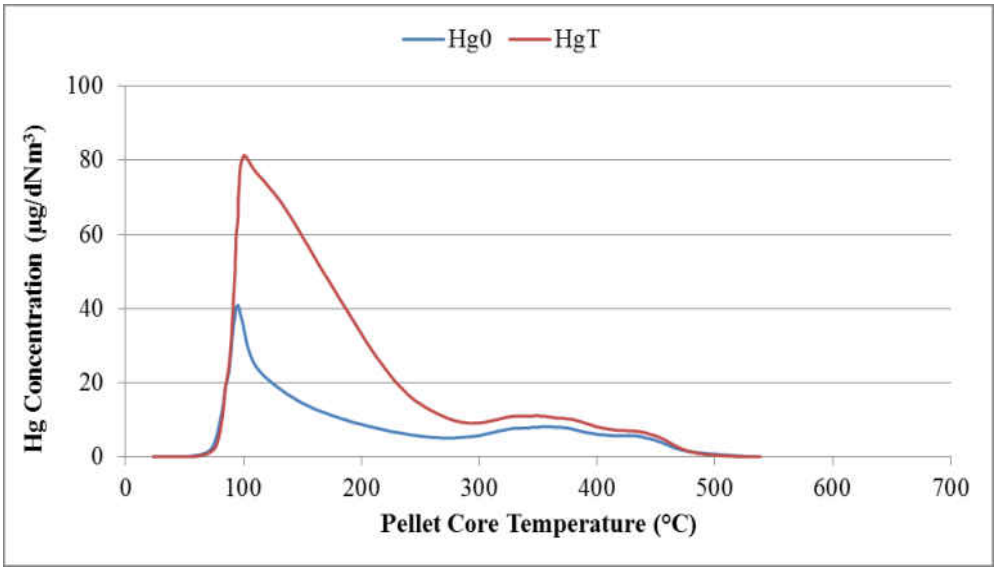

Figure 94 : Mercury release profile for Arcelor Mittal 0.1wt% loading run -3

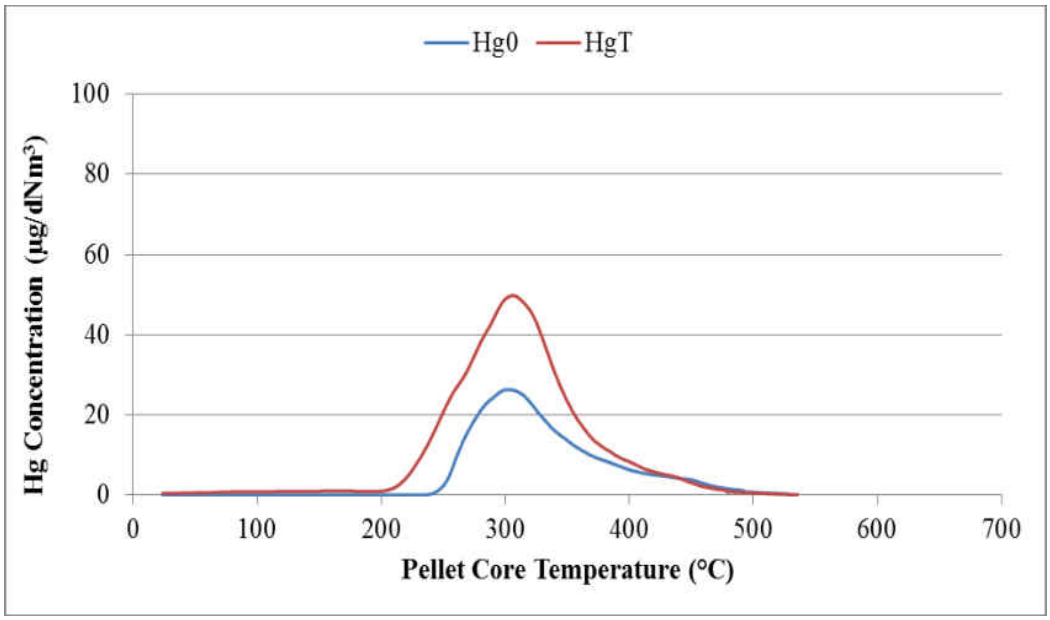

Figure 95 : Mercury release profile for Arcelor Mittal 0.1wt% replicate loading run - 4

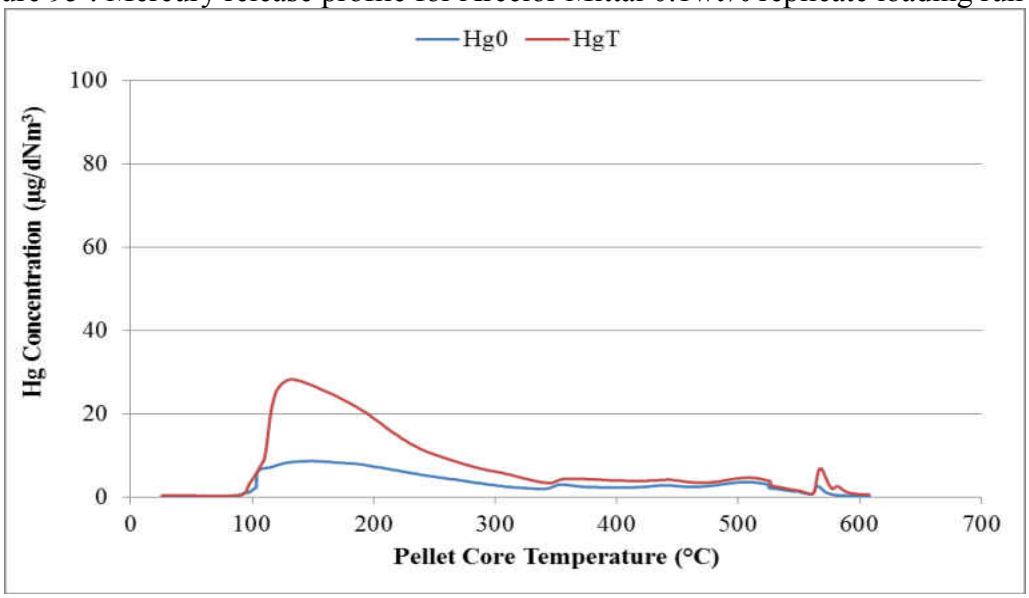

Figure 96 : Mercury release profile for Arcelor Mittal 0.5wt% loading run - 2

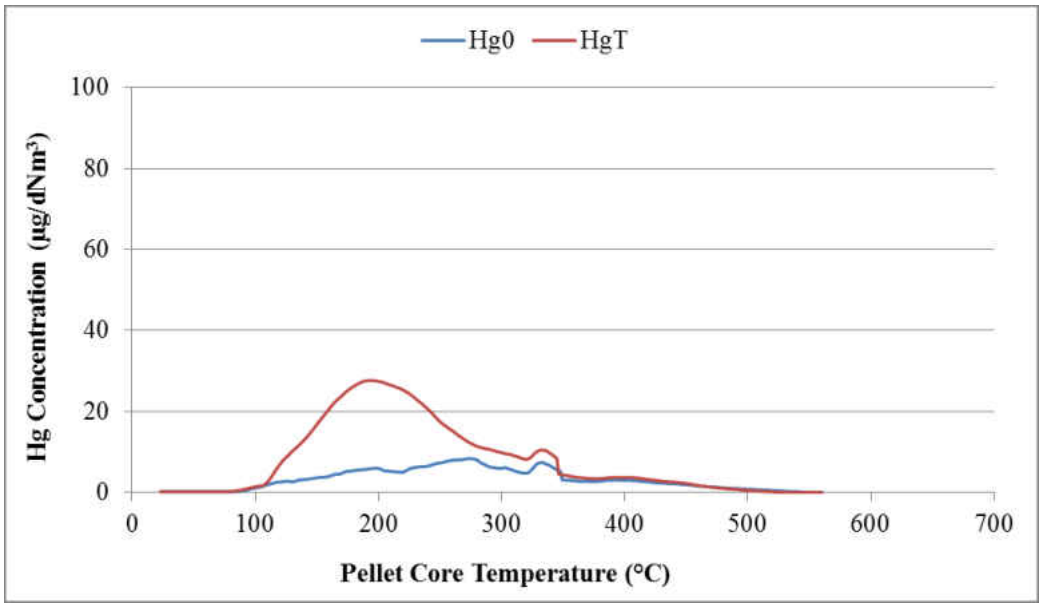

Figure 97 : Mercury release profile for Arcelor Mittal third 0.5wt% loading run - 3

Mercury Release Profiles - Keetac

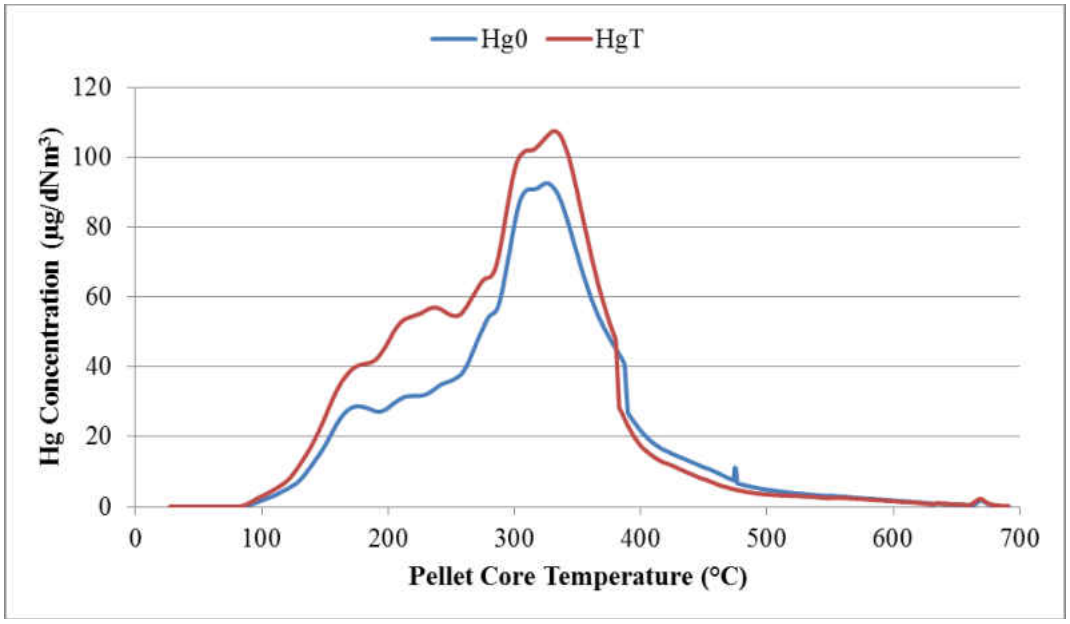

Figure 98 : Mercury release profile for Keetac baseline run – 2

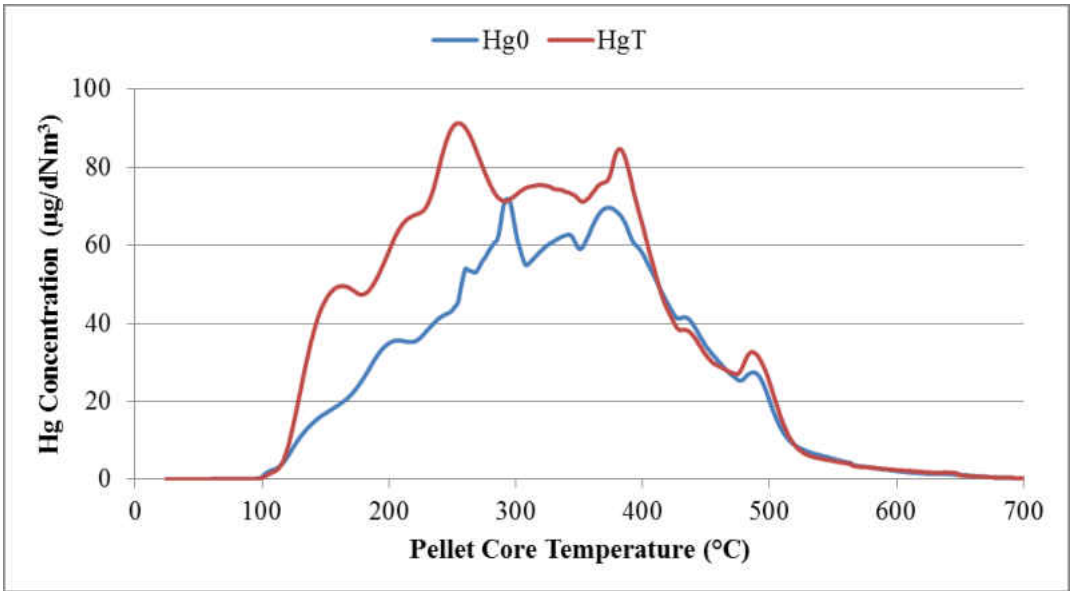

Figure 99 : Mercury release profile for Keetac baseline run - 3

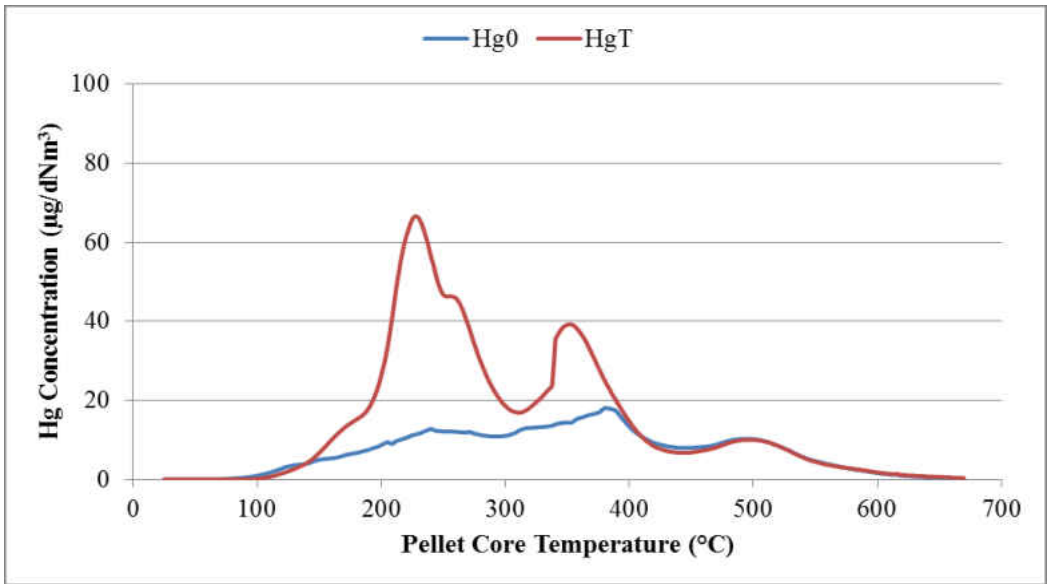

Figure 100 : Mercury release profile for Keetac second 0.1wt% run - 2

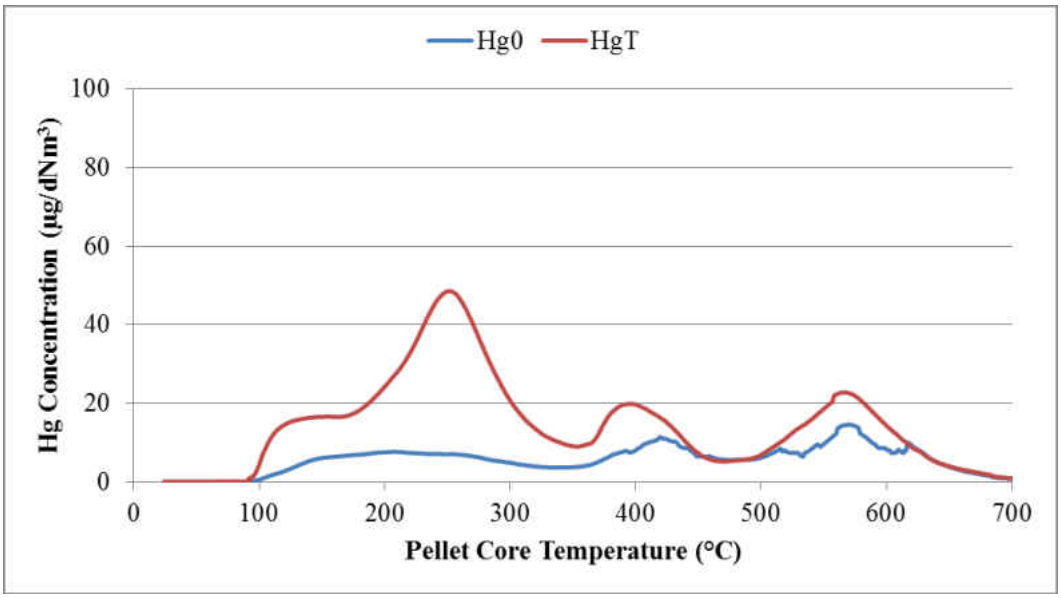

Figure 101 : Mercury release profile for Keetac replicate first 0.1wt% run -3

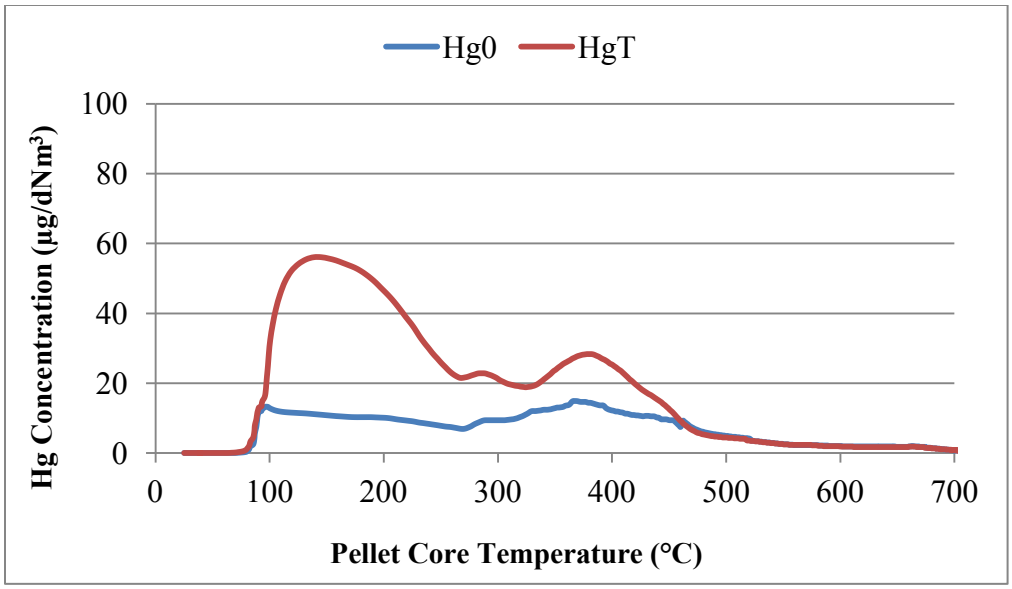

Figure 102 : Mercury release profile for Keetac replicate second 0.1wt% run – 4

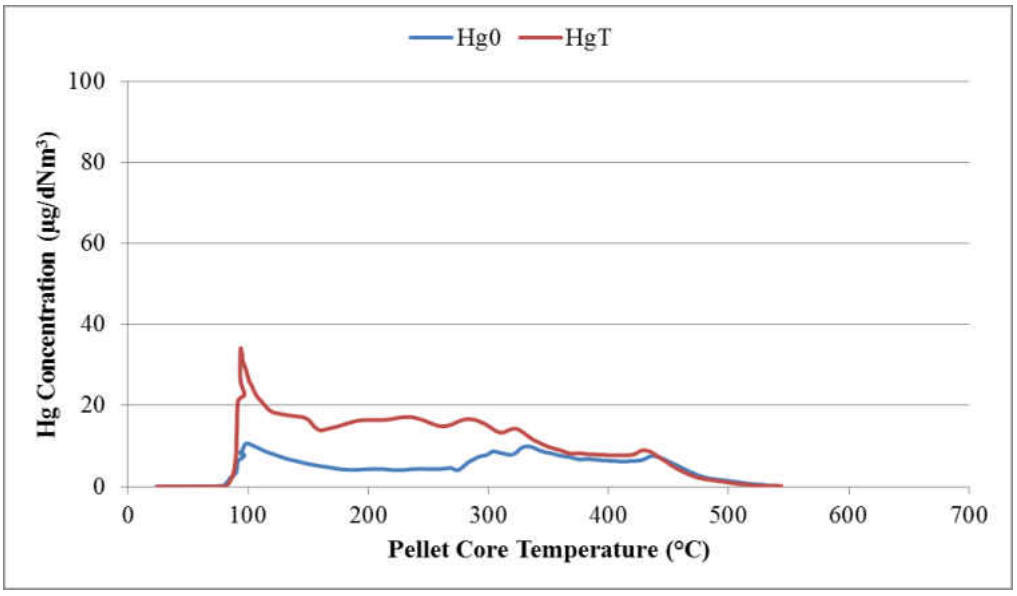

Figure 103 : Mercury release profile for Keetac second 0.5wt% run - 2

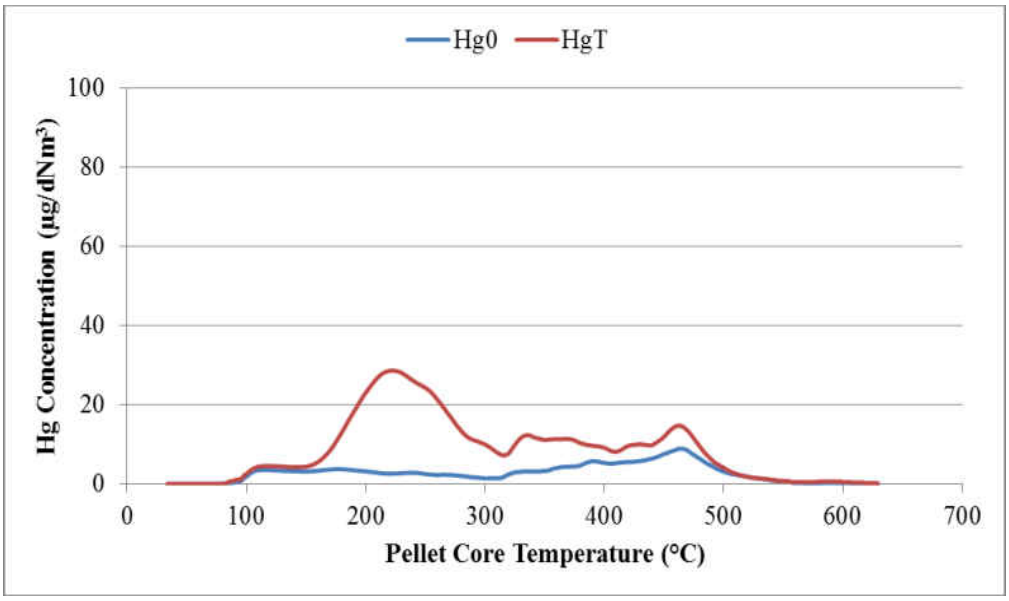

Figure 104 : Mercury release profile for Keetac third 0.5wt% run -3

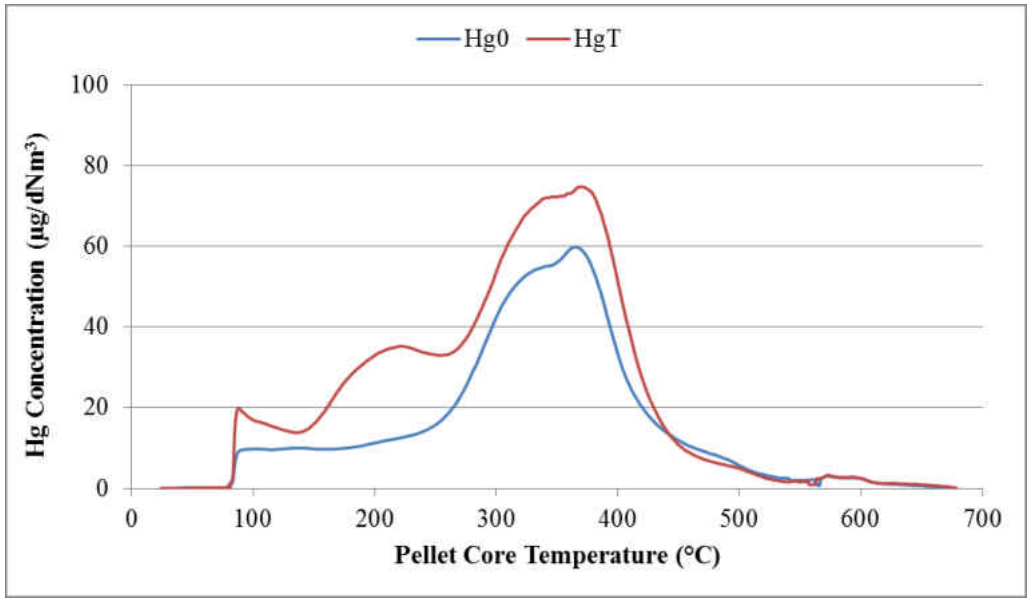

Figure 105 : Mercury release profile for Utac baseline run - 2

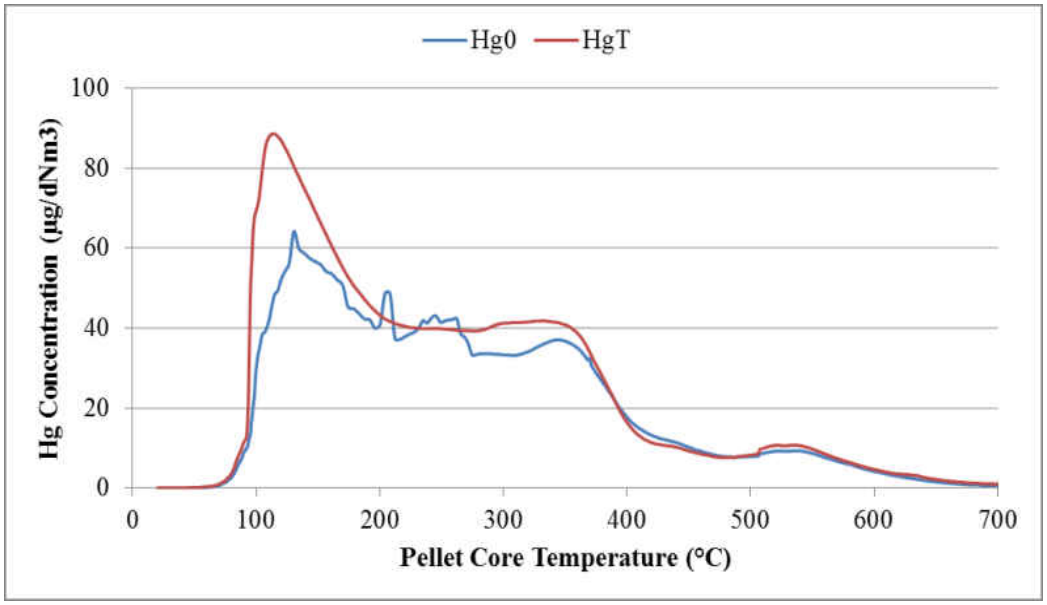

Figure 106 : Mercury release profile for Utac baseline run -3

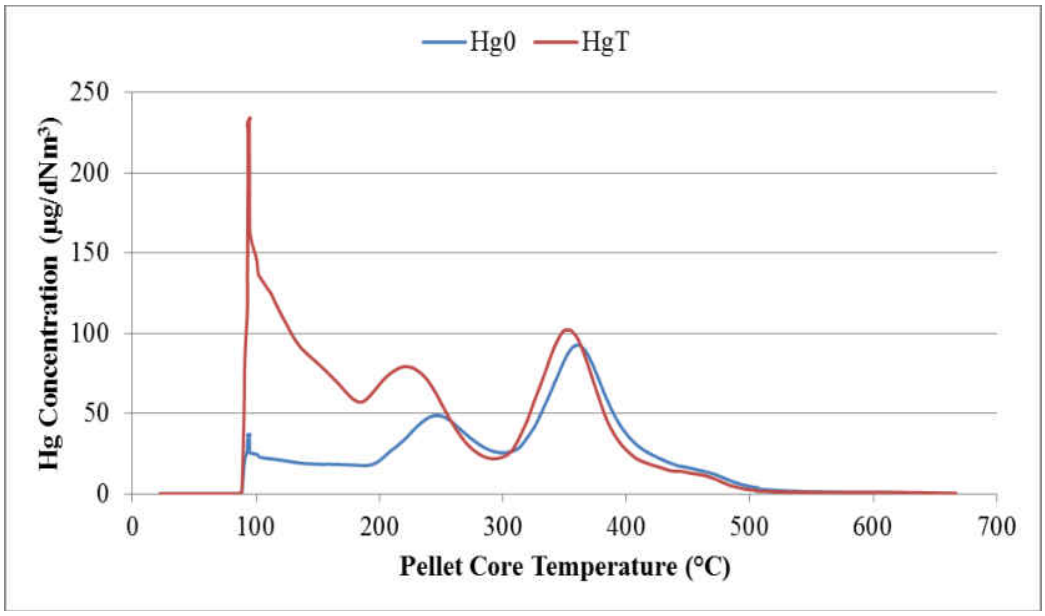

Figure 107 : Mercury release profile for Utac 0.1wt% run – 2

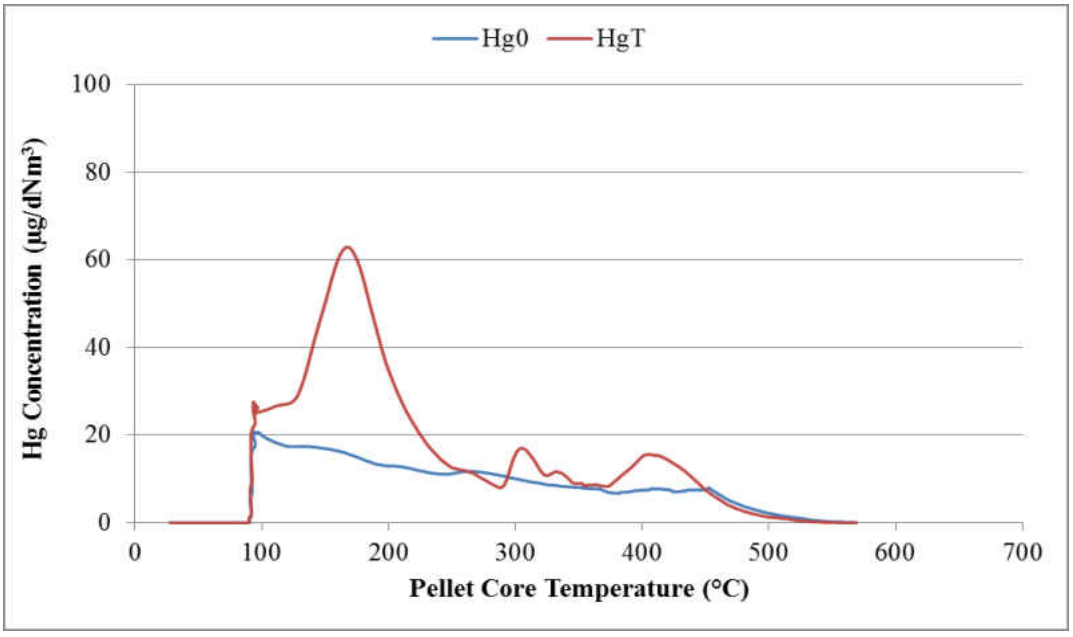

Figure 108 : Mercury release profile for Utac 0.5wt% run -2

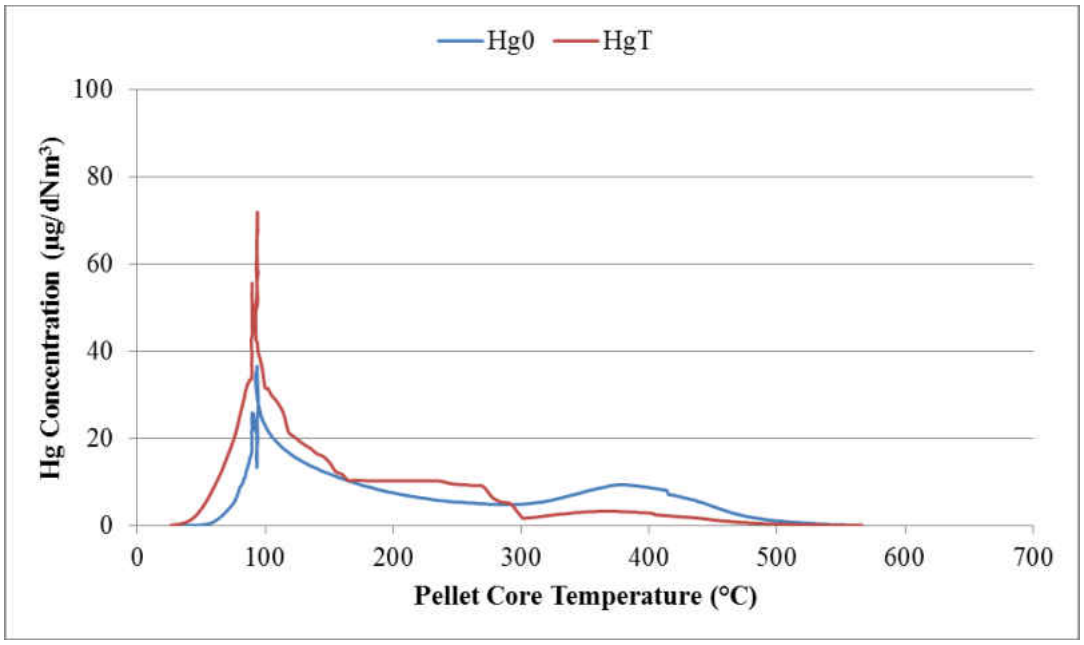

Figure 109 : Mercury release profile for Utac 0.5wt% run - 3

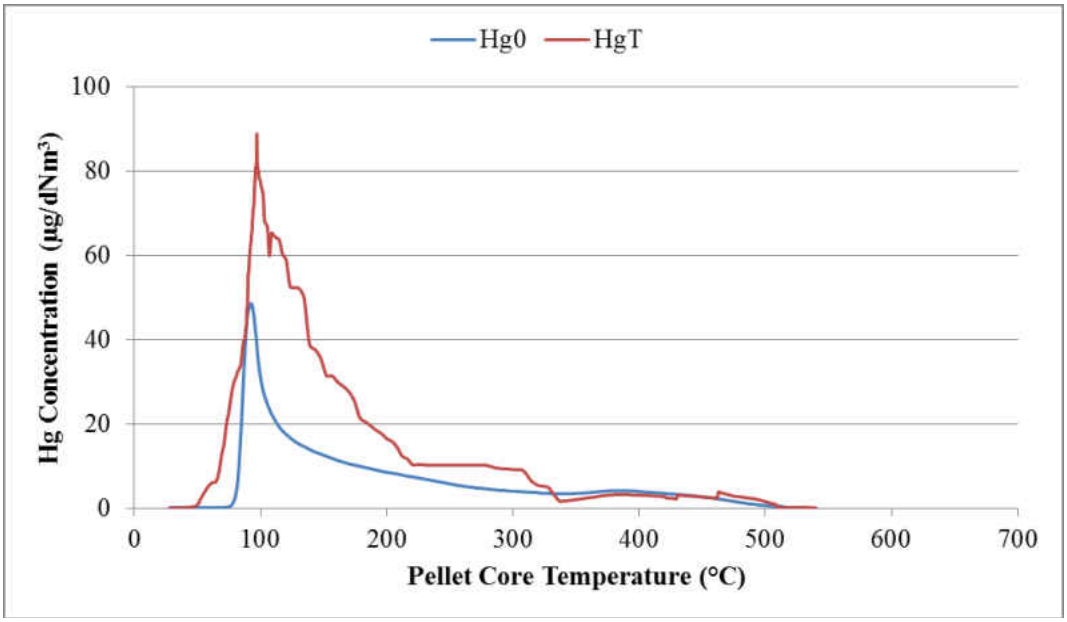

Figure 110 : Mercury release profile for Utac replicate second 0.5wt% run – 4

Mercury Release Profiles - Hibtac Standard Pellet

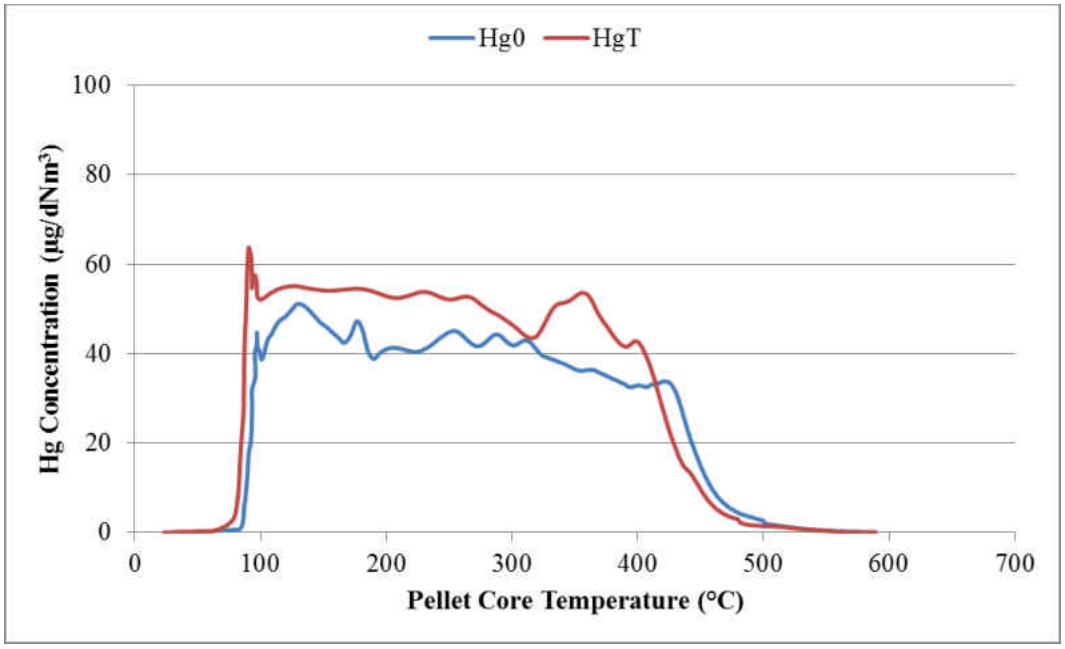

Figure 111 : Mercury release profile for Hibtac standard green ball baseline run – 2

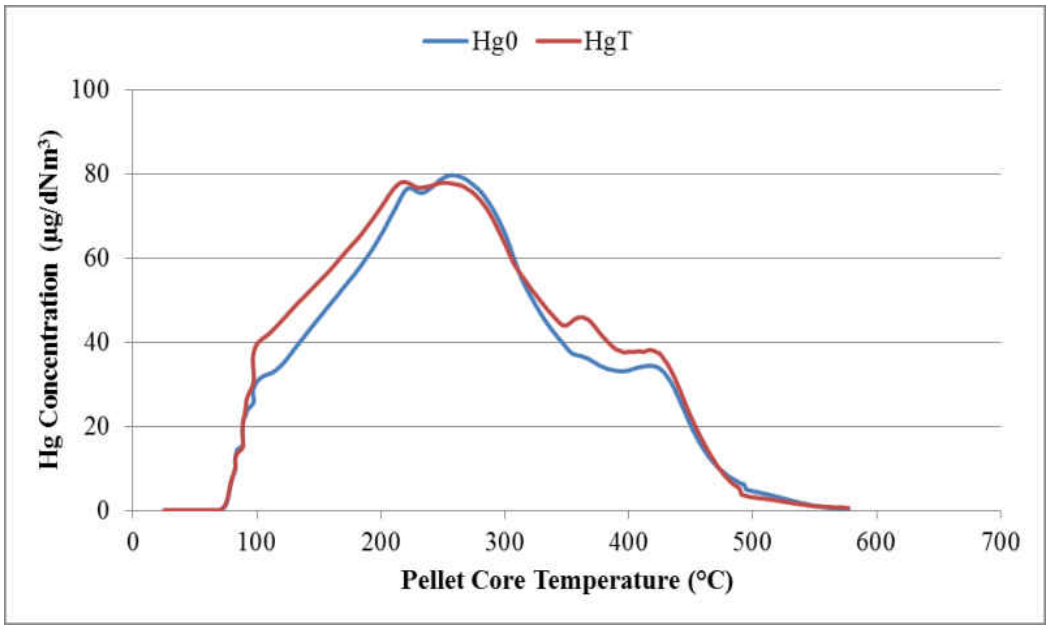

Figure 112 : Mercury release profile for Hibtac standard green ball baseline - 3

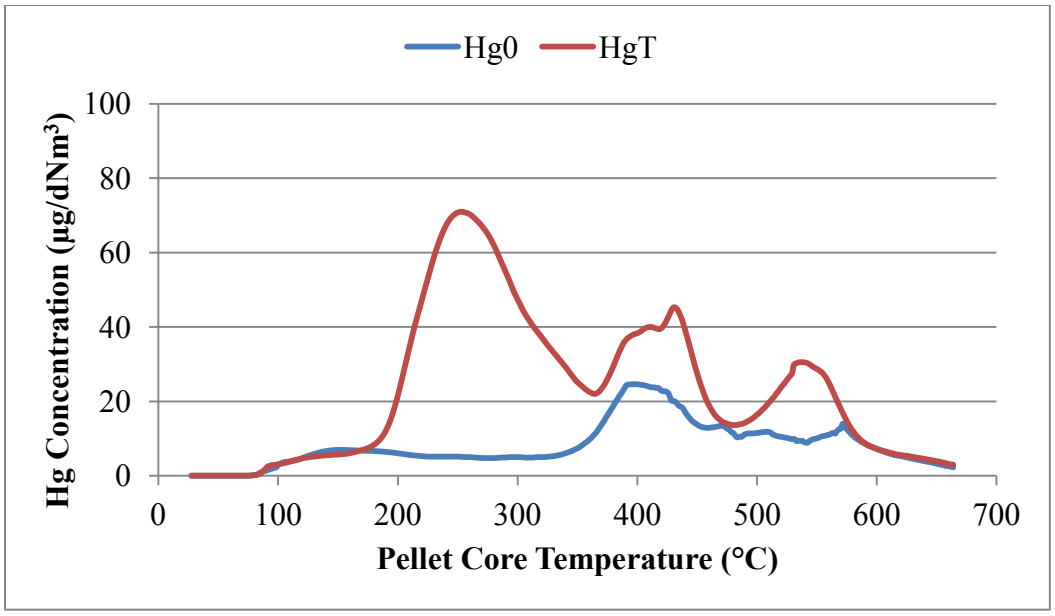

Figure 113 : Mercury release profile for Hibtac standard green ball 0.1wt% run – 2

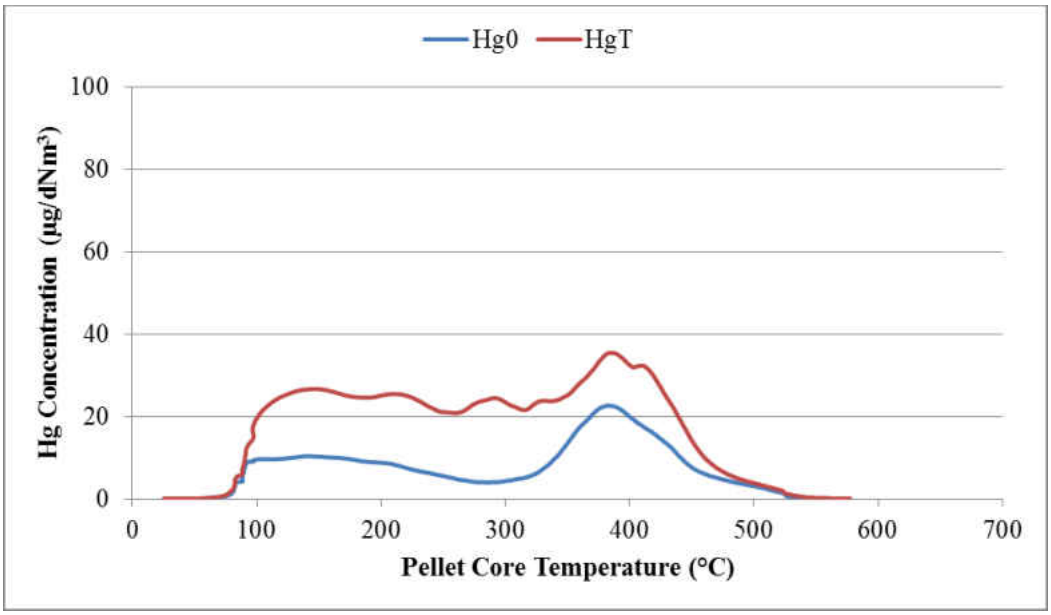

Figure 114: Mercury release profile for Hibtac standard green ball 0.1wt% run - 3

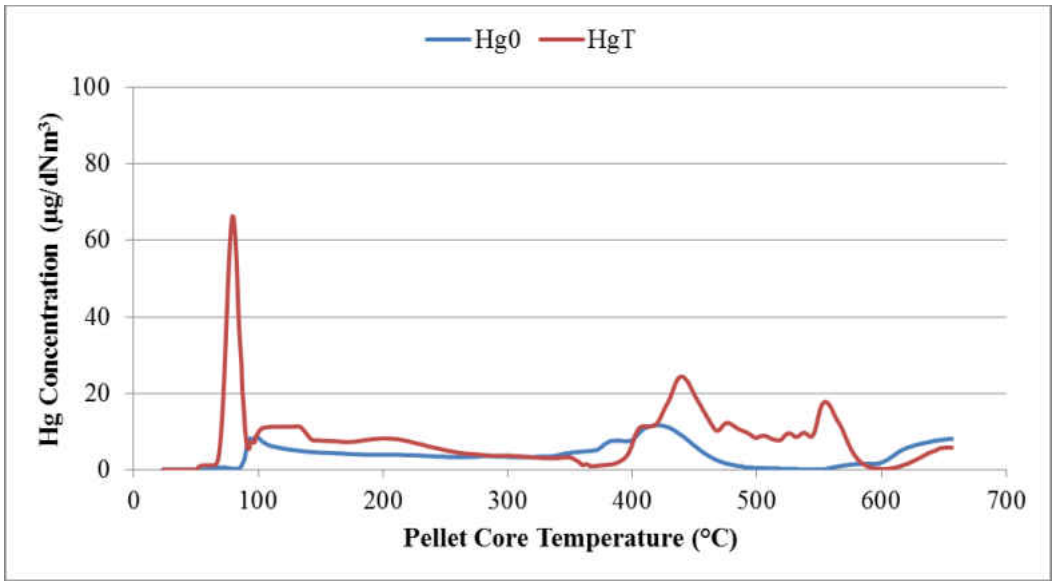

Figure 115: Mercury release profile for Hibtac standard green ball 0.5wt% run – 2

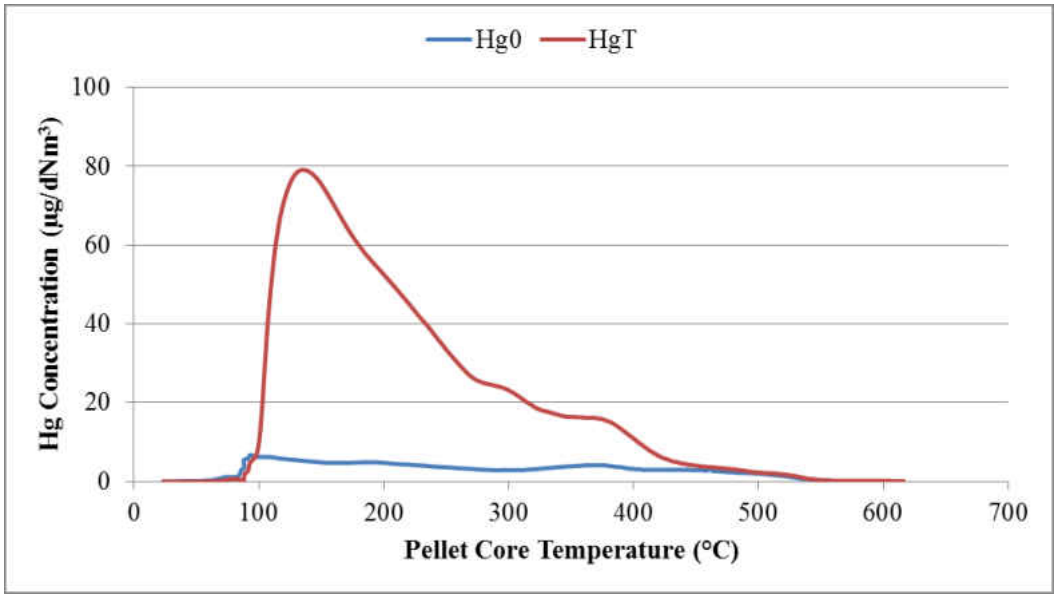

Figure 116 : Mercury release profile for Hibtac standard green ball 0.5wt% run - 3

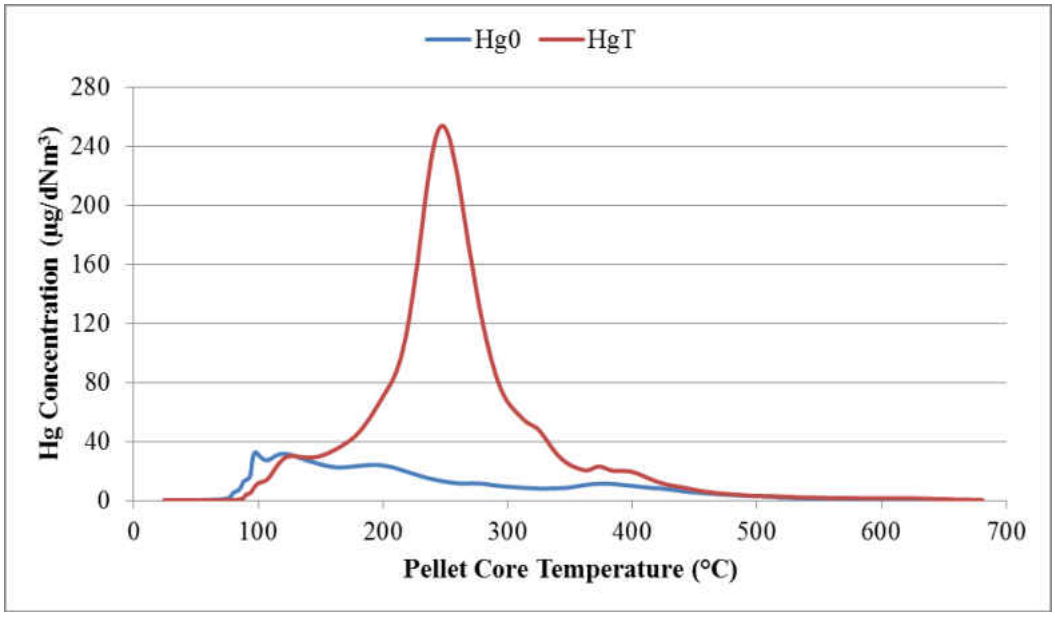

Figure 117 : Mercury release profile for Hibtac standard green ball 0.5wt% run – 4

Mercury Release Profiles - Hibtac High Compression Pellet

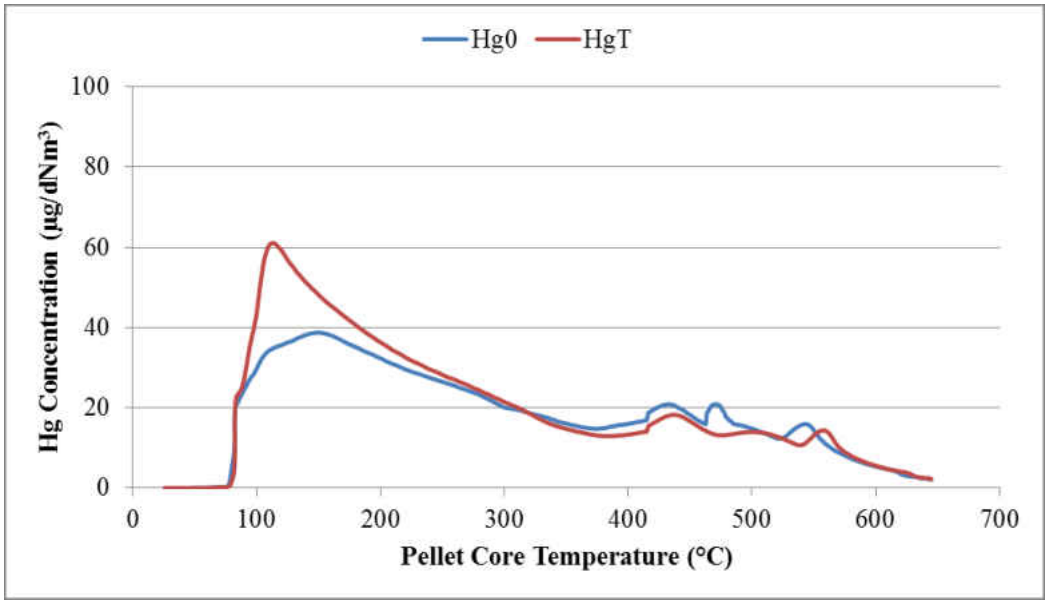

Figure 118 : Mercury release profile for Hibtac high compression green ball baseline run - 2

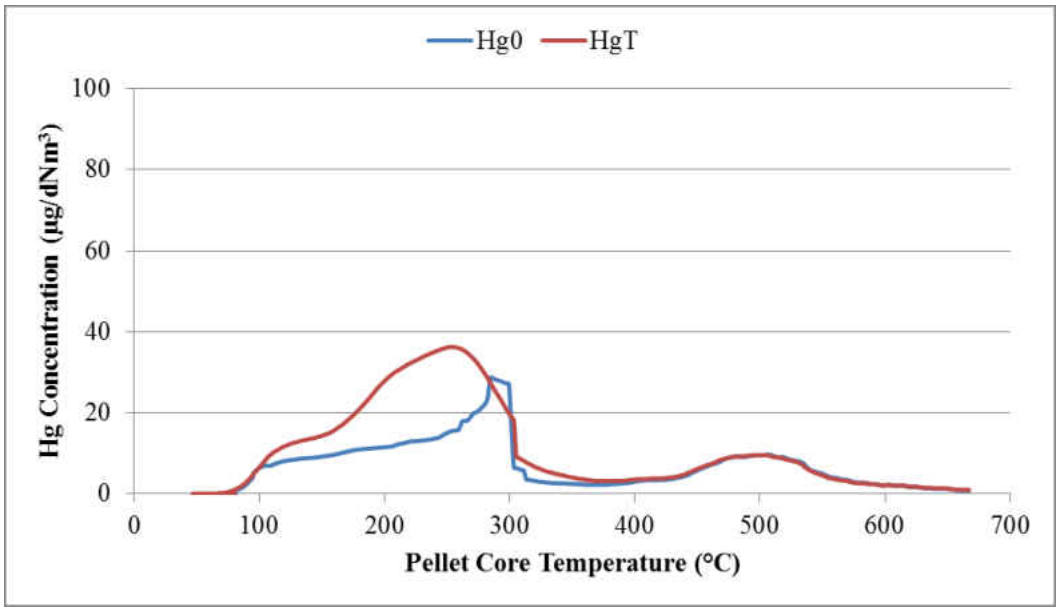

Figure 119 : Mercury release profile for Hibtac compression green ball baseline run -3

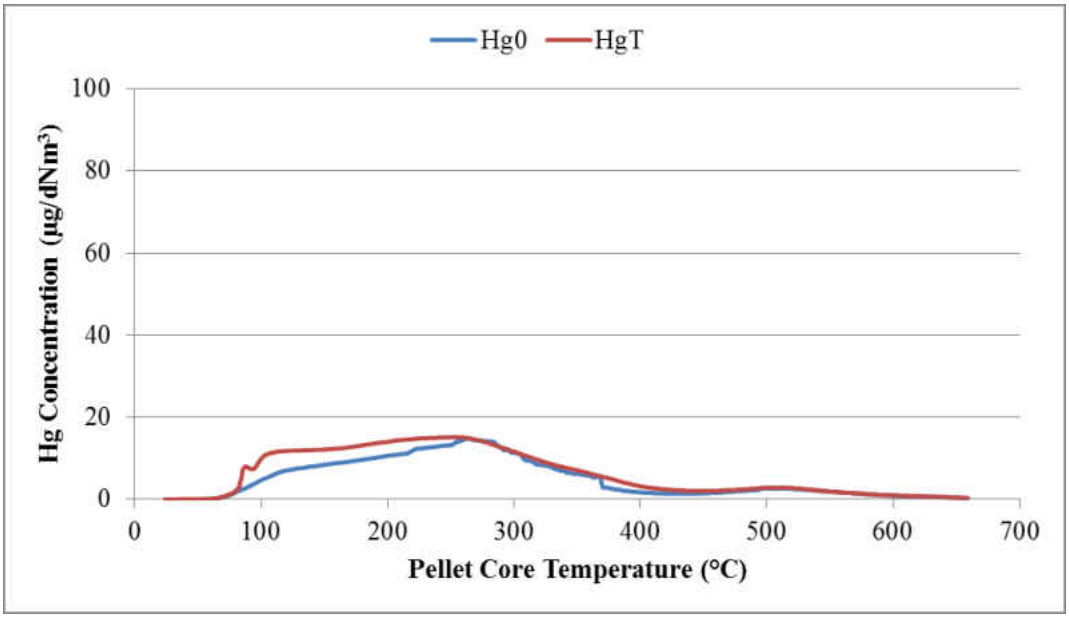

Figure 120 : Mercury release profile for Hibtac compression green ball – 4

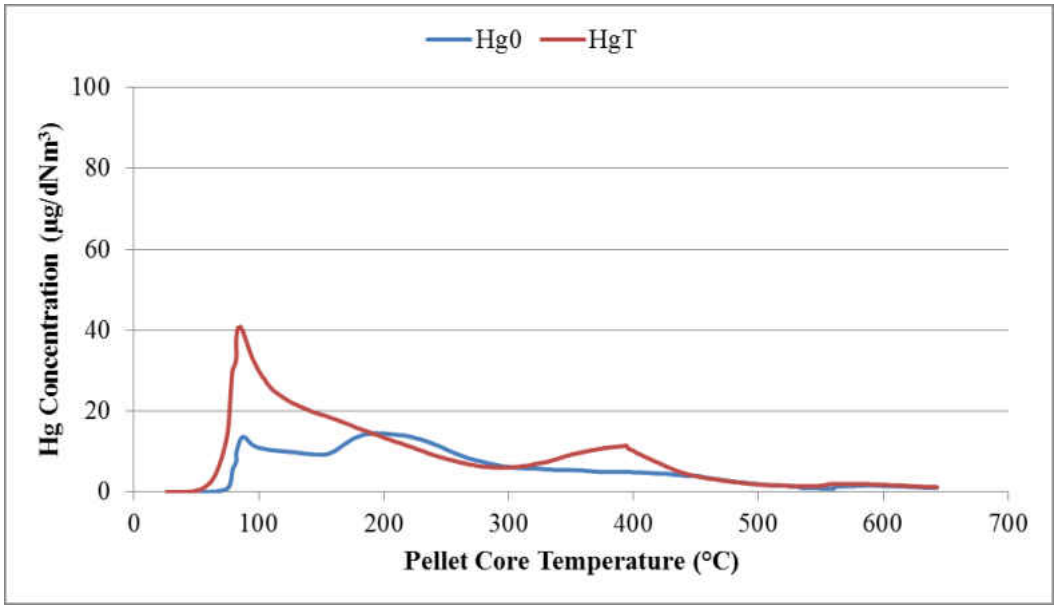

Figure 121 : Mercury release profile for Hibtac compression green ball 0.1wt% run -1

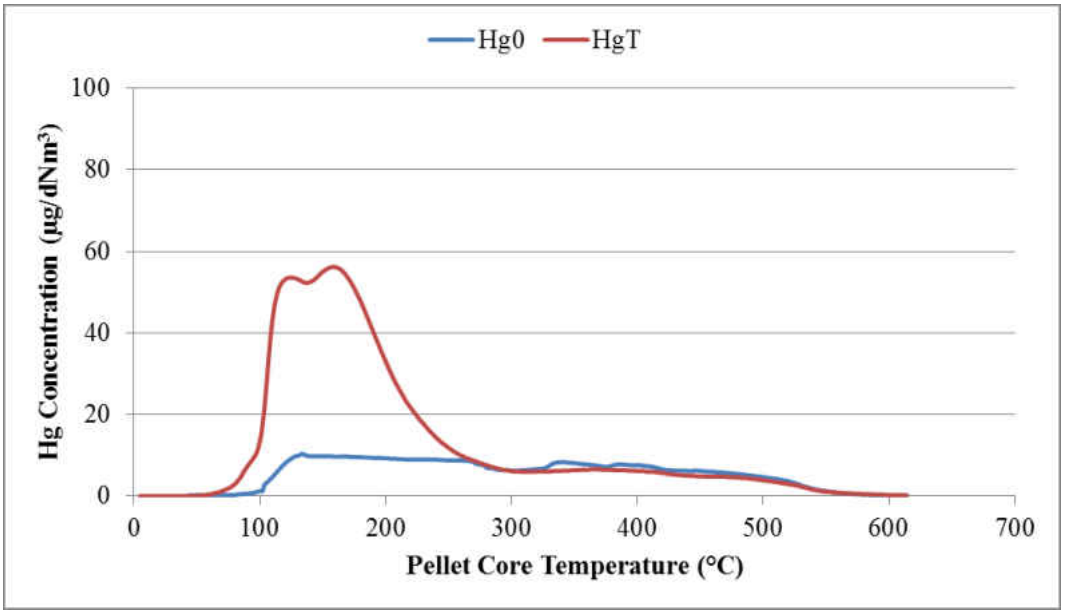

Figure 122 : Mercury release profile for Hibtac compression green ball 0.1wt% run – 2

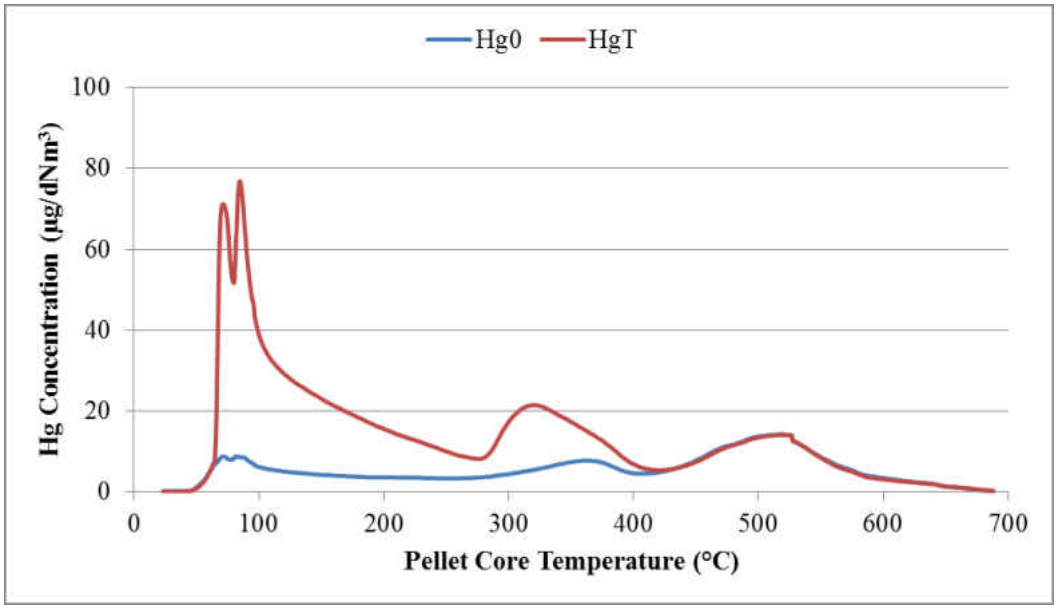

Figure 123 : Mercury release profile for Hibtac compression green ball 0.1wt% run -3

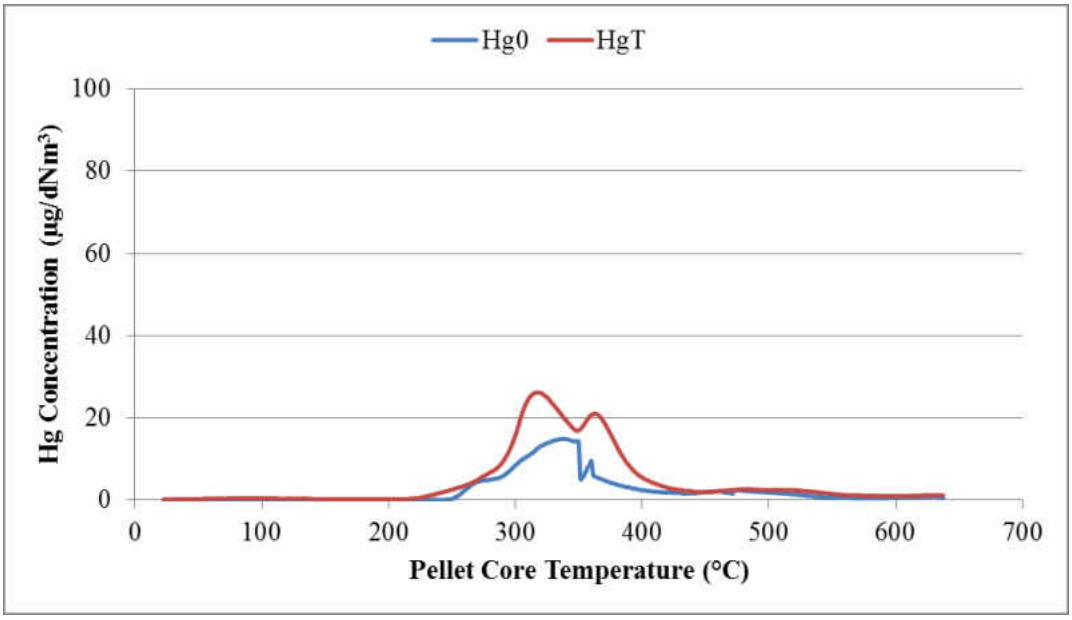

Figure 124 : Mercury release profile for Hibtac compression green ball 0.5wt% run – 2

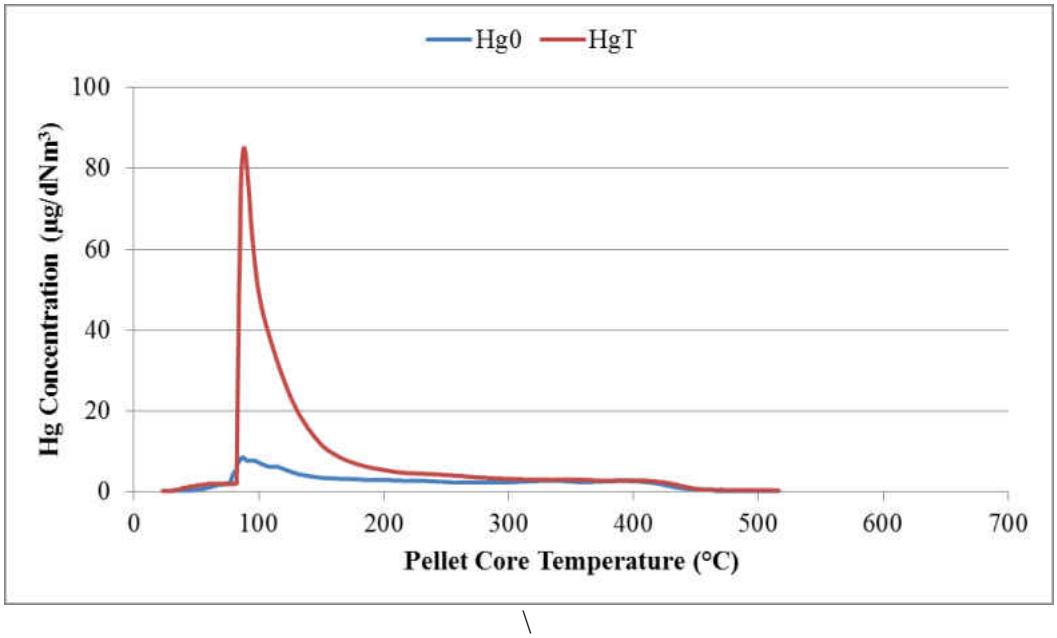

Figure 125 : Mercury release profile for Hibtac compression green ball 0.5wt% run - 3

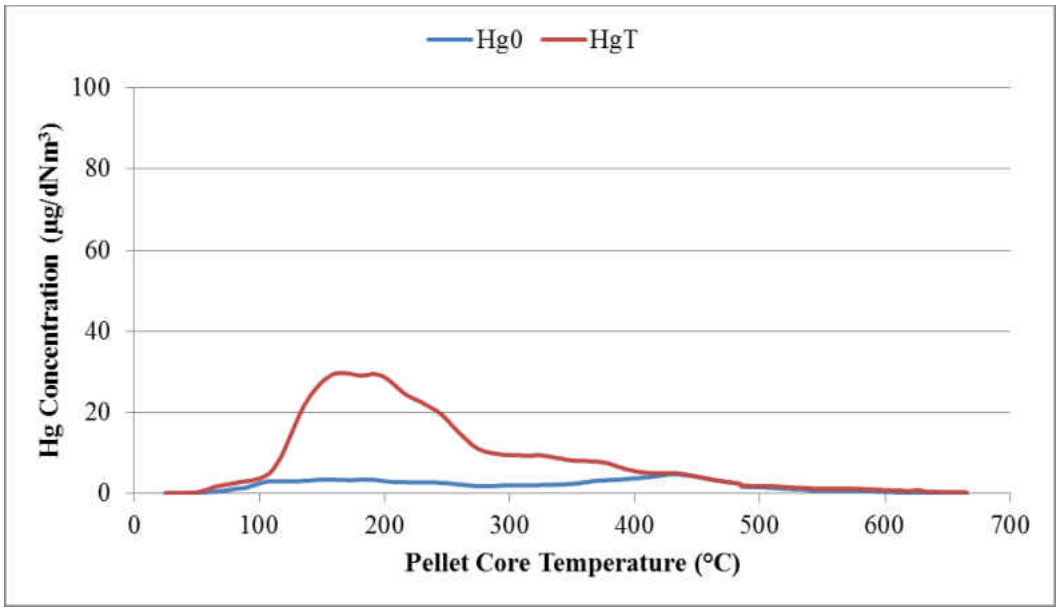

Figure 126 : Mercury release profile for Hibtac compression green ball 0.5wt% run - 4

References

1. Berndt M, Engesser J. Mercury transport in taconite processing facilities : (III) control method test results. 2007.

2. Hubbell B. Taconite mining and processing industry profile. 2001.

3. Berndt m. Mercury and mining in minnesota.

4. Laudal DL. Mercury control technologies for the taconite industry.

5. Heller K. Taconite iron ore NESHAP economic impact analysis. 2003.

6. Keating M.H. MKR. Mercury study report to congress. **1997**. united states environmental protection agency, EPA-452/R-97-003 through 010.

7. Overview of mining and mineral processing operations. In: .

8. Oberteuffer J. Magnetic separation: A review of principles, devices, and applications. IEEE Trans Magn. 1974;10(2):223-38.

9. Kelland D. High gradient magnetic separation applied to mineral beneficiation. IEEE Trans Magn. 1973;9(3):307-10.

10. Houot R. Beneficiation of iron ore by flotation—review of industrial and potential applications. Int J Miner Process. 1983;10(3):183-204.

11. Berndt M, Engesser J. Mercury transport in taconite processing facilities: (I) release and capture during induration.

12. Berndt M. Mercury transport in taconite processing facilities: (II) fate of mercury captured by wet scrubbers. 2005.

13. Berndt M, Engesser J. Mercury chemistry and mössbauer spectroscopy of iron oxides during taconite processing on Minnesota's iron range.

14. Galbreath KC. Mercury vaporisation characteristics of taconite pellets.

15. Zhou Y, Jin X, Mukovskii Y, Shvets I. Kinetics of oxidation of low-index surfaces of magnetite. Journal of Physics: Condensed Matter. 2003;16(1):1.

16. Sondreal EA, Benson SA, Pavlish JH, Ralston NVC. An overview of air quality III: Mercury, trace elements, and particulate matter. Fuel Process Technol. 2004;85(6):425-40.

17. French CL, Maxwell WH. Study of hazardous air pollutant emissions from electric utility steam generating units: Final report to congress. United States Environmental Protection Agency, Office of Air Quality Planning and Standards; 1998.

18. Murata K, Weihe P, Budtz-Jørgensen E, Jørgensen PJ, Grandjean P. Delayed brainstem auditory evoked potential latencies in 14-year-old children exposed to methylmercury. J Pediatr. 2004;144.

19. Harada M. Congenital minamata disease: Intrauterine methylmercury poisoning. Teratology. 1978;18(2):285-8.

20. National Research Council (US). Board on Environmental Studies, National Research Council (US). Committee on the Toxicological Effects of Methylmercury. Toxicological effects of methylmercury. National Academies Press; 2000.

21. Zheng L, Liu G, Chou CL. The distribution, occurrence and environmental effect of mercury in chinese coals. Sci Total Environ. 2007;384(1):374-83.

22. Berndt ME, Engesser J, Johnson A. On the distribution of mercury in taconite plant scrubber systems. Minnesota Department of Natural Resources Report. 2003.

23. Great lakes mercury emission reduction strategy.

24. Luo W, Lu Y, Wang B, Tong X, Wang G, Shi Y, et al. Distribution and sources of mercury in soils from former industrialized urban areas of beijing, china. Environ Monit Assess. 2009;158(1):507-17.

25. Zhao Y, Mann MD, Pavlish JH, Mibeck BAF, Dunham GE, Olson ES. Application of gold catalyst for mercury oxidation by chlorine. Environ Sci Technol. 2006;40(5):1603-8.

26. Blythe G, Richardson C, Lani BW, Rhudy RG, Strohfus M, Loritz L, et al. In: Pilot testing of oxidation catalysts for enhanced mercury control by wet FGD. Combined power plant air pollutant control mega symposium, washington DC; ; 2003.

27. Dunham GE, DeWall RA, Senior CL. Fixed-bed studies of the interactions between mercury and coal combustion fly ash. Fuel Process Technol. 2003;82(2):197-213.

28. Tan Y, Mortazavi R, Dureau B, Douglas MA. An investigation of mercury distribution and speciation during coal combustion. Fuel. 2004;83(16):2229-36.

29. Albert A, Evan J, Karash A, Hargis RA, William J. O'Dow d, and, Pennline HW. A kinetic approach to the catalytic oxidation of mercury in flue gas. Energy Fuels. 2006;20(5):1941-5.

30. Galbreath KC, Zygarlicke CJ. Mercury transformations in coal combustion flue gas. Fuel Process Technol. 2000 6;65-66(0):289-310.

31. Olson E, Crocker C, Benson S. Surface compositions of carbon sorbents exposed to simulated low-rank coal flue gases.

32. Pavlish JH, Sondreal EA, Mann MD, Olson ES, Galbreath KC, Laudal DL, et al. Status review of mercury control options for coal-fired power plants. Fuel Process Technol. 2003 8/15;82(2-3):89-165.

33. Benner B. Mercury release from taconite during heating. . 2005.

34. Edwin S. Olson, Jeffrey S. Thompson, John H. Pavlish. TRAPPING AND IDENTIFICATION OF OXIDIZED MERCURY SPECIES IN FLUE GAS.

35. Forsmo S. Influence of green pellet properties on pelletizing of magnetite iron ore. . 2007.

36. Schmidt E, Vermaas F. Differential thermal analysis and cell dimensions of some natural magnetites. Annals of Mineralogy. 1955;40:422-31.

37. Gruner JW. Organic matter and the origin of the biwabik iron-bearing formation of the mesabi range. Economic Geology. 1922;17(6):407-60.

38. Bentell L, Mathisson G. Oxidation and slag-forming process in dolomite-fluxed pellets based on magnetite concentrates. Scand J Metall. 1978;7(5):230-6.

39. Dianbing H, Ungían K, Zongcai U. A mathematical model for the process of magnetite oxidation. Acta Metallurgical Sinica. 1994;7:57-63.

40. Edström JO, Bitsianes G. Studies on some chemical reactions involved in the pelletizing and reduction of iron oxides: Study of the mechanism and kinetics of oxidation of green magnetite pellets; the phase CaO-2Fe2O3 in the system CaO-Fe2O3 and its importance as binder in ore pellets; reduktionsstrukturer hos järnpulver; solid state diffusion in the reduction of magnetite. Almqvist & Wiksells; 1958.

41. Edström J. Study of the mechanism and kinetics of oxidation of green magnetite pellets. Jernkontorets Ann. 1957;141:457-78.

42. Edstrom J, Bitsianes G. Solid state diffusion in the reduction of magnetite. Trans.AIME. 1955;203:760-5.

43. Papanastassiou D, Bitsianes G. Mechanisms and kinetics underlying the oxidation of magnetite in the induration of iron ore pellets. Metallurgical and Materials Transactions B. 1973;4(2):487-96.

44. Galbreath KC, Zygarlicke CJ, Tibbetts JE, Schulz RL, Dunham GE. Effects of NOx, α-Fe2O3, γ-Fe2O3, and HCl on mercury transformations in a 7-kW coal combustion system. Fuel Process Technol. 2005 1/25;86(4):429-48.

45. EPA Website title 40 part 63 : http://www.ecfr.gov/cgi-bin/text-idx?c=ecfr;rgn=div6;view=text;node=40%3A15.0.1.1.1.5;idno=40;sid=62df1232dc085efd1ee45c5a3ef05df8;cc=ecfr#40:15.0.1.1.1.5.187.5

47. Nasah, J.N.D. Thesis : Evaluating the effectiveness of proprietary additives in improving the capture and sequestration of oxidized mercury in scrubber systems, 2012, University of North Dakota

48. Srinivasachar, S., Benson S.A. Method of capturing mercury from flue gas, 2009 patent